CHARACTERIZATION OF RAT CAROTID BODY TYPE II CELLS

FUNCTIONAL CHARACTERIZATION AND CELLULAR PHYSIOLOGY OF RAT CAROTID BODY TYPE II CELLS

By SINDHUBARATHI MURALI, B.Sc. (Hons)

A Thesis

Submitted to the School of Graduate Studies

In Partial Fulfilment of the Requirements for the Degree

MASTERS OF SCIENCE

McMaster University

MASTER OF SCIENCE (2015) MCMASTER UNIVERSITY

(Department of Biology) Hamilton, Ontario

TITLE: Functional characterization and cellular physiology of rat carotid body type II cells

AUTHOR: Sindhubarathi Murali, B.Sc. (hons) (McMaster University)

SUPERVISOR: Professor Colin A. Nurse

NUMBER OF PAGES: xv; 134

ABSTRACT

The carotid body (CB) is a peripheral arterial chemoreceptor located at the carotid bifurcation. Receptor type I cells transduce blood-borne chemical stimuli into electrical signals and release the excitatory neurotransmitter ATP onto afferent terminals that project to the breathing centre located in the brainstem. For the longest time, glial-like type II cells within the CB were thought to be sustentacular cells that formed intimate associations with type I cells. Recently, it was hypothesized that type II cells have a paracrine function in CB chemotransduction by acting as an ATP amplifier and enhancing chemoexcitation (Zhang et al. 2012). Given this recent development, the primary goal of this thesis was to further elucidate the paracrine function of type II cells and characterize the signaling mechanisms involved in type I and type II cell interactions. Ratiometric calcium imaging was used to investigate type II cell sensitivity to two prominent CB neuromodulators, angiotensin II (ANG II) and 5-HT, in rat CB cultures. Both ANG II and 5-HT elicited large rises in intracellular Ca^{2+} ($\Delta[Ca^{2+}]_i$) that were present in the absence of extracellular Ca^{2+} and were inhibited by intracellular store depletion agents. ANG II and 5-HT acted on their respective G-protein coupled receptors, AT_1 receptor (AT_1R) and 5-HT_{2A} receptor (5-$HT_{2A}R$), to initiate these Ca^{2+} responses presumably via a PLC-IP_3 mediated mechanism. Interestingly, these Ca^{2+} responses were required to activate pannexin-1 channels (Panx-1), a channel that has been previously shown to be a conduit for ATP in type II cells (Zhang et al. 2012).

This thesis investigated a variety of type I and type II cell interactions using ratiometric Ca^{2+} imaging. We were specifically interested in determining whether type II cells were capable of indirectly responding to a chemostimulus such that the stimulus would elicit neurosecretion from type I cells and result in a secondary Ca^{2+} responses in type II cells. Isohydric hypercapnia and a depolarizing stimulus (30 mM KCl saline) were capable of eliciting *indirect* Ca^{2+} responses in type II cells. These secondary Ca^{2+} responses in type II cells were partially inhibited by suramin, a purinergic P2Y2 receptor antagonist, suggesting that ATP was the predominant neurotransmitter responsible for type I to type II crosstalk. Similarly, a selective agonist for type II cells, UTP, evoked indirect Ca^{2+} responses in nearby type I cells. Type II to type I cell communication was dependent on Panx-1 channels since the secondary Ca^{2+} responses in type I cells were inhibited by the Panx-1 blocker, carbenoxolone (5 µM). UTP-evoked *indirect* Ca^{2+} in type I cells were partially inhibited by adenosine A2 receptor antagonists suggesting that the neuromodulator, adenosine,

governs cross-talk between type II and type I cells. This study elucidates the importance of purinergic signaling in the bi-directional cross-talk between receptor type I cells and glial-like type II cells.

ACKNOWLEDGEMENTS

Firstly, I would like to thank my supervisor, Dr. Colin Nurse, for his guidance and encouragement throughout my entire Master's. Thank you to Colin for being such a dedicated, approachable, and understanding supervisor. I learnt many things from him over the years including how to be a confident presenter, applying Occam's razor when interpreting data, and how to improve my writing style so that it may be more eloquent. Undoubtedly, his excitement for science has made my Master's experience a pleasurable one.

Thank you to Cathy Vollmer for being an amazing lab mom and handling every lab debacle with calm, cool expertise; it is because of her that the Nurse lab runs so smoothly! Cathy is a patient teacher and her warm, kind demeanor was appreciated during frustrating times. I am forever grateful to Dr. Nikol Piskuric for being an amazing mentor and friend. Thank you for answering all my never-ending questions from the calcium imaging system to statistics to just about everything in academia. She is one of the most inspirational role-models in my life. I would like to thank Min Zhang for offering his incredible patching skills to the cause of my thesis. Thank you to Dr. Angela Scott for her wisdom and insight into both academic-related and personal issues. She has shown me what it is to be a strong, confident, charismatic female researcher. A big thank you to the wonderful and loving friends that I have made during graduate school: Natalie D'Silva, Marten Kaas, Tarushika Vasanthan, and Lana Shaya. Thanks guys for being so supportive, calming me down during my many panic attacks, and most importantly, for getting me out of the lab to experience life.

Finally, I would like to deeply thank my family for their unconditional love and support. Thank you to my best friend, Thenes Asokumaran, for being a comfort during stressful times, listening to me complain about bad experiment days, and for reminding me to have more confidence in myself and in my abilities. Thank you to Ammamma, Appappa, and Appamma for always making sure I'm happy, fed, and for being my second set of parents. You guys are the biggest source of joy in my life. Last, but certainly not least, thank you to my wonderful parents for believing in me and being so supportive with my life decisions. Thank you Amma and Appa for always being so proud of me and encouraging me to pursue my dreams.

TABLE OF CONTENTS

LIST OF FIGURES AND TABLES

CHAPTER 1

CHAPTER 2

CHAPTER 3

CHAPTER 4

CHAPTER 5

LIST OF ABBREVIATIONS

α,β-MeADP	α,β-methyleneADP
5-HT	5-hydroxytryptamine (serotonin)
AB	aortic body
ACE	angiotensin converting enzyme
ACh	acetylcholine
Ado	adenosine
ADP	adenosine disphosphate
AMP	adenosine monophosphate
AMPK	AMP-activated protein kinase
ANG II	angiotensin II
AT_1R	angiotensin 1 receptor
ASIC	acid-sensitive ion channel
ATP	adenosine triphosphate
BBS	bicarbonate-buffered solution
BK	voltage- and Ca^{2+} - sensitive big conductance K^+ channel
$[Ca^{2+}]_i$	intracellular free Ca^{2+} concentration
CB	carotid body
CBS	cystathionine β-synthase
CBX	carbenoxolone
CIH	chronic intermittent hypoxia
CH	chronic hypoxia

CHF	chronic heart failure
CO_2	carbon dioxide
CSE	cystathionine γ-lyase
CSN	carotid sinus nerve
DA	dopamine
EC_{50}	concentration of agonist causing a half maximal response
ENT	equilibrative nucleoside transporter
fura-2/AM	fura-2 acetoxymethyl ester
GABA	γ-aminobutyric acid
GFAP	glial fibrillary acidic protein
H_2S	hydrogen sulphide
IP_3	ionsitol 1,4,5-triphosphate
LTF	long-term facilitation
mRNA	messenger ribonucleic acid
NBTI	S-(4-nitrobenzyl)-6-thioinosine
NO	nitric oxide
O_2	oxygen
Panx	pannexin
P2X	iontropic purinergic receptor
P2Y	metabotropic purinergic receptor
PCO_2	partial pressure of carbon dioxide
PKC	protein kinase C
PN	petrosal neuron

PO_2	partial pressure of oxygen
RAS	renin-angiotensin system
ROS	reactive oxygen species
SCG	superior cervical ganglion
S.E.M	standard error of the mean
TASK	TWIK-related acid sensitive K^+ channel
TWIK	tandem P domain weak inward rectifier K^+ channel
UTP	uridine triphosphate

CHAPTER 1

General Introduction

As the final acceptor of electrons in the mitochondrial respiratory chain, oxygen (O_2) is vital to cellular energy (i.e. ATP) production and therefore to the survival of all aerobic organisms. In mammals, O_2 is delivered to the tissues by the respiratory and circulatory systems. The respiratory system ensures that O_2-rich air enters the lungs and that CO_2-rich air is expelled. One of the most important functions of the respiratory system is to adjust ventilation to meet changes in O_2 consumption and CO_2 production, thereby maintaining homeostasis in the organism. On the other hand, the cardiovascular system controls the amount and rate of delivery of O_2 to all cells in the body. Both systems work to ensure that the partial pressure of oxygen (PO_2) and carbon dioxide (PCO_2) in arterial blood are kept within close limits.

The respiratory and cardiovascular systems are reflexively controlled by a number of specialized sensors that detect the chemical composition of arterial blood. The chemical signals that are sensed include, but are not limited to, changes in PO_2, PCO_2, and/or acid [H^+]. These sensors, known as the central and peripheral chemoreceptors, relay chemosensory information to the respiratory and cardiovascular centres in the brainstem, which coordinate the sensory input and in turn send impulses to control ventilation and cardiovascular responses, respectively. The central chemoreceptors, located in the medulla of the brainstem, are most important for the minute-to-minute control of ventilation. They sense blood pCO_2 and pH via changes in pH of the cerebrospinal fluid resulting in an increase of sympathetic and respiratory activity (Neubauer and Sunderram 2004; Spyer and Gourine 2009). In contrast, the peripheral chemoreceptors located primarily in the carotid and aortic bodies are polymodal sensors responsible for eliciting hypoxia (low PO_2)-evoked hyperventilation. Of these peripheral chemoreceptors, the carotid bodies (CBs)

are the most important for sensing reductions in PO_2 (hypoxia), although it is now well accepted that they are capable of detecting several sensory modalities including high CO_2 (hypercapnia), acidosis, low glucose, and temperature (Gonzalez et al. 1994; López-Barneo 2003; Kumar and Bin-Jaliah 2007). Afferent petrosal neurons (PNs) transmit sensory information originating in the CB to the respiratory control center or central pattern generator, which interprets the strength and duration of the stimulus by a frequency code and adjusts the ventilatory response accordingly (Gonzalez et al. 1994; Teppema and Dahan 2010). The removal of the CBs in animals and humans greatly attenuates the ventilatory and cardiovascular responses to hypoxia (Lugliani et al. 1971; Bureau et al. 1985; Winter 1991). Interestingly, CB hyperactivity is associated with several pathophysiological conditions including sleep apnea, congestive heart failure, hypertension, and chronic obstructive pulmonary disease (Schultz 2011; Kumar and Prabhakar 2012). However, despite their clinical importance, the mechanisms underlying sensory processing in the CB are not fully understood. One of the goals of this thesis is to contribute new knowledge in this area by focusing on the roles of CB neurochemicals and cell-cell interactions using a culture model of dispersed CB cells. An introduction to the general anatomical organization and main cellular elements in the CB is considered below.

In mammals, the peripheral chemoreceptors are the carotid bodies (CBs), situated at the bifurcation of the common carotid arteries, and the aortic bodies (ABs) that are diffusely distributed near the aortic arch. CB receptor cells, known as glomus or type I cells, detect chemical stimuli in the arterial blood and transduce them into an electrical signal; this leads to an increase in intracellular calcium ($[Ca^{2+}]_i$) and neurosecretion onto sensory petrosal nerve endings resulting in an increase in action potential firing in the carotid sinus nerve (CSN) (Peers and Buckler 1995; López-Barneo 1996). Within the CB chemoreceptor complex, type I receptor cells are ensheathed by processes of glial-like type II cells. Research in peripheral chemoreception has justifiably focused on the type I cell, but the intimate associations between them and the glial-like type II cell suggests that the type II cells may also play a significant role in modulating CB signalling. In the central nervous system, glial cells, such as astrocytes, actively participate in synaptic signalling by releasing neuroactive substances (Eroglu and Barres 2010). Until recently, it remained unclear whether type II cells of the CB played an active role in chemotransduction. Their presumed passive role was challenged with the demonstration that they expressed P2Y2 receptors, which are activated by ATP or UTP leading to a rise in $[Ca^{2+}]_i$ (Xu et al. 2003). The activation of these P2Y2

receptors on type II cells leads to the opening of a large pore, pannexin-1 (Panx-1) channels thereby facilitating further ATP release (Zhang et al. 2012). Thus, the type II cells have the potential to enhance the excitatory drive at the chemosensory synapse by amplifying ATP levels in the vicinity of the sensory afferent nerve terminal. This mechanism of "ATP-induced ATP release" suggests a paracrine function for type II cells during chemoexcitation. The aim of my thesis will be to further characterize the modulatory role of type II cells in chemoreception, and work to identify novel neuroactive substances involved in the cell-to-cell interactions within the CB.

Structural organization of the carotid body

The paired carotid bodies (CB) are located between the internal and external carotid arteries, where they sample the chemical composition of the arterial blood. The CB is reported to be the most richly vascularised organ in the body and morphometric measurements indicate that one-quarter to one-third of its volume is occupied by capillaries and venules (De Castro 1968; McDonald 1981). Penetration by a dense network of thin-walled, fenestrated capillaries provides the CB with a rich arterial blood supply for the delivery of the sensory stimuli. This dense network of small vessels originates from one or more small arteries that branch off of the common carotid artery. The CB is strategically placed for monitoring blood chemicals just before they reach the brain, a critical organ that is quite sensitive to oxygen and glucose deprivation (McDonald 1981).

The CB is a small organ, roughly egg-shaped, and measures 0.6 x 0.6 x 1.5 mm in the rat (McDonald 1975). In mammals, the organ is adjacent to the superior cervical sympathetic ganglion (SCG) and nodose ganglion and receives its sensory innervation from the carotid sinus nerve (CSN), a branch of the glossopharyngeal nerve (IXth cranial nerve) (McDonald 1981). The adult CB is comprised of clusters of parenchymal chemoreceptor type I (glomus) cells penetrated by glia-like type II cells. Individual clusters of glomus and type II cells are separated by walls of connective tissue, which converge on the surface to form a capsule surrounding the whole organ (Gonzalez et al. 1994).

The receptor type I (glomus) cells originate from the neural crest (Pearse et al. 1973) and are round or ovoid with a diameter of 8-15 μm. They constitute 57% of the total cells in human carotid bodies to 79% in rat carotid bodies (McDonald 1981). Type I cells are organized into clusters that are surrounded by a layer of connective tissue. They have the morphological characteristics of cells that actively synthesize and package substances for secretion. The

cytoplasm has a well-developed Golgi apparatus, extensive endoplasmic reticulum, numerous mitochondria, and a variety of dense- and clear-cored synaptic vesicles that contain various neurotransmitters (McDonald 1981). Glomus cells form afferent and efferent chemical synapses with sensory nerve endings and appear to be in synaptic contact with each other. In addition to chemical synapses, the expression of the gap junction subunit connexin 43 suggests the presence of electrical coupling and the importance of intercellular communication between neighbouring glomus cells (McDonald 1975; Monti-Bloch 1990; Jiang and Eyzaguirre 2003; Eyzaguirre 2007).

Type II cells have been variously described as sheath or sustentacular cells and are considered to be "glial-like" due to similarities shared with Schwann and satellite cells (McDonald 1981). Consistent with their glial cell origin, they immunostain positively for glial fibrillary acid protein (GFAP) (Pardal et al. 2007). Though present in fewer numbers, type II cells form an intimate association with glomus cells (McDonald 1981). Their cylindrical cell bodies extend cytoplasmic processes of variable lengths that interdigitate glomus cell clusters. A major goal of this thesis is to elucidate possible physiological roles of type II cells. As discussed in more detail later on, their morphology suggests that they may form paracrine cell-cell interactions with several adjacent glomus cells. The most striking differences between glomus and type II cells are type II cells do not respond directly to chemostimuli (Xu et al. 2003; Zhang et al. 2012), and lack synaptic vesicles at the ultrastructural level (McDonald 1981).

The CB is innervated mainly by sensory fibres of the CSN, a branch of the glossopharyngeal nerve. Data from axonal degeneration studies in the rat CB have shown that 95% of the nerve endings that innervate type I clusters are part of unipolar neurons, whose cell bodies lie in the petrosal (sensory) ganglion of the glossopharyngeal nerve (McDonald 1975). Afferent endings contact type I cells as either small bouton-like endings or wide calyx-shaped endings, and contain ~10x more small clear-core vesicles than dense-core vesicles (McDonald and Mitchell 1975). Retrograde-labelling studies have confirmed that neuronal cell bodies which lie in the distal portion of the petrosal ganglion have axons terminating in the CB (Katz and Black 1986). The axonal terminals of petrosal ganglion neurons (PNs) form synapses with neurons in the nucleus tractus solitarius in the medulla oblongata. Electron micrographs of CB sections have demonstrated that type I cells and the afferent fibres form specific synaptic connections (Morgan et al. 1975). This is consistent with the notion that type I cells have an important role in transmitting

sensory information through the CSN into the central nervous system. A proportion of the nerve endings that terminate within the CB belong to autonomic efferent neurons, whose cell bodies reside in microganglia embedded within the carotid sinus and glossopharyngeal nerves. These neurons express nitric oxide synthase, and they are the source of the efferent inhibition within the CB since nitric oxide (NO) inhibits the sensory discharge in the CSN (Alcayaga et al. 1999; Campanucci et al. 2012).

Carotid body chemosensing mechanisms

The CB detects a variety of arterial chemical signals including: a change in the partial pressure of oxygen (PO_2), PCO_2, [H^+], and [glucose]. There are numerous studies demonstrating that type I cells are the chemotransducer element for most, if not, all of these chemostimuli, and are capable of transduction via the regulation of ion channel activity (Gonzalez et al. 1994; Peers and Buckler 1995; Lopez-Barneo et al. 2001; Zhang and Nurse 2004; Nurse 2005). In response to the chemical stimuli, type I cells transduces them into a change in membrane potential or action potential frequency leading to elevations of $[Ca^{2+}]_i$, and neurosecretion onto afferent nerve terminals. The CB then relays this information to the respiratory centre in the brainstem, which coordinates the sensory input and in turn sends impulses to the respiratory muscles. The respiratory muscles then control ventilation and restores the arterial blood composition. The chemosensing mechanisms for hypoxia, hypercapnic and acid stimuli follow this general pattern.

Oxygen Sensing

Hypoxia leads to the inhibition of O_2-sensitive K^+ channels within type I cells, which results in the depolarization of the plasma membrane (Gonzalez et al. 1994; Peers and Buckler 1995; Prabhakar and Overholt 2000; Lopez-Barneo et al. 2001). The closing of a K^+ channel moves the membrane potential away from the K^+ equilibrium potential (~ - 80 mV) and toward the equilibrium potentials of other ions with positive Nernst potentials (e.g. Na^+ or Ca^{2+}), thus resulting in the depolarization of the type I cell. Lopez-Barneo et al. (1988) were the first to report that hypoxia could selectively inhibit a lower conductance (40 pS), voltage-gated, Ca^{2+}-insensitive K^+ channel in adult rabbit type I cells (Lopez-Barneo et al. 1988; Ganfornina and López-Barneo 1992). Since then, it is evident that there are clear species differences when considering the nature of the O_2-sensitive K^+ channels and within a given species there appears to be more than one type of channel. For example, in rat type I cells there is strong evidence to support 2 candidates, i.e. a

voltage- and Ca^{2+}-sensitive large-conductance (BK) channel (Peers 1990; Peers and Wyatt 2007) and a voltage-insensitive, TWIK-related acid-sensitive (TASK)-like tandem-P domain background K^+ channel (Buckler 1997; Buckler et al. 2000). Kim et al. (2009) suggests that the main O_2-sensitive background K^+ channel in the rat consists of a TASK1/3 heteromultimer. It is fairly evident that the closure of a K^+ conductance is the initial step of hypoxia chemotransduction, however the means by which this closure occurs is still not clear.

The mechanism by which type I cells initially "sense" physiological stimuli, such as hypoxia, remains controversial. The most popular hypothesis concerning the identity of the O_2-sensor has been the 'mitochondrial hypothesis' (Kemp 2006; Buckler 2007). The key observation supporting this hypothesis is that the carotid body is rapidly and powerfully excited by numerous inhibitors of mitochondrial energy metabolism such as uncouplers, electron transport chain inhibitors, and inhibitors of ATP synthase (Buckler 2007). The precise link or links between mitochondrial function and background K^+-channel activity has not yet been fully resolved; one possible link between the two involves the AMP-activated protein kinase (AMPK). AMPK is a kinase activated by a rise in the cytosolic AMP: ATP ratio and therefore, a finely tuned metabolic sensor. Wyatt et al. (2006) demonstrated that the pharmacological activation of AMPK caused the inhibition of both BK and TASK K^+ channels resulting in type I cell depolarization.

Another CB O_2 sensing pathway, independent of mitochondrial inhibition, involves the gasotransmitter, H_2S, a signaling gas that regulates neuronal transmission (Kimura et al. 2005; Olson 2011; Kumar and Prabhakar 2012; Prabhakar and Peers 2014). Normally, there are low basal levels of H_2S within type I cells since the H_2S-synthesizing enzymes, cystathionine-γ-lyase (CSE) and cystathionine β-synthase (CBS), are inhibited. Hypoxia, through unknown mechanisms, removes this tonic inhibition on both enzymes allowing for endogenous H_2S production. Observations from *in vitro* CB preparations have shown that supraphysiological doses of H_2S evoked type I cell depolarization and $[Ca^{2+}]_i$ elevation (Buckler 2012; Makarenko et al. 2012). H_2S facilitates cellular excitation via a few mechanisms, which include either inhibition of BK (Li et al. 2010) and/or TASK K^+ channels (Buckler 2012) or activation of voltage-gated L-type Ca^{2+} channels (Peng et al. 2010). The most compelling evidence for the H_2S hypothesis comes from studies utilising transgenic CSE knock-out models. Mice deficient in CSE had an impaired ventilatory response to hypoxia and displayed diminished hypoxia-evoked rises in $[Ca^{2+}]_i$,

catecholamine secretion, and CSN activity (Peng et al. 2010; Makarenko et al. 2012). There is doubt whether the H_2S hypothesis is separate from the mitochondrial hypothesis since Buckler (2012) demonstrated that the effects of H_2S on CB type I cells occur via the impairment of mitochondrial function. H_2S is a recognized mitochondrial inhibitor that binds to and deactivates complex IV, resulting in run-down of mitochondrial electron transport and $[ATP]_i$. Buckler (2012) argued that a significant proportion of CB activation caused by endogenous H_2S production occurs secondary to a reduction in mitochondrial ATP synthesis and cellular energy status. Further work is required in order to elucidate O_2 sensing pathways within the CB.

After membrane depolarization, the next step is calcium entry via voltage-gated calcium channels. Hypoxia elicits a fast, sustained increase in $[Ca^{2+}]_i$ followed by Ca^{2+} fluctuations. The magnitude of the Ca^{2+} response is graded with the degree of hypoxia; i.e. a greater $[Ca^{2+}]_i$ response with decreasing PO_2 levels (Buckler and Vaughan-Jones 1994). Buckler & Vaughan-Jones (1994) demonstrated that the source of calcium is extracellular since the hypoxia-induced rise in $[Ca^{2+}]_i$ was completely abolished in the absence of external calcium. This observation was confirmed with intact carotid body preparations where hypoxia-induced increases in both afferent CSN discharge and dopamine release were inhibited by Ca^{2+} -free media and attenuated by L-type Ca^{2+}-channel antagonists (Shaw et al. 1989; Shirahata and Fitzgerald 1991; Obeso et al. 1992). Membrane depolarization is required for the activation of voltage-gated Ca^{2+} channels as seen with experiments that simultaneously measure membrane potential and $[Ca^{2+}]_i$. Hypoxia depolarized type I cells and caused a rapid rise in $[Ca^{2+}]_i$; however, when cells were voltage-clamped at their resting potentials, hypoxia produced a smaller and slower rise in $[Ca^{2+}]_i$ (Buckler and Vaughan-Jones 1994). Type-1 cell express a number of different voltage-gated Ca^{2+}-channels including L-, N-, P/Q-, R-, and T-type channels, although only L- and P/Q-type channels appear to be strongly coupled to neurosecretion (Rocher et al. 2005).

Hypercapnia/Acid Sensing

The chemotransduction of hypercapnic and acidic stimuli involves the acidification of type I cell intracellular pH. Evidence for this is based on observations that membrane permeant carbonic anhydrase inhibitors, such as acetazolamide, slowed and attenuated hypercapnia-evoked membrane depolarization in type I cells and CSN discharge in response to hypercapnic acidosis (Hanson et al. 1981; Rigual et al. 1991; Iturriaga et al. 1993; Zhang and Nurse 2004). The

production of acid (H^+) is an important step in the transduction of hypercapnic stimuli since carbonic anhydrase accelerates the hydration of CO_2. Once the acid is internally produced, it results in the inhibition of TASK K^+ channels followed by membrane depolarization (Buckler and Vaughan-Jones 1994). Type I cells are also capable of responding to extracellular acidosis via cation-selective, acid-sensitive ion channels (ASIC 1 & 3) (Tan et al. 2007). Tan et al. (2007) found that extracellular acidosis generated both transient and sustained currents and depolarization; the initial transient response was consistent with the activation of ASICs whereas the sustained response was consistent with the inhibition of TASK K^+ channels. Similar to hypoxia, hypercapnia or respiratory acidosis (PCO_2/H^+) is abolished in Ca^{2+}-free media and substantially inhibited by 2 mM Ni^{2+}, a general voltage-gated Ca^{2+} channel blocker (Rocher et al. 1991). PCO_2/H^+ produces a biphasic Ca^{2+} response due to the combined effects of CO_2 and H^+ on intracellular pH. Type I cells initially respond to PCO_2/H^+ with a rapid transient Ca^{2+} response followed by a secondary, gradual decline to levels above basal Ca^{2+} levels. In comparison, isohydric hypercapnia (PCO_2 increases in normal pH) elicits the initial Ca^{2+} peak but not the sustained Ca^{2+} response whereas isocapnic (metabolic) acidosis (low pH in normal PCO_2) only causes the sustained Ca^{2+} response (Buckler and Vaughan-Jones 1993). The rapid transient Ca^{2+} response is due to a fast intracellular acidification as a result of carbonic anhydrase catalyzing the hydration of CO_2 whereas the slow, sustained phase results from a sustained decrease in intracellular pH due to prolonged extracellular acidification. The acid/hypercapnic-induced rise in type I cell $[Ca^{2+}]_i$ serves as a signal for neurosecretion (Rocher et al. 1991).

Neurotransmitters of the carotid body

Chemoreception in the carotid body involves the concerted actions of multiple neurotransmitters and neuromodulators released from type I cells (Nurse 2005; Nurse 2010; Kumar and Prabhakar 2012). Recent evidence suggests type II cells may also be involved (Zhang et al. 12). Some of these neurochemicals include but are not limited to: acetylcholine (ACh), ATP, dopamine (DA), serotonin (5-HT), angiotensin II (ANG II), γ-aminobutyric acid (GABA), adenosine (Ado), and histamine (Nurse 2005; Nurse 2010; Kumar and Prabhakar 2012). My working hypothesis is that these neurochemicals may participate not only in synaptic transmission from type I cells to sensory afferent terminals, but also in paracrine and autocrine interactions

involving type I cells and type II cells. Here, I present a brief overview of current knowledge about the roles of CB neurotransmitters and neuromodulators that are relevant to this thesis.

ATP: a key CB excitatory neurotransmitter

Zhang et al. (2000) determined the identity of the CB excitatory neurotransmitters using a functional co-culture model in which isolated clusters of rat type I cells were juxtaposed with dissociated PNs. They found that the combined application of the P2X (purinergic) receptor blocker and nicotinic ACh receptor (nAChR) blocker completely abolished the post-synaptic excitatory responses recorded in PNs during hypoxia and acid hypercapnia (Zhang et al. 2000; Zhang and Nurse, 2004). In experiments utilizing *in vitro* preparations of the isolated, superfused CB-attached CSN, both hypoxia-evoked (rat) and acidosis-evoked (cat) CSN activity were inhibited by the simultaneous blockade of purinergic and nicotinic receptors (Zhang et al. 2000; Varas et al. 2003).

ATP-sensitivity of afferent PNs has been demonstrated in the rat, mouse, and cat (Alcayaga et al. 2000; Zhang et al. 2000; Rong et al. 2003). Electrophysiological and single-cell RT-PCR studies conducted on co-cultures suggested that PN purinergic receptors consisted of heteromeric P2X2 and P2X3 subunits (Prasad et al 2001), This was confirmed with immunofluorescence experiments on rat CB tissue sections demonstrating the co-localization of these subunits in afferent nerve terminals (Zhang et al. 2000; Prasad et al. 2001). The essential role of the P2X2 subunit was demonstrated in transgenic mice lacking the P2X2 subunit where the ventilatory response to hypoxia was attenuated and this was correlated with a reduction in hypoxia-evoked CSN discharge (Rong et al. 2003). In comparison, P2X3-knockout mice had a normal hypoxia ventilatory response suggesting that the P2X2 is a critical subunit at least in these animals (Rong et al. 2003). However, in the rat CB-sinus nerve preparation Niane et al. (2011) confirmed the importance of the P2X3 subunit using selective antagonists to block both basal and hypoxia-induced CSN discharge. In other studies using luciferin-luciferase bioluminescence assays, hypoxia-evoked release of ATP was demonstrated in isolated whole CBs, CB tissue slices, and CB cultures (Buttigieg J. & Nurse 2004; Conde and Monteiro 2006). These studies provide confirmation that ATP is a key neurotransmitter released from type I cells during chemoexcitation and that postsynaptic homomeric P2X2, P2X3, and/or heteromeric P2X2/3 receptors contribute to this ATP-mediated synaptic transmission.

Adenosine: an excitatory neuromodulator

Adenosine (Ado), a purine nucleoside, plays an excitatory role in ventilation as seen in both rats (Monteiro and Ribeiro 1987; Monteiro and Ribeiro 1989) and humans (Watt and Routledge 1985; Watt et al. 1987). First, exogenous Ado administration results in a stimulatory effect upon carotid body chemoafferent discharge in the cat both *in vivo* (McQueen and Ribeiro 1981; McQueen and Ribeiro 1983) and *in vitro* (Runold et al. 1990) as well as in the rat (Vandier et al. 1999). Second, hypoxia-evoked CSN discharge is substantially reduced in the presence of either the non-specific Ado receptor inhibitors, 8-phenyl-theophylline in cats (McQueen and Ribeiro 1986), or caffeine in rats (Conde et al. 2006). Third, the excitatory effect of Ado on the CB is sufficient to enhance ventilation by increasing respiratory frequency, tidal volume, and minute ventilation (Monteiro and Ribeiro 1987). It has been proposed that Ado is generated endogenously in the CB since these ventilatory effects are abolished by CSN section and may have a protective effect to increase O_2 delivery (Kumar and Prabhakar 2012).

There is an extracellular and intracellular source of Ado, both of which are a result of ATP metabolism. The extracellular source of Ado is due to the breakdown of ATP released during chemotransmission by ectonucleotidases. ATP within the synapse is broken down into adenosine monophosphate (AMP) in the presence of ectonucleoside triphosphate diphosphohydrolyase 1. Ado is produced from the cleavage of AMP by membrane-bound, 5'-nucleotidase or by the hydrolysis of S-adenosylhomocysteine (Kumar and Prabhakar 2012). Alternatively, Ado can be produced from intracellular ATP catabolism and released into the synapse through a bidirectional equilibrative nucleoside transporter (ENT) (Baldwin et al. 1999). Extracellular Ado was detected when whole CBs were exposed to normoxic conditions *in vitro* and the amount of Ado recovered was reduced in the presence of the ecto-5'-nucleotidase inhibitor, α,β-methylene ADP (AOPCP), but not by the ENT blocker, S-(4-nitrobenzyl)-6-thioinosine (NBTI). This suggests that the Ado produced during normoxia occurs predominantly via extracellular ATP catabolism (Conde and Monteiro 2004). During hypoxia there is an increase in intracellular production and consequent release of Ado that is suppressed by pharmacological inhibition of ENT and ecto-5'-nucleotidase. This suggests that the release of Ado from the CB during hypoxia arises from both extracellular ATP catabolism and nucleoside transporter mechanisms (Conde and Monteiro 2004).

Ado acts on a number of specific, G-protein coupled, P1 purinoceptors located on the pre- and post-synaptic membranes. Molecular, pharmacological, and immunohistochemical techniques have identified A_{2A} and A_{2B} receptors on type I cells and petrosal neurons (McQueen and Ribeiro 1986; Kobayashi et al. 2000; Conde et al. 2006). Both receptors seem to contribute to enhanced secretion of CB neurotransmitter(s) and excitation of the afferent nerve terminal. Caffeine, a non-selective A_2 receptor antagonist, inhibited catecholamine secretion and CSN discharge under normoxic and hypoxic conditions (Conde and Monteiro 2006). Specific antagonists for both the A_{2A} and the A_{2B} receptors reduced hypoxia-evoked increases in CSN discharge frequency, suggesting that both subtypes contribute to the modulating effect of Ado on chemosensory discharge (Conde et al. 2006). The external application of Ado to type I cells resulted in a rise in $[Ca^{2+}]_i$ that was inhibited by the selective A_{2A} receptor blocker, SCH58261 (Xu et al. 2006). The rise in $[Ca^{2+}]_i$ was mimicked by the cAMP activator forskolin, abolished by the PKA inhibitor H89, and was augmented by anandamide, a TASK-1 K^+ channel blocker. These results suggested that Ado, acting via A_{2A} receptors, produces a PKA-dependent inhibition of TASK-like K^+ channels in the rat CB (Xu et al. 2006). Specific A_{2A} receptor antagonists have been shown to inhibit both hypoxia-evoked receptor potentials and Ado-evoked Ca^{2+} signals in type I cells (Xu et al. 2006; Nurse and Piskuric 2013). Ado, acting via A_{2B} receptors, is known to increase cAMP in rabbit type I cells thus, potentiating the release of catecholamines in response to hypoxia (Pérez-García et al. 1991; Chen et al. 1997; Conde et al. 2008). Chronic hypoxia has been shown to enhance A_{2B} receptor signaling in rat CB type I cells facilitating an augmented stimulus-evoked catecholamine secretion (Livermore and Nurse 2013).

5-HT: A biogenic amine and excitatory neuromodulator

5-Hydroxytryptamine (5-HT; serotonin) is one of several neuromodulators within the CB that act on ionotropic and/or metabotropic receptors to shape the chemoexcitory response. 5-HT has been identified in type I cells of the CB of many species, including the mouse (Oomori et al. 1994), rat (Gronblad et al. 1983), cat (Abramovici et al. 1991), and humans (Perrin et al. 1986). Type I cells express the $5\text{-}HT_{2A}$ receptor (Zhang et al. 2003), a G-protein-coupled receptor for serotonin that preferentially couples to $G_{q/11}$ to increase hydrolysis of inositol phosphates and elevate cytosolic $[Ca^{2+}]$ (Finkbeiner 1993). Zhang et al. (2003) found that the $5\text{-}HT_{2A}$ selective antagonist, ketanserin, was able to block spontaneous discharge seen in type I clusters and

exogenous 5-HT application induced membrane depolarization and/or rhythmic spiking. The mechanism for the 5-HT-induced membrane depolarization was a PKC-dependent inhibition of an unidentified, resting K^+ conductance, which sometimes led to action potentials. The pre-synaptic effect of 5-HT is mediated through this autocrine/paracrine signalling pathway that augments the receptor potential and chemoexcitatory response via a positive feedback loop (Zhang et al. 2003; Nurse 2005).

5-HT has many effects on respiration. For instance, exogenous application of 5-HT to the rat CB produces hyperventilation which is correlated with an increase in CSN activity and can be abolished by CSN section (Sapru and Krieger 1977). Despite this observation, there is controversy surrounding the participation of 5-HT in acute hypoxia signalling. A study on intact rat CBs detected spontaneous, but not hypoxia-evoked 5-HT release using HPLC. However, the authors discovered a role for ketanserin-sensitive 5-HT_2 receptors in modulating the decay phase of the hypoxic sensory responses (Jacono et al. 2005). In contrast, hypoxia-evoked responses recorded in postsynaptic PNs in functional co-cultures were suppressed by 5-HT_{2A}-selective antagonists, ketanserin and/or ritanserin (Zhang et al. 2003). Furthermore, 5-HT has been implicated in long-term facilitation (LTF), a long-lasting increase in sensory discharge associated with exposures to chronic intermittent hypoxia (CIH) (Peng et al. 2006). These authors found that intermittent exogenous application of 5-HT can evoke sensory LTF in isolated CBs in vitro; also, the 5-HT – induced sensory LTF was abolished by 5-HT_{2A} receptor antagonists and/or PKC inhibitors. In summary, it was proposed that intermittent release of 5-HT during CIH and subsequent 5-HT_{2A} receptor stimulation gave rise to chronic up-regulation in PKC activity, thus increasing NADPH oxidase activity and ROS generation to induce sensory LTF and CB hypersensitivity (Peng et al. 2009).

RT-PCR experiments revealed that CB type I cells and PNs express 5-HT_{5A} receptors suggesting that this receptor may play a role in arterial chemoreception (Wang et al. 2000). To my knowledge, there are no studies elucidating the physiological implications of the 5-HT_{5A} receptor within the CB. In general, the 5-HT_5 receptor subfamily is the least well understood of all the 5-HT receptor families (Noda et al. 2004). The 5-HT_{5A} is predominantly expressed by astrocytes to mediate a mechanism for neuronal suppression; the activation of this receptor led to the inhibition of adenylate cyclase via coupling to PTX sensitive G_i/G_o proteins (Carson et al. 1996). Nodal et

al. (2003) suggested that 5-HT_{5A} receptors coupled to multiple signal transduction pathways and were capable of regulating intracellular Ca^{2+} via ADP-ribosyl cyclase activity and IP_3-mediated mechanisms. For example, one pathway led to the inhibition of ADP-ribosyl cyclase activity and cyclic ADP ribose formation, a compound that targets type II ryanodine receptors to release Ca^{2+} from mitochondrial stores. An alternative pathway was presumed to cause IP_3-mediated increase in intracellular Ca^{2+}, leading to the transient opening of K^+ channels. The K^+ currents were partially inhibited by PTX suggesting that there may be crosstalk between G_i/G_o and PKC signalling pathways, and/or the 5-HT_{5A} receptor may couple to G_q to mediate the conventional IP_3-signaling cascade (Noda et al. 2003). In summary, 5-HT_{5A} receptor signalling appears more complicated than what was previously assumed.

So far, the sites of action for 5-HT are presumed to be presynaptic, i.e. on chemoreceptor type I cells, or postsynaptic, i.e. on afferent nerve endings which express the 5-HT_{2A} receptor, the 5-HT_{5A}, and/or the ligand-gated, ionotropic, 5-HT_3 receptor (Zhong et al. 1999; Wang et al. 2000). However, preliminary data from our lab suggest that this view may be an oversimplification, as glia-like type II cells are also potential targets for 5-HT. In this thesis I will extend these studies in order to elucidate the role of 5-HT in the physiology of type II cells.

Angiotensin II: A carotid body neuropeptide

As mentioned above, the CB is highly vascularised with blood perfusion that exceeds the needs of local tissue metabolism (McDonald 1981). Circulating hormones and locally produced substances from the vasculature, all of which include vasoactive peptides such as angiotensin II (ANG II), act as autocrines and paracrines that could regulate the excitability of type I cells. ANG II is a key component of the renin-angiotensin system (RAS) that is involved in blood pressure regulation and fluid homeostasis. The expression and localization of several key RAS components within the CB suggests the existence of an intrinsic RAS. The compulsory component for an intrinsic RAS, angiotensinogen, was detected in type I cells (Lam and Leung 2002). In addition to angiotensinogen mRNA and protein, angiotensin converting enzyme (ACE) mRNA expression has been demonstrated in type I cells (Lam and Leung 2002). This local angiotensin system contributes to CB sensitization during chronic heart failure (CHF), as well as chronic and intermittent hypoxia (Schultz 2011; Kumar and Prabhakar 2012). During CHF, CB chemosensitivity is enhanced, leading to sympathetic hyperactivity and the exacerbation of the

disease progression (Schultz 2011). These findings seem to be consistent with an excitatory role for ANG II signalling in CB function.

Peripheral infusion of ANG II stimulates respiration in anesthetized animals, in part via stimulation of the carotid chemoreflex (Jennings 1993; Ohtake and Jennings 1993). ANG II modulates the basal CSN discharge in the ex vivo CB by inducing a brief inhibition followed by a major excitation. Losartan, a selective angiotensin 1 receptor (AT_1R) antagonist, abolishes both the inhibitory and excitatory effects of exogenous ANG II (Allen 1998). Allen et al. (1998) detected a high density of ANG II receptors in the CB using autoradiography. Using spectrofluorimetry, Fung et al. (2001) demonstrated that a proportion of type I cells (40%) responded to ANG II with an increase in $[Ca^{2+}]_i$ that could be reversibly blocked by pre-treatment with losartan but not by PD-123319, an AT_2R antagonist. This study is consistent with immunohistochemical findings that localized AT_1R in some, but not all chemoreceptor lobules of the CB (Fung et al. 2001). The AT_1R co-localized with cells expressing the catecholamine biosynthetic enzyme, tyrosine hydroxylase (TH), a marker for CB type I cells (Fung et al. 2001). These findings are consistent with the notion that AT_1Rs expressed in type I cells mediate the carotid chemoreceptor response to ANG II. The activation of AT_1R stimulates the phospholipase C pathway in the plasma membrane and leads to the formation of 1,2-diacylglycerol and inositol-1,4,5-triphosphate (IP_3). IP_3 in turn stimulates Ca^{2+} release from the endoplasmic reticulum, leading to an elevation in intracellular Ca^{2+} (Balla et al. 1998). In addition to AT_1R, mRNA transcripts for AT_2R were also found in the CB (Fung et al. 2002). Although the activation of the AT_2R results in a wide spectrum of effects however, its role in the CB is unknown (Fung 2014). In a recent study, type II cells were shown to respond to ANG II (100 nM) with large rises in $[Ca^{2+}]_i$ (Tse et al. 2012). The effect of ANG II on the physiology of type II cells will be explored further in this thesis.

Paracrine interactions involving type II cells

ATP released from type I cells also has paracrine effects on the surrounding glia-like type II cells. In the central nervous system, glial cells play an active role in synapse integration and act as modulators of synaptic transmission (Allen and Barres 2009). Until recently, it remained unclear whether type II cells of the CB played an active role in chemotransduction and participated in synaptic activity. Their presumed passive role was challenged with the demonstration that they

expressed purinergic P2Y2 receptors, which are activated by ATP or UTP, leading to a rise in $[Ca^{2+}]_i$ (Xu et al. 2003). The authors raised the possibility that ATP-evoked Ca^{2+} responses in type II cells could mediate paracrine interactions in the CB since ATP is released from type I cells during hypoxia (Xu et al. 2003).

Many neuron-glial interactions are mediated by pannexin-1 (Panx) channels that secrete signalling molecules that are active at the synapse. For example, ATP release from cultured astrocytes via Panx-1 channels can activate purinergic signalling mechanisms (Iglesias et al. 2009). Using immunohistochemistry, Zhang et al. (2012) detected the expression of Panx-1 channels on type II cells, but not type I cells, in both tissue sections and CB cultures. Given these data, Zhang et al. (2012) hypothesized that activation of P2Y2 receptors on type II cells led to Panx-1 channel opening via a Ca^{2+}-dependent mechanism. They found that P2Y2 agonists, UTP and ATP, opened a non-selective cation channel, which was blocked by the Panx-1 antagonist, carbenoxolone (CBX). The authors demonstrated that the selective activation of P2Y2 receptors on type II cells led to release of ATP, which increased excitation of juxtaposed petrosal neurons (PN) via ligand-gated P2X2/3 receptors. They suggested that the type I, type II cells, and PN formed a tripartite synapse where ATP played a central role. Thus, ATP release from type I cells during chemoexcitation activated P2Y2 receptors on type II cells, leading to the opening of Panx-1 channels and further release of ATP (Fig. 1). This "ATP-induced ATP-release" mechanism amplifies the [ATP] in the vicinity of the sensory nerve terminals thereby enhancing afferent excitation (Zhang et al. 2012).

Pannexin-1 Channels

The pannexin (Panx) family consists of three members: Panx-1, 2, & 3, however, Panx-1 is the most ubiquitously expressed in the central nervous system and several organs (Barbe et al. 2006). The Panx family possesses a similar membrane topology to the gap-junction connexins, consisting of cytoplasmic N- and C-termini, four transmembrane domains, two cysteine-containing extracellular loops, and one cytoplasmic loop (Scemes et al. 2007). Unlike most connexins, Panx family members are capable of forming non-selective 'hemi-channels' with pores large enough to release molecules such as ATP, glutamate, and/or lactate under normal physiological conditions (Dubyak 2009; MacVicar and Thompson 2010). The presence of high levels of glycosylation in the extracellular loops of Panx proteins is thought to prevent intimate

contact with Panx proteins of neighbouring cells (Scemes et al. 2007). There is now considerable evidence that Panx-1 proteins form single membrane channels that connect the cytoplasm to the extracellular space (MacVicar and Thompson 2010).

Electrophysiological studies have determined some biophysical properties of Panx-1 channels. When Panx-1 channels were expressed in *Xenopus* oocytes, they induced a large whole cell membrane current and were initially reported to mediate intercellular communication (Bruzzone et al. 2003). The whole-cell current carried by Panx-1 channels is related to their large unitary conductance of ~70-550 pS, which may reflect different recording conditions, cell type properties, or sub-conductance states (Locovei et al. 2006; Kienitz et al. 2011; Ma et al. 2012). In some instances, Panx-1-mediated currents are outwardly rectifying and require depolarization for activation (Bruzzone et al. 2003; Ma et al. 2009). However, in most instances Panx-1 channels do not show a strong voltage-dependence typical of their counterpart i.e. connexin hemichannels (Bruzzone et al. 2003). Instead, Panx-1 currents recorded in response to ischemia, NMDAR stimulation, mechanical disruption, and metabotropic receptor activation display a current-voltage (I-V) relationship that is linear with a reversal potential close to zero (Bao et al. 2004; Thompson et al. 2006; Zoidl et al. 2007; Thompson et al. 2008; Thompson and MacVicar 2008; MacVicar and Thompson 2010; Zhang et al. 2012).

Panx-1 channels are known to participate in ATP-mediated modulations of neurotransmission in many different systems. In the central nervous system, for example, it was demonstrated that low glucose opened Panx-1 channels in rat hippocampal CA3 pyramidal neurons resulting in ATP release (Kawamura et al. 2010). This ATP was then degraded by ectonucleotidases into adenosine (Dunwiddie et al. 1997), leading to the opening of ATP-sensitive K^+ channels via A1 receptors and downregulation of neuronal activity (Kawamura et al. 2010). In mammalian taste buds, tastant molecules activate gustatory receptors leading to the opening of Panx-1 channels and subsequent ATP release. The released ATP then activates purinergic receptors on presynaptic cells that, in turn, release 5-HT to stimulate centrally- projecting sensory afferents (Huang et al. 2007; Romanov et al. 2007; Romanov et al. 2008). Erythrocytes are capable of releasing ATP via Panx-1 channels in response to low O_2 tension (Sridharan et al. 2010). ATP that is released from the erythrocytes binds to purinergic receptors on vascular endothelium, which results in the local generation of vasodilators including NO (Sprague et al. 1996). Finally, Panx1-

ATP signaling has also been implicated in the propagation of astrocytic Ca^{2+} wave signaling. Astrocytes participate in long-range signaling by releasing glutamate and ATP into the extracellular space (Bennett et al. 2003). ATP then activates metabotropic, purinergic P2Y receptors expressed by neighbouring astrocytic cells leading to an increase in IP_3 and subsequent intracellular Ca^{2+} release resulting in Panx1 activation. This process continues facilitating the propagation of a regenerative signal to neighbouring astrocytic cells in the form of a Ca^{2+} wave (Venance et al. 1997; Guthrie et al. 1999; Iglesias et al. 2009). The activation of Panx1 channels may require IP_3 and/or Ca^{2+}-dependent process forming a connection between activation of metabotropic receptors and the opening of Panx channels (Barbe et al. 2006).

Main technique used in this thesis

Ratiometric Ca^{2+} Imaging

Ratiometric Ca^{2+} imaging was used to monitor changes in $[Ca^{2+}]_i$ in type I and II cells given that Ca^{2+} is an important second messenger during chemotransduction in type I cells and glial signalling in type II cells. An advantage of this technique is it allows for the simultaneous recording of $[Ca^{2+}]_i$ in many different cells. This technique utilizes a fluorescent dye called fura-2, which is a Ca^{2+} ion selective chelator. When fura-2 binds to Ca^{2+}, the dye shifts its maximum excitation (absorption) spectrum from 380 nm to 340 nm. However, the maximum fluorescence emission (at ~ 510 nm) is relatively independent of the Ca^{2+} ion concentration. Therefore, the ratio of emission observed at 340 nm versus 380 nm excitation indicates the bound: free fura-2 giving a good measure of intracellular Ca^{2+} concentration (Tsien 1989). This ratio is obtained every 2 seconds throughout the entire experiment so that changes in $[Ca^{2+}]_i$ can be monitored in response to applied stimuli. The Grynkiewicz equation is used to convert ratio values into absolute values (Grynkeiwicz G. 1985). Ratiometric Ca^{2+} imaging is an effective method for measuring the $[Ca^{2+}]_i$ because it reduces the effects of uneven dye loading, variable cell thickness, loss/leakage of the dye, and photobleaching (Grynkeiwicz G. 1985; Tsien 1989).

Cells are loaded with the fluorescent dye by incubating them at 37°C in a dilute solution of cell permeable acetoxymethyl (AM) ester linked to fura-2 (fura-2/AM; 2.5 µM). Inside the cells fura-2/AM is cleaved by non-specific cytoplasmic esterases liberating the active Ca^{2+} sensitive dye. The active form of the dye is negatively charged and thus has a low leakage rate. As a result,

the dye accumulates in the cytosol where it can function as a Ca^{2+} ion indicator. This thesis primarily uses this technique to elucidate the paracrine function of type II cells.

Goals and organization of this thesis

The primary goal of this thesis was to provide a physiological characterization of rat CB glial-like type II cells and elucidate potential mechanisms by which they may participate in sensory processing. At the start of this project it was evident that type II cells were capable of responding to a host of CB neurotransmitters and neuromodulators with rises in intracellular Ca^{2+}. I chose to focus on two important CB neuromodulators, ANG II and 5-HT, based on the magnitude and frequency of the type II cell Ca^{2+} responses and their implication in CB pathophysiological conditions. To this end, I was interested in characterizing the paracrine function of type II cells, specifically looking at the signal transduction mechanisms mediating ANG II and 5-HT responses, as well as addressing type I and type II cell crosstalk.

The main body of this thesis is written in a 'sandwich' style and is composed of one published, peer-reviewed manuscript, and two manuscripts that are in preparation for submission.

The first data chapter, Chapter 2 (published in J. Physiol. 2014), explores the hypothesis that ANG II activates G-protein coupled receptors on type II cells resulting in the regulation of intracellular Ca^{2+}, leading to the opening of Panx-1 channels. I used ratiometric Ca^{2+} imaging to characterize and compare ANG II- and ATP/UTP-evoked $[Ca^{2+}]_i$ responses in type II cells versus type I cells. Electrophysiology (performed by Min Zhang) was used to investigate ANG II-evoked Panx1-currents. In Chapter 3, I showed that 5-HT exerts paracrine actions on type II cells via G-protein coupled receptors resulting in IP_3-mediated Ca^{2+} release from intracellular stores. In the final data chapter (Chapter 4), I explored whether a CB chemostimulus such as isohydric hypercapnia was capable of eliciting crosstalk between type I and type II cells. Finally, Chapter 5 presents a general discussion of the data from Chapters 2-4, possible future directions, and the physiological implications of this work.

Figure 1. Paracrine activation of glial-like type II cells of the rat carotid body: Role of ATP. During chemoexcitation, receptor type I cells release the neurotransmitter, ATP, leading to direct excitation of petrosal afferent terminals via P2X2/3Rs. This ATP that is released can also have paracrine effects by activating purinergic P2Y2 receptors located on type II cells leading to the release of even more ATP via pannexin-1 channels. This "ATP-induced ATP-release" mechanism amplifies the [ATP] in the vicinity of the sensory nerve terminals thereby enhancing afferent excitation. Zhang et al. (2012) proposed that the type I, type II, and petrosal afferent neuron formed a tripartite synapse where purinergic signaling was crucial. This thesis aims to elucidate the paracrine role of type II cells in carotid body chemosensing. Figure was adapted from Zhang et al. (2012).

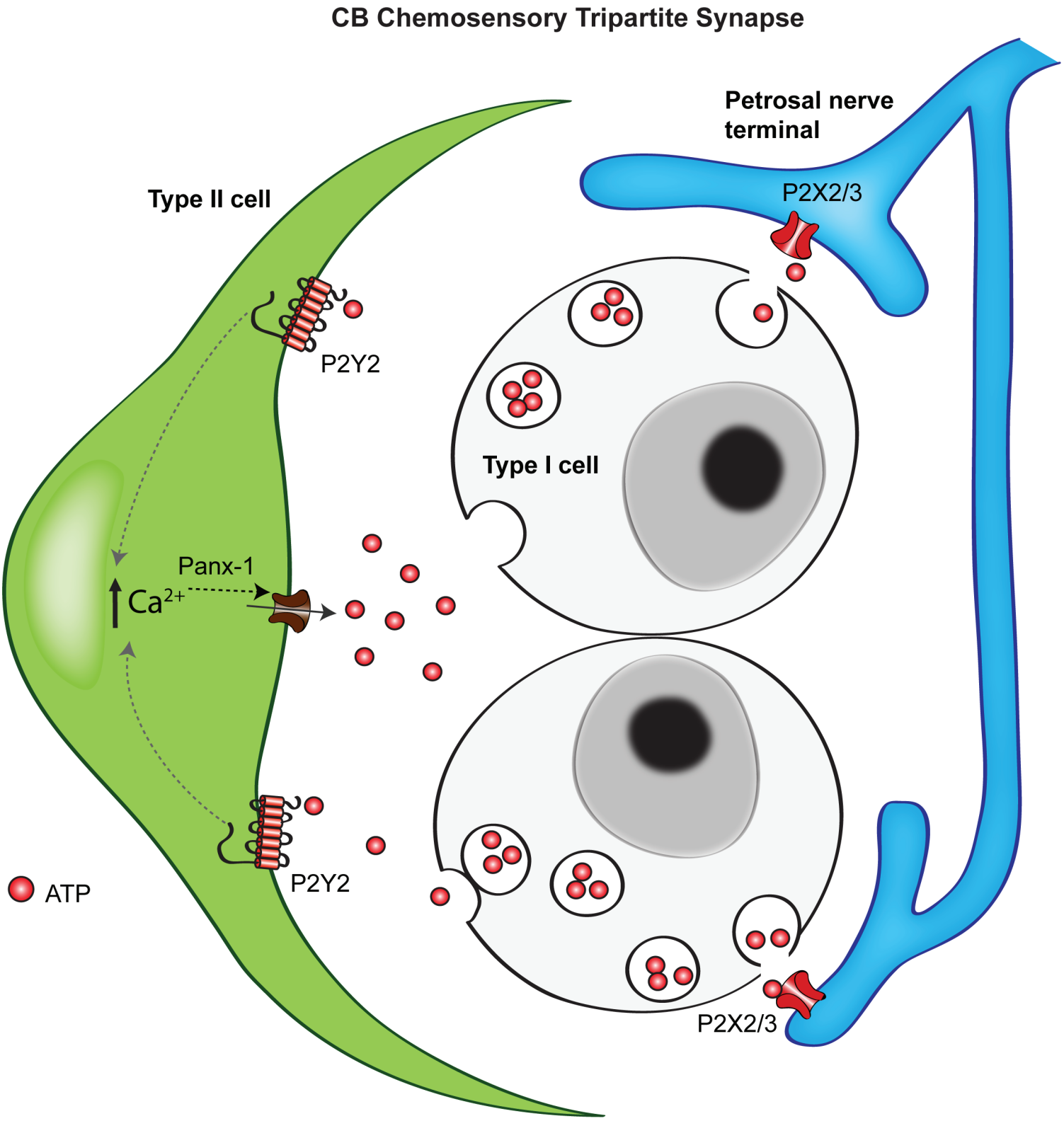
CB Chemosensory Tripartite Synapse
Petrosal nerve terminal
P2X2/3
Type II cell
P2Y2
Type I cell
Panx-1
Ca2+
P2Y2
ATP
P2X2/3

CHAPTER 2

Angiotensin II mobilizes intracellular calcium and activates pannexin-1 channels in rat carotid body type II cells via AT_1 receptors

The work in this chapter has been published as,

Murali, S., Zhang, M. and Nurse, C.A. (2014) *The Journal of Physiology*, **592**(21): 4747-4762

I initiated the study, prepared the cultures, carried out all the Ca^{2+} imaging experiments and data analysis and helped prepare the figures. Min Zhang performed all the electrophysiological experiments, analyzed the data, and helped prepare the figures. Colin A. Nurse was involved in the planning and designing of all the experiments, helped to interpret the data, and wrote the first draft of the manuscript. All authors approved the final version of this manuscript.

Abstract

A local angiotensin-generating system is present in the carotid body (CB) and increased angiotensin II (ANG II) signaling contributes to enhanced CB excitation in chronic heart failure (CHF) and after chronic or intermittent hypoxia. ANG II actions have thus far been attributed solely to stimulation of AT_1 receptors (AT_1R) on chemoreceptor type I cells. Here, we show that in dissociated rat CB cultures, ANG II also stimulates glial-like type II cells, identified by P2Y2-receptor induced intracellular Ca^{2+} elevation ($\Delta[Ca^{2+}]_i$). ANG II induced a dose-dependent (EC_{50} ~8 nM), robust $\Delta[Ca^{2+}]_i$ in type II cells that was reversibly abolished by the AT_1R blocker, losartan (1 µM). The ANG II-induced $\Delta[Ca^{2+}]_i$ persisted in Ca^{2+}-free medium but was sensitive to store depletion with cyclopiazonic acid (1 µM). Similar to P2Y2R agonists, ANG II (20-1000 nM) activated pannexin-1 (Panx-1) current that was reversibly abolished by carbenoxolone (5 µM). This current arose with a variable delay and was reversibly inhibited by losartan. Repeated application of ANG II often led to current run-down, attributable to AT_1R desensitization. When applied to the same cell the combined actions of ANG II and ATP on Panx-1 current were synergistic. Current induced by either ligand was inhibited by BAPTA-AM (1 µM), suggesting that intracellular Ca^{2+} signaling contributed to Panx-1 channel activation. Because open Panx-1 channels release ATP, a key CB excitatory neurotransmitter, it is plausible that paracrine stimulation of type II cells by ANG II contributes to enhanced CB excitability, especially in pathophysiological conditions such as CHF and sleep apnea.

Introduction

The chemosensory carotid body (CB) plays an important role in the reflex control of ventilation, as well as in the autonomic control of cardiovascular functions (Kumar and Prabhakar 2012). CB stimulation during hypoxemia enhances cardiovascular performance and protects vital organs via an increase in sympathetic efferent activity and circulatory levels of vasoactive hormones including the octapeptide, angiotensin II (ANG II) (Marshall 1994). ANG II is a key component of the renin-angiotensin system (RAS) that is involved in blood pressure regulation and fluid homeostasis. Interestingly, however, a locally-generating, renin-independent RAS system has been described in the CB (Lam and Leung 2002), and hyperactivity within this system is associated with several pathophysiological conditions such as chronic heart failure (CHF) and exposures to chronic and intermittent hypoxia (Ding et al. 2011; Kumar and Prabhakar 2012). Indeed, both systemic and tissue RAS are activated during hypoxia, leading to an increase in plasma ANG II (Zakheim et al. 1976), and infusion of exogenous ANG II in the peripheral circulation stimulates cardiorespiratory functions (Ohtake and Jennings 1993; Li et al. 2006). Moreover, superfusion of the isolated rat CB with ANG II *in vitro* increases afferent nerve discharge (Allen 1998), and perfusion of the vascularly- isolated rabbit carotid sinus region with ANG II augments the hypoxia-evoked CB chemoreceptor discharge (Li et al. 2006). Taken together, these studies indicate that ANG II signaling pathways play an important excitatory role in CB function.

Studies on the role of ANG II in the CB have so far focused on the chemoreceptor type I cells. Autoradiographic studies have revealed a high density of angiotensin AT_1 receptors (AT_1R) over type I cell clusters of the rat CB (Allen, 1998), and both angiotensin converting enzyme (ACE) and angiotensinogen (the precursor of ANG II) are expressed in type I cells (Leung *et al.*, 2000; Lam & Leung, 2003). While the role of endogenous ANG II in the normal CB function remains unclear (Li *et al.*, 2006), there is functional evidence that exogenous ANG II causes a concentration-dependent increase in intracellular Ca^{2+} in isolated rat type I cells via losartan-sensitive AT_1R (Fung *et al.*, 2001). Also, transcripts for both $AT_{1a}R$ and $AT_{1b}R$ have been detected by RT-PCR in whole rat CB and there is immunohistochemical evidence for AT_1R protein expression in type I cells of rat and rabbit CB (Fung *et al.*, 2001; Li *et al.*, 2006). Importantly, components of the local RAS system in the CB are regulated by different patterns of hypoxia

exposure, and the type I cells seem to be a major target (Leung *et al.*, 2000; Lam *et al.*, 2014). For example, in a recent study, exposure to chronic intermittent hypoxia led to upregulation of RAS components in the rat CB, in association with enhanced type I cell intracellular Ca^{2+} responses to exogenous ANG II (Lam *et al.*, 2014).

Recent evidence from this laboratory suggests that sensory processing in the rat CB may involve not only the chemoreceptor type I cells, which release the excitatory neurotransmitter ATP, but also adjacent sustentacular, 'glial-like' type II cells (Nurse 2010; Nurse and Piskuric 2012; Zhang et al. 2012). It was proposed that during chemotransduction paracrine stimulation of P2Y2 receptors on type II cells may help boost the ATP signal, and therefore CB excitation, by activating pannexin-1 (Panx-1) channels which act as conduits for ATP release (Zhang et al. 2012). P2Y2R stimulation leads to a rise in intracellular Ca^{2+} in type II cells (Xu et al. 2003; Zhang et al. 2012), and this is thought to be a trigger for Panx-1 channel opening. Interestingly, it was briefly noted in a recent review that type II cells may also respond to ANG II with a rise in intracellular Ca^{2+} (Tse et al. 2012), raising the possibility that ANG II actions in the CB may be more complex than initially thought. In the present study we extend this initial observation and show that ANG II, acting via AT_1R in type II cells, induces a robust increase in intracellular Ca^{2+}, which in turn leads to Panx-1 channel activation. These data strongly suggest that the excitatory role of ANG II in the CB likely involves dual actions at both type I and type II cells.

Methods

Ethical approval

All procedures for animal handling and tissue dissections were carried out according to the guidelines of the Canadian Council on Animal Care (CCAC) and institutional guidelines.

Cell cultures of dissociated rat carotid body

Carotid bifurcations from 9-14 day old rats (Wistar, Charles River, Quebec, Canada) were excised bilaterally, after the animals were first rendered unconscious by a blow to the back of the head, followed immediately by decapitation. The carotid bodies (CBs) were isolated from the surrounding tissue and dissociated cell cultures prepared according to established procedures, described in detail elsewhere (Zhong et al. 1997; Zhang et al. 2000). Briefly, the excised CBs were

incubated for 1 h at 37°C in a physiological salt solution containing 0.1% trypsin (Sigma-Aldrich, Oakville, Ontario, Canada) and 0.1% collagenase (Gibco, Grand Island, NY, USA), followed by mechanical dissociation and trituration. The dispersed cell suspension was allowed to adhere to the central wells of modified tissue culture dishes; the wells were pre-coated with a thin layer of Matrigel (BD Biosciences, Mississauga, Ontario, Canada). The cells were cultured in basic growth medium (BGM) consisting of F-12 nutrient medium supplemented with 10% fetal bovine serum, 1% penicillin-streptomycin, 1% glutamine, 0.3% glucose, and 3 μg ml^{-1} insulin, as in previous studies (Zhang et al. 2000; Zhang et al. 2012). To enrich for type II cells and facilitate recordings, the growth medium was switched after 12 hr to Cosmic-BGM containing: 50% BGM plus 50% of modified BGM where 10% fetal bovine serum was replaced with 5% fetal bovine serum and 5% Cosmic calf serum (Hyclone Laboratories Inc. Utah, USA). Our previous study demonstrated that there were no obvious differences in the properties of type II cells cultured in BGM vs. Cosmic-BGM (Zhang et al. 2012). In some experiments, phorbol 12-myristate 13-acetate (PMA; 100 nM) was added to the culture medium in attempts to minimize AT_1 receptor desensitization (Zhang et al. 1996). Cultures were grown at 37°C in a humidified atmosphere of 95% air-5% CO_2. Patch clamp recordings were usually carried out in 5-7 day-old CB cultures, which permitted optimal recordings from isolated 'solitary' type II cells; the Ca^{2+} imaging experiments were typically carried out after ~48 h in culture.

Intracellular Ca^{2+} measurements

Intracellular free Ca^{2+} concentration ($[Ca^{2+}]_i$) was monitored using the fluorescent Ca^{2+} indicator fura-2 AM (Molecular Probes, Eugene, OR, USA), as previously described (Piskuric and Nurse 2012; Zhang et al. 2012). Cells were loaded with 2.5 μM fura-2 AM diluted in standard bicarbonate-buffered solution (BBS) for 30 min at 37°C, and subsequently washed for ~15 min to remove free dye. The BBS used in Ca^{2+} imaging experiments had the following composition (in mM): $NaHCO_3$, 24; NaCl, 115; glucose, 5; KCl, 5; $CaCl_2$, 2 and $MgCl_2$, 1; the pH was maintained at ~7.4 by bubbling with a 5% CO_2-95% air mixture. Ratiometric Ca^{2+} imaging was performed using a Nikon Eclipse TE2000-U inverted microscope (Nikon, Mississauga, ON, Canada) equipped with a Lambda DG-4 ultra-high-speed wavelength changer (Sutter Instrument Co., Novato, CA, USA), a Hamamatsu OCRCA-ET digital CCD camera (Hamamatsu, Sewickley, PA, USA) and a Nikon S-Fluor 40x oild-immersion objective lens with a numerical aperture of 1.3.

Dual images at 340 nm and 380 nm excitation (510 emission) were acquired every 2 s, with an exposure time of 100-200 ms. Pseudocolour ratiometric data were obtained using Simple PCI software version 5.3. All experiments were performed at 35-37°C, and cells were continuously perfused with BBS to maintain an extracellular pH of ~ 7.4.

The imaging system was calibrated using the Fura-2 Calcium Imaging Calibration Kit from Molecular Probes (Cat. No. F-6774). Photometric data at 340 nm and 380 nm excitation (510 emission) were obtained for 11 buffers of known Ca^{2+} concentrations from Ca^{2+}-free (0 µM) to saturating Ca^{2+} (39 µM). After correcting for background fluorescence, these values were used to calculate the following ratios as follows: 'R' is the 510 nm emission intensity at 340 nm excitation to 510 nm emission intensity at 380 nm excitation; R_{min}, the ratio at zero free Ca^{2+}; $R_{max,}$ the ratio at saturating Ca^{2+}; and β, the fluorescence intensity with excitation at 380 nm for zero free Ca^{2+} (F_{380max}), to the fluorescence intensity at saturating free Ca^{2+} (F_{380min}). The intracellular free [Ca^{2+}] was obtained after substituting these ratios into the Grynkiewicz equation (Grynkiewicz et al. 1985) as follows:

$$[Ca^{2+}]_i = K_d \frac{[R - R_{\min}]}{[R_{\max} - R]} \beta$$

where R_{min} = 0.18, R_{max} = 7.81, β = 12.29, K_d = 225 nM and R is the ratio obtained during the experiment for a given cell. For most experiments statistical analysis was performed using Repeated Measures ANOVA with Tukey's Multiple Comparison Test *post hoc* test, as indicated in text.

Electrophysiology

Nystatin perforated-patch whole cell-recording was used to monitor ionic currents in type II cells as previously described (Zhang et al. 2000; Zhang et al. 2012). All recordings were carried out at ~35°C and the cells were perfused with standard BBS containing (in mM): $NaHCO_3$, 24; NaCl, 115; KCl, 5; $CaCl_2$, 2; $MgCl_2$, 1; glucose, 10, and sucrose, 12; at pH 7.4 maintained by bubbling with 5% CO_2-95% air mixture. The pipette solution contained (mM): potassium gluconate, 115; KCl, 25; NaCl, 5; $CaCl_2$, 1; Hepes, 10, and nystatin 200 µg.ml^{-1}; at pH 7.2. Agonists (e.g. ANG II, ATP) were applied by a 'fast perfusion' system utilizing a double-barreled pipette assembly as previously described (Zhong et al. 1997; Zhang et al. 2000; Zhang et al. 2012). Current measurements under voltage clamp were obtained the aid of a MultiClamp 700A patch

clamp amplifier and a Digidata 1322A analog-to-digital converter (Axon Instruments Inc., Union City, CA, USA), and the data stored on a personal computer. Data acquisition and analysis were performed using pCLAMP software (version 9.0; Axon Instruments Inc.). Because of the desensitization properties of the AT_1 receptor and long latency of the ANG II-induced current, we used a repeated ramp protocol to obtain an estimate of the reversal potential of $I_{ANG\ II}$. Starting with a holding potential of -60 mV, the voltage was ramped every 6 sec from -40 to +20 mV over a period of 700 msec. The ramp protocol was first applied just before ANG II exposure (to obtain the control I-V plot) and then the cycle was repeated at 6 sec intervals throughout the ANG II exposure period. The ANG II -induced I-V plot during the peak or plateau phase of the current was selected and then subtracted from the initial control plot so as to obtain the $I_{ANG\ II}$ difference current and an estimate of the reversal potential. For multiple comparisons of ionic currents or current density (pA/pF; obtained by dividing peak current by whole cell capacitance), ANOVA was used and the level of significance was set at $P < 0.05$.

Reagents and drugs

The following reagents and drugs were obtained from Sigma-Aldrich (Oakville, ON): ATP, UTP, angiotensin II (ANG II), losartan potassium, and carbenoxolone (CBX).

Results

The majority of the experiments described below were carried out on isolated 'solitary' type II cells to eliminate or minimize secondary or indirect effects from neighboring type I cells. Such effects may arise within type I cell clusters as a result of the known stimulatory actions of ANG II on type I cells (Fung et al. 2001; Ding et al. 2011). A few experiments were done on type I cells, present within characteristic clusters that are readily identified in these cultures under phase contrast microscopy (Nurse 2010). In Ca^{2+} imaging experiments, type II cells were routinely identified by the presence of a robust increase in intracellular Ca^{2+} ($\Delta[Ca^{2+}]_i$) during exposure to the selective P2Y2 receptor agonist, UTP (Xu et al. 2003; Piskuric and Nurse 2012; Tse et al. 2012; Zhang et al. 2012). The absence of cross-talk from type I to type II cells was confirmed by the lack of a $\Delta[Ca^{2+}]_i$ response in type II cells during perfusion with the depolarizing stimulus high K^+ (30 mM), which stimulates neurosecretion from type I cells in similar CB cultures (Buttigieg

and Nurse 2004; Livermore and Nurse 2013). The 'n' values reported in text refer to the number of culture dishes sampled, where the Ca^{2+} response of each dish was taken as the mean peak $\Delta[Ca^{2+}]_i$ value obtained from 10-15 randomly chosen cells. Cells with basal $[Ca^{2+}]_i$ greater than 200 nM, or cells whose baseline exhibited continuous ramping during the experiment, were excluded from analyses. In voltage clamp experiments, solitary type II cells were first 'tentatively' identified by their elongated morphology, and subsequently confirmed by their characteristic electrophysiological profile, including the presence of activatable Panx-1 currents (Duchen et al. 1988; Zhang et al. 2012).

Angiotensin II induces a rise in intracellular Ca^{2+} in type II cells via AT_1 receptors: comparison with type I cells

As exemplified in Fig. 1A, perfusion of ~2 day-old CB cultures with ANG II led to a dose-dependent increase in intracellular Ca^{2+} ($\Delta[Ca^{2+}]_i$) in type II cells, identified by the presence of a positive $\Delta[Ca^{2+}]_i$ response to UTP (100 µM), but not high K^+. In one experimental series, the majority of UTP-sensitive type II cells (401/537; ~75%) were also sensitive to ANG II. A plot of the dose-response curve for ANG II versus $\Delta[Ca^{2+}]_i$ indicated an EC_{50} of approximately 8 nM, a value comparable to that previously reported for ANG II acting at AT_1 receptors in rat podocytes (EC_{50} =3 nM; (Henger et al. 1997)). Repeated application of a high dose of ANG II (100 nM) tended to produce diminishing $\Delta[Ca^{2+}]_i$ responses in a given cell (Fig. 1B), probably due to receptor desensitization which is a well- known property of AT_1 receptors (Zhang et al. 1996; Guo et al. 2001). A histogram showing the time course of this desensitization phenomenon is shown in Fig. 1D.

Previous studies in rat CB using western blot, *in situ* hybridization, RT-PCR and immunohistochemical techniques revealed high expression of AT_1 receptors (AT_1R), localized predominantly to type I cells (Leung et al. 2000; Fung et al. 2001; Lam and Leung 2002). It was therefore of interest to determine whether or not the ANG II-induced $\Delta[Ca^{2+}]_i$ responses in type II cells were also mediated by AT_1 receptors. First, we confirmed that ANG II elicited a rise in $[Ca^{2+}]_i$ in type I cells present in the same cultures (Fig. 2A). Notably, a comparison of the relative magnitude of the peak $\Delta[Ca^{2+}]_i$ evoked by the same dose of ANG II revealed that type II cells generated a much more robust Ca^{2+} response than type I cells (Fig. 2B). The mean $\Delta[Ca^{2+}]_i$ induced

by 100 nM ANG II was ~ 95 nM in type II cells compared to ~ 32 nM for type I cells; the latter value was comparable to that previously reported for rat type I cells (~20 nM; (Fung et al. 2001)). In a few cases, we confirmed that the type II cell responses did not arise secondarily from ANG II-induced release of ATP from type I cells using the P2Y2R blocker, suramin; the mean (± s.e.m.) $\Delta[Ca^{2+}]_i$ response was 76.6 ± 12.8 nM for ANG II (100 nM), 59.5 ± 12.2 nM for ANG II plus 100 μM suramin, and 68.6 ± 12.4 nM for ANG II after washout of suramin (n =3 dishes; p> 0.05).

The ANG II-induced rise in $\Delta[Ca^{2+}]_i$ in type II cells was completely inhibited by the specific AT_1R blocker, losartan (1 μM), and the effect was reversible (Fig. 2C); a scatter plot of $\Delta[Ca^{2+}]_i$ responses before, during, after losartan is shown in Fig. 2D. Losartan significantly reduced the proportion of ANG II-responsive type II cells by 95% (only 30/545 cells that initially responded to ANG II did so in the presence of losartan); also, the mean $\Delta[Ca^{2+}]_i$ response was reduced by 97% (mean $\Delta[Ca^{2+}]_i$ before and during losartan was 101 ± 9.3 nM vs. 3.1 ± 1.8 nM, n = 10 dishes; Repeated Measures ANOVA with Tukey's Multiple Comparison Test *post hoc* test, $p < 0.05$). After wash-out of losartan there was an ~80% recovery of the original ANG II-evoked Ca^{2+} response. We also confirmed that the ANG II-induced response in type I cells was also inhibited by losartan (Fig. 2C), as previously reported (Fung et al. 2001). Taken together these data imply that functional AT_1R are expressed in both type I and type II cells of rat CB.

Angiotensin II-induced Ca^{2+} transients in type II cells originate mainly from intracellular stores

In general, ANG II- AT_1R signaling is mediated either via entry of extracellular Ca^{2+} through Ca^{2+} channels or activation of the phosphotidylinositol- IP_3 pathway coupled to Ca^{2+} release from internal stores (Balla et al. 1991; Henger et al. 1997; Goette and Lendeckel 2008; Ding et al. 2011). To determine whether the ANG II-induced $\Delta[Ca^{2+}]_i$ in type II cells arose principally from entry of extracellular Ca^{2+}, we first monitored Ca^{2+} transients in nominally Ca^{2+}-free medium. As shown in Fig. 3A, Ca^{2+} transients evoked by 100 nM ANG II were not significantly altered in Ca^{2+}-free medium, consistent with a predominant release from intracellular stores; mean ± s.e.m. $\Delta[Ca^{2+}]_i$ in calcium-free solution was 80.6 ± 15 nM, whereas the mean ± s.e.m. in normal calcium was 105.0 ± 17 nM (n = 9 dishes; Mann Whitney test, p = 0.3). In order to avoid the effect of desensitization, the first ANG II-evoked Ca^{2+} responses were compared either

in the presence or absence of extracellular Ca^{2+}. Fig. 3B illustrates this comparison as a scatter plot of the ANG II-induced $\Delta[Ca^{2+}]_i$ in type II cells in normal (2 mM) and zero Ca^{2+} solutions. To confirm a major role for Ca^{2+} release from intracellular stores, we monitored Ca^{2+} transients in presence of the store-depleting agent, cyclopiazonic acid (CPA; 10 µM). As shown in Fig. 3C, D, the ANG II-induced $\Delta[Ca^{2+}]_i$ was markedly inhibited by CPA, suggesting that Ca^{2+} release from stores was a major contributor to ANG II-AT_1R signaling in type II cells; the mean ± s.e.m $\Delta[Ca^{2+}]_i$ in control vs CPA-containing solutions was 88 ± 9.7 vs. 13.5 ± 2.0 nM; n = 12 dishes; Friedman Test with Dunn's Multiple Comparison Test, $p < 0.05$).

Angiotensin II-induced signaling activates pannexin-1 currents in type II cells

We next determined whether or not ANG II -induced signaling led to the activation of Panx-1 currents in type II cells, as previously demonstrated for ATP acting via P2Y2 receptors (Zhang et al. 2012). As exemplified in Fig. 4A, ANG II caused a dose-dependent activation of Panx-1 currents that arose with a variable delay. A plot of peak Panx-1 current density (pA/pF; at -60 mV holding potential) vs ANG II concentration over the dose range 20 -1000 nM is shown in Fig. 4B. Often, the ANG II-evoked Panx-1 current showed more than one plateau or multiple peaks (Figs. 4A, 5B); in such cases the largest peak value seen in the inward current trace was used in constructing the dose-response curve. The variability in the delay of current activation versus ANG II concentration is plotted in Fig. 4C, and is reminiscent of a similar observation noted during P2Y2R-induced activation of Panx-1 currents in these cells (Zhang et al. 2012). Panx-1 currents in type II cells could not be activated at a concentration of 10 nM ANG II or less (n = 10), at least within 100 sec of exposure.

To confirm that the ANG II-activated current ($I_{ANG\ II}$) displayed the expected properties of Panx-1 currents we first measured the reversal potential (E_{rev}). In our previous study, P2Y2R stimulation activated Panx-1 current with a E_{rev} near ~ 0 mV (Zhang et al. 2012). Because of current run-down observed during repeated ANG II applications due to receptor desensitization (see below), as well as variability in response latency, we used a repeated ramp protocol to estimate E_{rev} of the ANG II difference current ($I_{ANG\ II}$) as described in Methods. As exemplified in Fig. 4D1 for a type II cell exposed to 100 nM ANG II, E_{rev} of $I_{ANG\ II}$ was ~ -6 mV; the mean E_{rev} for a group of 5 cells was -5.7 ± 2.6 mV, consistent with opening of non-selective ion channels. Indeed, when

both ANG II and ATP were tested on the same cell, as exemplified in Figs. 4D1,D2, E_{rev} was indistinguishable for the two agonists, even though each acted at its own distinct receptor; for ATP the mean E_{rev} was -3.2 ± 1.8 mV (n =5) .

Final validation that ANG II activated Panx-1 currents in type II cells was obtained using the selective blocker carbenoxolone (CBX) at low concentrations (5 µM), thought to block Panx-1 channels but not gap junctional channels (Barbe et al. 2006; Ma et al. 2009). As in our previous study using P2Y2R agonists (Zhang et al. 2012), the ANG II-induced inward current at -60 mV holding potential was reversibly abolished by 5 µM CBX (Fig. 5A,C; n= 5), consistent with Panx-1 channels as the current carrier.

Pannexin-1 current activation by angiotensin II is mediated via AT_1 receptors in type II cells

Given that AT_1R is the major ANG II receptor subtype expressed in the rat CB (Leung et al. 2000; Fung et al. 2001; Lam and Leung 2002), and that AT_1R mediated the ANG II -induced rise in $[Ca^{2+}]_i$ in type II cells (see above), we investigated whether Panx-1 current activation was also mediated via AT_1R using the selective blocker, losartan (de Gasparo et al. 2000). As exemplified in Fig. 5B, the ANG II-induced Panx-1 current in type II cells was reversibly abolished by losartan (1 µM); a histogram of the ANG II-induced Panx-1 current density (pA/pF; at -60 mV holding potential) for a group of 4 cells before, during, and after exposure to 1 µM losartan is shown in Fig. 5D.

Consistent with the well-known desensitization properties of the AT_1R (see above), repeated application of ANG II to the same cell routinely resulted in Panx-1 current run-down, as exemplified in Fig. 6A. The time course of decay of $I_{ANG\ II}$ current density (at -60 mV holding potential) during repeated applications of ANG II over a 20 min period is shown in Fig. 6C. This contrasts with the effect of ATP acting via P2Y2R on Panx-1 current which typically remained stable during repeated applications of ATP over the same time period (Fig. 6B, C). Current run-down was not due to 'inactivated' or non-functional Panx-1 channels because the current could be promptly restored (within 2 min), soon after run-down induced by high doses of ANG II (100 nM-1 µM), by simply applying ATP to the same cell (e.g. Fig. 6D; n = 4 cells). Taken together, these data indicate that both the ANG II-induced rise in $[Ca^{2+}]_i$ and Panx-1 current activation are mediated via functional AT_1R expressed in type II cells.

Combined actions of angiotensin II and ATP lead to a synergistic activation of pannexin-1 current in type II cells

Over the course of this study it was routinely observed that solitary type II cells often responded to both ATP/UTP and ANG II with a rise in intracellular Ca^{2+} or activation of Panx-1 current. While ANG II in the pM range can produce physiological effects at AT_1R in the intact CB (Allen 1998; Peng et al. 2011), relatively higher doses ($\geq$ 20 nM) were required to activate Panx-1 current, at least within 100 sec of application. Given that during CB chemoexcitation, it is unlikely ANG II will be acting alone, we wondered whether its actions might be complementary to those of other excitatory mediators such as ATP. Indeed, we found that doses of ANG II and ATP (below the EC_{50} and near the foot of their respective dose-response curves) interacted synergistically when applied to the same cell. First, as exemplified in Fig. 7A, when a near-threshold dose of ATP (10 µM) sufficient to activate the Panx-1 current was combined with a 'subthreshold' dose of ANG II (10 nM) that failed to do so in a given cell, there was a >1.5x potentiation of the ATP-evoked response (n=3 cells). Second, whereas each of the doses 10 µM ATP and 20 nM ANG II activated a detectable Panx-1 current when applied separately to the same type II cell, the current was markedly potentiated when the same doses were applied together (Fig. 7B). A histogram showing mean Panx-1 current density (pA/pF) for a group of 5 cells exposed to 10 µM ATP and 20 nM ANG II separately, and then in combination, is shown in Fig. 7C. These data suggest the current response from the combined application was more-than-additive, and was ~1.6x larger than the sum of the two separate applications ($p< 0.05$; Fig. 7C). Interestingly, during the combined application the latency of the current response was significantly shorter than the minimum observed for either ligand acting alone (Fig. 7D; $p <0.01$).

Angiotensin II- and ATP-induced pannexin-1 current in type II cells requires a rise in intracellular Ca^{2+}

In oocyte expression systems, cytoplasmic Ca^{2+} in the micromolar range was sufficient to activate human Panx-1 channels (Locovei et al. 2006), however, the requirement for a rise in $[Ca^{2+}]_i$ has been questioned in another study (Ma et al. 2009). To test whether or not the rise in

cytoplasmic Ca^{2+} elicited in type II cells by ANG II and ATP (Xu et al. 2003; Zhang et al. 2012) was necessary for activation of the Panx-1 current, we used the membrane permeable Ca^{2+} chelator, BAPTA-AM (1 μM). As exemplified in Figs. 8 A,B, the Panx-1 current induced by either ANG II or ATP was reversibly inhibited by BAPTA; pooled data from cells exposed to ANG II or ATP are summarized in Fig. 8C,D, respectively. Taken together, these data support the notion that a rise in cytoplasmic Ca^{2+} is required for Panx-1 channel activation by both agonists.

Discussion

The presence of a locally-generating, renin-independent, ANG II system was identified in the carotid body (CB) many years ago and has generated much interest and speculation about its physiological function (Lam and Leung 2002; Li et al. 2007; Ding et al. 2011; Peng et al. 2011). The present study has highlighted a novel aspect of ANG II signaling in the rat CB involving sustentacular, glial-like type II cells. Prior to this study, the focus of ANG II actions was understandably centered on CB chemoreceptor type I cells, because they expressed functional AT_1 receptors (AT_1R), as well the biosynthetic machinery for ANG II synthesis (Allen 1998; Fung et al. 2001; Lam and Leung 2002; Ding et al. 2011). However, we provide strong evidence that type II cells, which are normally found in intimate association with type I cells in the CB, are also likely to be an important target for the actions of ANG II. In particular, we show that ANG II acting via losartan-sensitive AT_1R induces a robust increase in intracellular Ca^{2+} in isolated type II cells; this in turn leads to the activation of Panx-1 channels, which we recently showed act as conduits for ATP release from these cells (Zhang et al. 2012). We are unaware of any other studies demonstrating a link between ANG II signaling and the activation of Panx-1 channels; however, these channels are known to facilitate release of ATP as well as other chemical signals from a variety of cell types (MacVicar and Thompson 2010; Sridharan et al. 2010). Previous immunohistochemical studies reported the presence of positive AT_1R-immunoreactivity in CB type I cells, however, these studies did not include tests for whether or not type II cells were also immuno-positive (Leung et al. 2000; Li et al. 2006). We did not attempt to co-localize AT_1R immunoreactivity with known type II cell markers because as many as six commercially available AT_1R antibodies have recently been found to be non-specific, when tested on AT_1 knock-out animals (Benicky et al. 2012). We also confirmed the previous findings of Fung *et al*. (2001)

indicating that ANG II stimulates a rise in intracellular Ca^{2+} in rat type I cells via AT_1R; however, these Ca^{2+} signals tended to be much smaller in magnitude than those recorded in type II cells. In the latter study, the source of the AT_1R -mediated rise in intracellular Ca^{2+} in rat type I cells was not identified (Fung *et al*., 2001). However, in rabbit type I cells ANG II has been reported to exert an excitatory effect mediated via AT_1R and activation of NADPH oxidase, leading to inhibition of various K^+ channels, membrane depolarization, and voltage-gated Ca^{2+} entry (Schultz, 2011). These data suggest that during AT_1R stimulation the source of the $[Ca^{2+}]_i$ rise in type I cells is extracellular, in contrast to type II cells where the source is intracellular (this study). Also, as discussed below, the ANG II- AT_1R signaling pathway in type II cells leads to the activation pannexin-1, non-selective, ion channels. This contrasts with the inhibition of voltage-gated K^+ ($I_{K(V)}$) channels seen in type I cells (Schultz & Li, 2007; Schultz, 2011), which appear to lack pannexin-1 channel expression at least in the rat (Zhang *et al*., 2012).

Angiotensin II-AT_1R-Pannexin 1 signal transduction pathway in type II cells

Ratiometric fura-2 imaging experiments revealed that ANG II elicited a rise in intracellular Ca^{2+} ($\Delta[Ca^{2+}]_i$) in type II cells that persisted in Ca^{2+}-free medium, but was sensitive to intracellular store depletion with cyclopiazonic acid. The principal ANG II receptor subtype involved was the AT_1R because the $\Delta[Ca^{2+}]_i$ responses were reversibly abolished by the specific AT_1R blocker, losartan (de Gasparo et al. 2000). These observations suggest ANG II- AT_1R signaling in type II cells occurs mainly via the ubiquitous G-protein coupled, phosphatidyl inositol -IP_3 pathway, whereby activation of phospholipase C leads to the generation of IP_3 which in turn triggers Ca^{2+} release from the endoplasmic reticulum (Guo et al. 2001). The AT_1 receptors are known to undergo rapid internalization and desensitization upon repeated stimulation (Zhang et al. 1996; Guo et al. 2001), and this property was the likely basis for the progressive decrease in $\Delta[Ca^{2+}]_i$ responses seen with repetitive ANG II applications. The estimated EC_{50} for the ANG II-AT_1R evoked Ca^{2+} responses was ~8 nM, a value comparable to that seen in other cell types with this technique (Henger et al. 1997); in competitive binding studies, the IC_{50} for ANG II at AT_1R was reported to be ~8 nM (Bosnyak et al. 2011).

Perforated-patch, whole-cell recordings from type II cells revealed that ANG II caused a dose-dependent activation of Panx-1 currents with a reversal potential near 0 mV, consistent with

the opening of non-selective ion channels. As expected for the involvement of AT_1R, these currents were reversibly blocked by losartan (1 μM). Panx-1 current run-down was commonly observed during repeated ANG II applications, probably because of AT_1R desensitization (see above); however, for reasons that are presently unclear current run-down was not obvious immediately after recovery from AT_1R blockade by losartan. Also, because the current could be robustly restored immediately after ANG II -induced run-down by simply activating a different (ATP-P2Y2R) signaling pathway, loss of Panx-1 channel function could not account for the run-down. The latency of ANG II-induced Panx-1 current in 'solitary' type II cells was quite variable, typically >25 sec, and depended on agonist concentration. During AT_1R signal transduction cascades, the ANG II -induced signal can arise with latencies that vary from seconds in the case of PLC-IP_3 -mediated release of Ca^{2+} from stores, to minutes in cases where other downstream signals (e.g. mitogen-activated protein kinase) are activated (Guo et al. 2001). In our previous studies using ATP (10 - 250 μM) to stimulate P2Y2R, the latency of Panx- current varied typically between 6 and 14 sec for 'solitary' type II cells; by contrast, for type II cells present within chemoreceptor clusters, the latency was much shorter (< 3 sec) (Zhang et al. 2012). In present study, the experiments were done on 'solitary' type II cells where coupling within the signaling pathway was probably less efficient than in cell clusters, perhaps contributing to the longer latencies. An interesting observation was that the latency of Panx-1 current activation by ANG II in 'solitary' type II cells appeared consistently shorter (<12 sec) if the cells were first 'primed' by exposure to a P2Y2R agonist such as ATP. Further studies are required to clarify the underlying mechanism.

Physiological significance and clinical relevance

Using immunofluorescence, we previously demonstrated that Panx-1 channels are expressed in GFAP-positive type II cells in tissue sections of rat carotid body (CB) *in situ*, and in cultured dissociated CB cells (Zhang et al. 2012). Moreover, we showed that when these channels were activated in isolated type II cells using the P2Y2R agonist UTP, they acted as conduits for release of ATP, a key CB excitatory neurotransmitter (Nurse 2010; Nurse and Piskuric 2012; Zhang et al. 2012). In light of these findings, a plausible physiological role of ANG II signaling in type II cells is to stimulate Panx-1 channel opening and consequently ATP release, which could

serve as a boost for CB excitation. The EC_{50} for ANG II as determined by Panx-1 current activation was ~76 nM, a value ~ 9x higher than that observed using Ca^{2+} imaging. In fact, Panx-1 currents were not detectable (at least with a latency <100 sec) at 10 nM ANG II which is near the EC_{50} value based on intracellular Ca^{2+} measurements. These data suggest that a threshold level of intracellular Ca^{2+} may need to be reached for Panx-1 channel activation, or some other lower affinity process needs to be activated in parallel with the rise in Ca^{2+}, or combinations of these. It is arguable whether an increase in intracellular Ca^{2+} is a general pre-requisite for Panx-1 channel activation in different cell types (Locovei et al. 2006; Ma et al. 2009). However, in the present study the necessity for a rise in intracellular Ca^{2+} was demonstrated in experiments where Panx-1 currents were almost completely and reversibly blocked in the presence of the membrane permeable Ca^{2+} chelator, BAPTA-AM (1 μM). Whether intracellular Ca^{2+} acts by binding directly to the Panx-1 channel in type II cells, or via some other (e.g. PKC) pathway, remains to be determined. Nonetheless, we cannot rule out the possibility that additional converging signaling pathways, for example activation of Src family kinases (Weilinger et al. 2012), are required for Panx-1 current activation.

The role of the local ANG II-generating system in normal CB function remains unclear. However, there are several pathophysiological conditions where upregulation of this local system occurs. These include conditions where animals are exposed to chronic or intermittent hypoxia (Leung et al. 2000; Lam and Leung 2003; Lam et al. 2014), and in patients or animal models experiencing chronic heart failure (CHF) (Li et al. 2007; Ding et al. 2011). After exposure to chronic hypoxia, AT_1R mRNA and protein expression increases in the rat CB and there is enhanced AT_1R-mediated excitation of CB afferent activity (Leung et al. 2000). In the case of chronic intermittent hypoxia (CIH), a condition associated with sleep-disordered breathing, there is increased angiotensinogen, AT_1R mRNA, and AT_1R protein expression in the CB, as well as increased type I cell Ca^{2+} responses to exogenous ANG II (Lam et al. 2014). In CHF rabbits, but not sham controls, pharmacological inhibition of AT_1R decreases CB chemoreceptor discharge to hypoxia, in association with increased hypoxic sensitivity of type I cells (Li et al. 2006; Li et al. 2007; Ding et al. 2011). In light of the accompanying increased local CB and systemic levels of ANG II in CHF (Ding et al. 2011), it is plausible that ANG II-AT_1R signaling via type II cells may contribute to sensitization of CB sensory discharge via Ca^{2+}-dependent activation of Panx-1 channels and release of ATP. Indeed, this ATP release from type II cells may be further facilitated

by the observed synergistic interactions between P2Y2R and AT_1R signal transduction pathways. In particular, we found that when low doses (< EC_{50}) of ANG II and ATP were applied to the same type II cell there was a synergistic enhancement of Panx-1 currents, which would be expected to cause further augmentation of ATP release and sensitization of CB function. In CHF, this increased CB sensitization appears maladaptive as it serves to exacerbate the tonic sympathetic hyperactivity associated the disease progression (Li et al. 2007; Ding et al. 2011).

In conclusion, the present study has revealed a novel Ang II-AT_1R signaling pathway in glial-like type II cells of the rat carotid body leading to activation of Panx-1 channels, which act as conduits for release of ATP (Nurse and Piskuric 2012; Nurse 2014). Given that ATP is a key excitatory CB neurotransmitter, we propose that activation of this signaling pathway has the potential to contribute to CB excitation. This is especially likely to occur in pathophysiological conditions of exaggerated CB excitation such as chronic heart failure and sleep-disordered breathing, where components of the local ANG II-AT_1R system are upregulated (Lam et al. 2004; Ding et al. 2011; Kumar and Prabhakar 2012; Lam et al. 2014).

Acknowledgements

This work was supported by a Discovery grant from the Natural Sciences and Engineering Research Council of Canada (NSERC) to C.A.N. S.M. currently holds a CIHR/NSERC CGS-M graduate scholarship award. We thank Cathy Vollmer and Dr. Nikol Piskuric for their assistance.

Figure 1. Effects of angiotensin II (ANG II) on intracellular calcium transients in type II cells. The effects of increasing doses of ANG II (10, 50, 100 nM) on intracellular Ca^{2+} concentration ($[Ca^{2+}]_i$) in a type II cell is shown in A; for type II cell identification note typical increase in Ca^{2+} ($\Delta[Ca^{2+}]_i$) to UTP (100 µM), but not high K^+ (30 mM). B. Dose-response relation for ANG II -induced $\Delta[Ca^{2+}]_i$ in type II cells; a fit of the dose-response curve with the Hill equation yielded an EC_{50} = 7.7 nM (n=15 dishes). C. Decrease in $[Ca^{2+}]_i$ responses in type II cells with repeated exposures to 100 nM ANG II, attributable to receptor desensitization. D. Time-course of the reduction in $\Delta[Ca^{2+}]_i$ responses in type II cells after 1, 6, and 11 min exposure to 100 nM ANG II; * indicates $p< 0.05$; ** $p< 0.01$; ***$p< 0.001$, Repeated Measures ANOVA with Tukey's Multiple Comparison Test *post hoc* test.

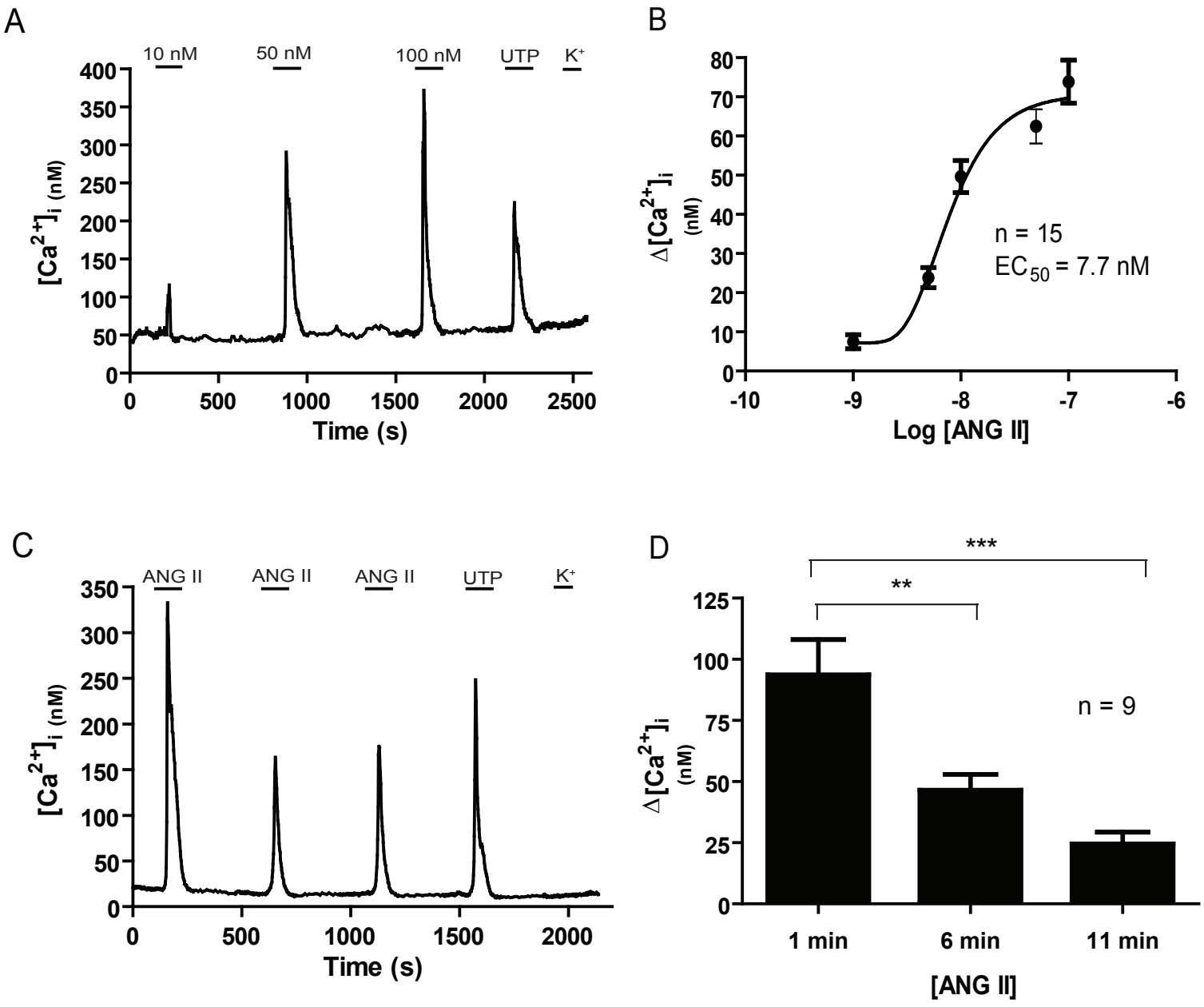
A
10 nM
50 nM
100 nM
UTP
K+
[Ca2+]i (nM)
Time (s)
B
Δ[Ca2+]i (nM)
n = 15
EC50 = 7.7 nM
Log [ANG II]
C
ANG II
ANG II
ANG II
UTP
K+
[Ca2+]i (nM)
Time (s)
D
***
**
n = 9
Δ[Ca2+]i (nM)
1 min
6 min
11 min
[ANG II]

Figure 2. Comparison of the effects of angiotensin II (ANG II) in type II versus type I cells and role of AT_1 receptors. In A, ANG II (100 nM) causes a rise in intracellular Ca^{2+} concentration ($[Ca^{2+}]_i$) in both a type II cell and a type I cell in the same culture; note the type II cell, which responds to UTP but not high K^+, elicits a more robust Ca^{2+} response than the type I cell, which responds to high K^+ but not UTP. Comparison of mean ± s.e.m. $[Ca^{2+}]_i$ responses in type II versus type I cells after exposure to 100 nM ANG II is shown in B (n=9 dishes; 10-15 cells sampled per dish). In C, the ANG II-induced rise in $[Ca^{2+}]_i$ is reversibly abolished by the selective AT_1 receptor blocker, losartan (1 μM), in both the type II cell and a type I cell within the cluster identified in D. Summary data from 10 dishes are shown in E. *indicates $p< 0.05$; ** $p< 0.01$; ***$p< 0.001$.

FIGURE 2

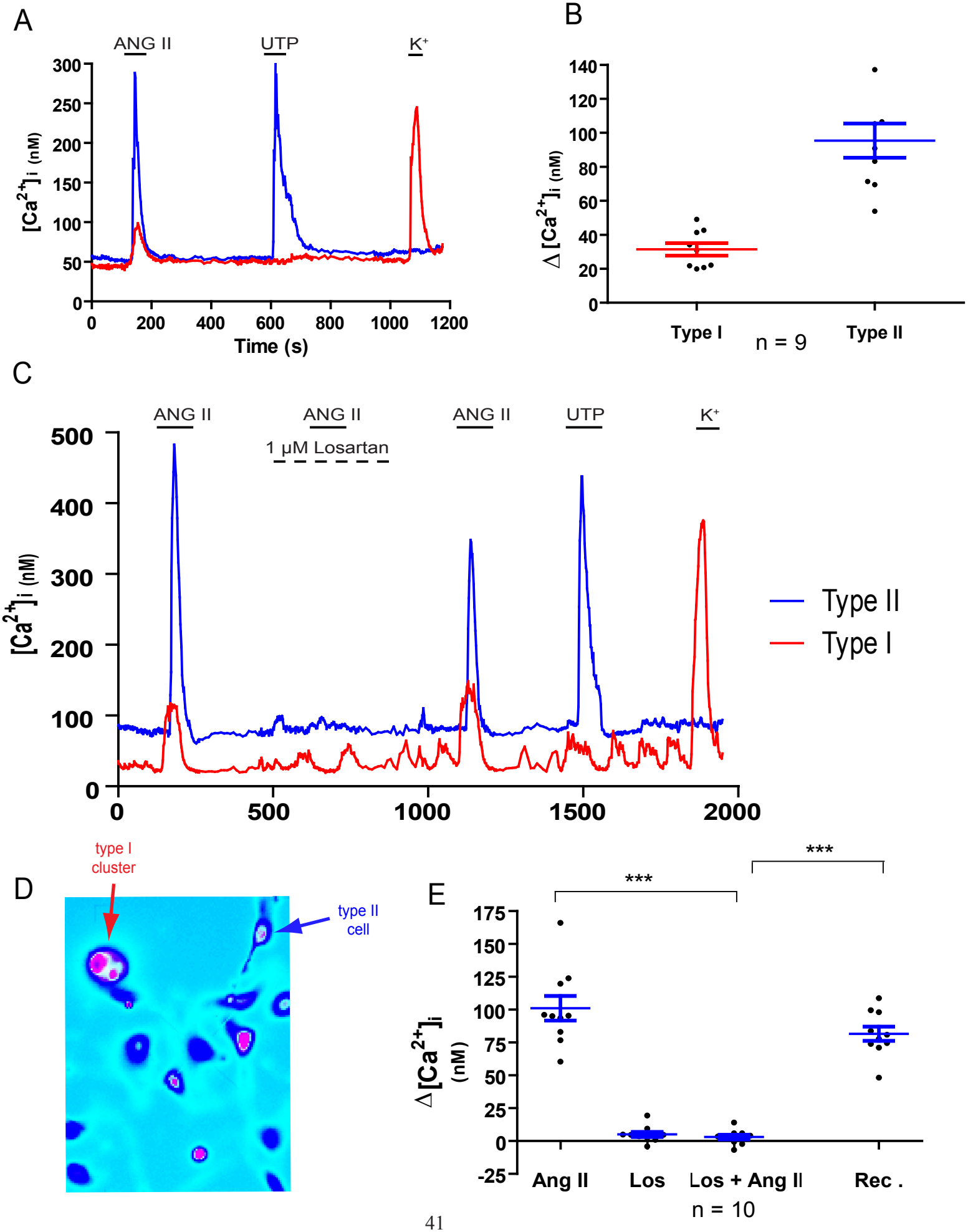
A
ANG II
UTP
K+
[Ca2+]i (nM)
Time (s)
B
Δ [Ca2+]i (nM)
Type I
Type II
n = 9
C
ANG II
ANG II
ANG II
UTP
K+
1 μM Losartan
[Ca2+]i (nM)
Type II
Type I
D
type I cluster
type II cell
E
***
***
Δ[Ca2+]i (nM)
Ang II
Los
Los + Ang II
Rec .
n = 10

Figure 3. Role of intracellular stores in angiotensin II -induced rise in $[Ca^{2+}]_i$ in type II cells. In A, the ANG II-induced rise in $[Ca^{2+}]_i$ persists in solution containing nominally-free extracellular Ca^{2+} (0 Ca^{2+}).; summary data of mean ± s.e.m. Ca^{2+} responses from 9 dishes are shown in B. In C, the ANG II-induced rise in $[Ca^{2+}]_i$ is inhibited by cyclopiazonic acid (CPA; 10 μM); note small Ca^{2+} response on exposing cells to CPA alone. Summary data of $\Delta[Ca^{2+}]_i$ from type II cells in 12 dishes before, during, and after CPA are shown in D. * indicates $p< 0.05$; ** $p< 0.01$; ***$p< 0.001$.

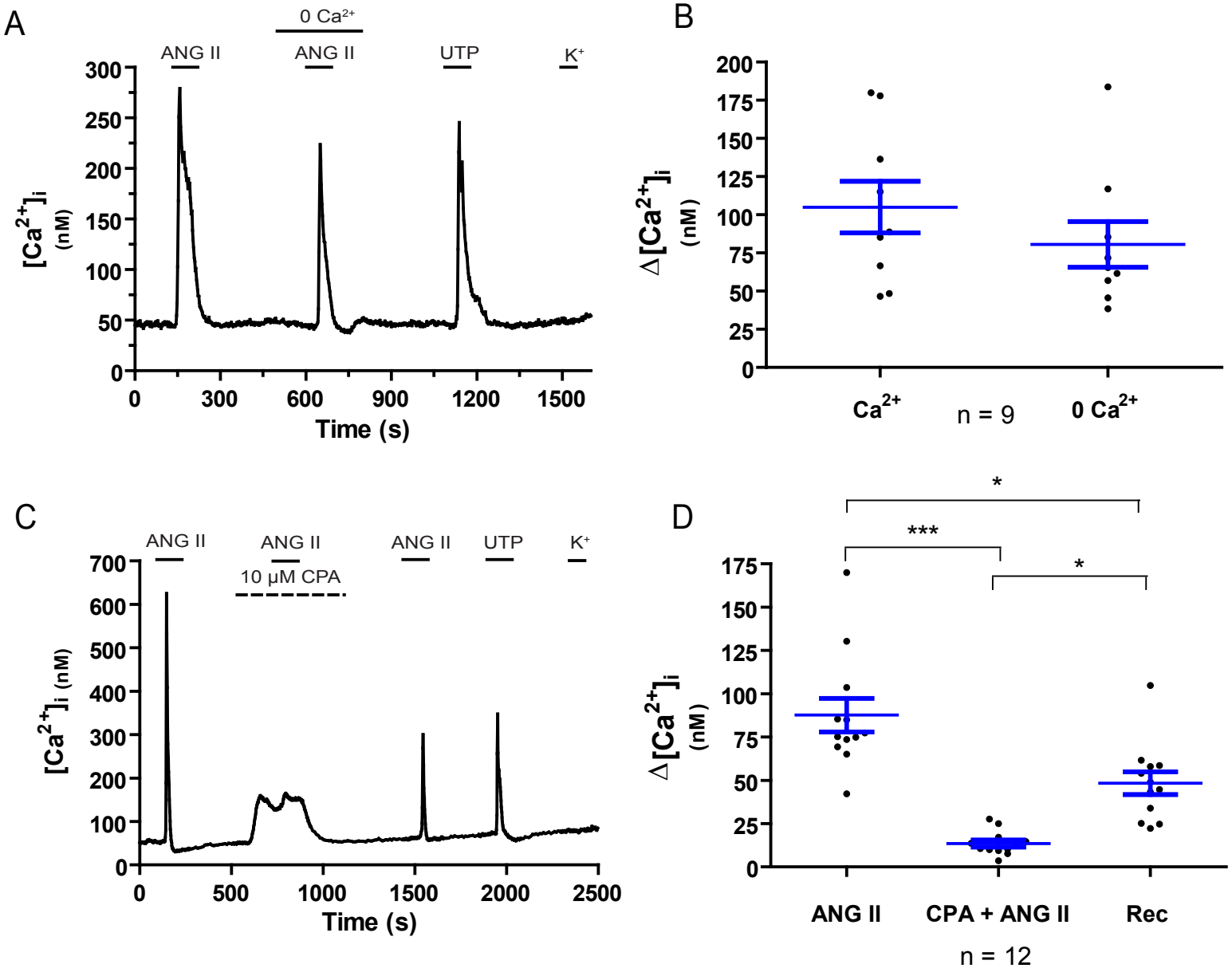
A
0 Ca2+
ANG II
ANG II
UTP
K+
[Ca2+]i (nM)
Time (s)
B
Δ[Ca2+]i (nM)
Ca2+
n = 9
0 Ca2+
C
ANG II
ANG II
ANG II
UTP
K+
10 μM CPA
[Ca2+]i (nM)
Time (s)
D
*
***
*
Δ[Ca2+]i (nM)
ANG II
CPA + ANG II
Rec
n = 12

Figure 4. Dose-dependence and reversal potential of ANG II-induced current in type II cells. In A, application of angiotensin II (ANG II) by a rapid perfusion system induced a dose-dependent inward current that arose with a variable latency; holding potential = -60 mV. The dose-response curve of peak current density (I pA/pF) versus ANG II concentration is shown in B (n = 5-7 cells); a fit of the dose-response curve with the Hill equation yielded an EC_{50} of 76 nM. A plot of latency of the peak current response versus ANG II concentration is shown in C for the same cells. In D1, an estimate of the reversal potential of the ANG II-induced current was obtained for a type II cell using a ramp protocol (holding potential -60 mV; ramp from -40 to +20 mV over 700 msec, repeated every 6 sec) described in Methods; the dotted curve shows the $I_{ANG\ II}$ difference current, obtained by subtracting the current evoked in presence of 100 nM ANG II from the control current, reversed at ~ -6 mV for this cell. In D2, the same cell was tested in a similar way using ATP, which was previously shown to activate Panx-1 current in type II cells via P2Y2R (Zhang et al. 2012); the I_{ATP} difference current in D2 showed a similar reversal potential as $I_{ANG\ II}$, as expected if both ligands activated the same target, i.e. Panx-1 channels. D1 and D2 are representative of 5 cells treated with this protocol.

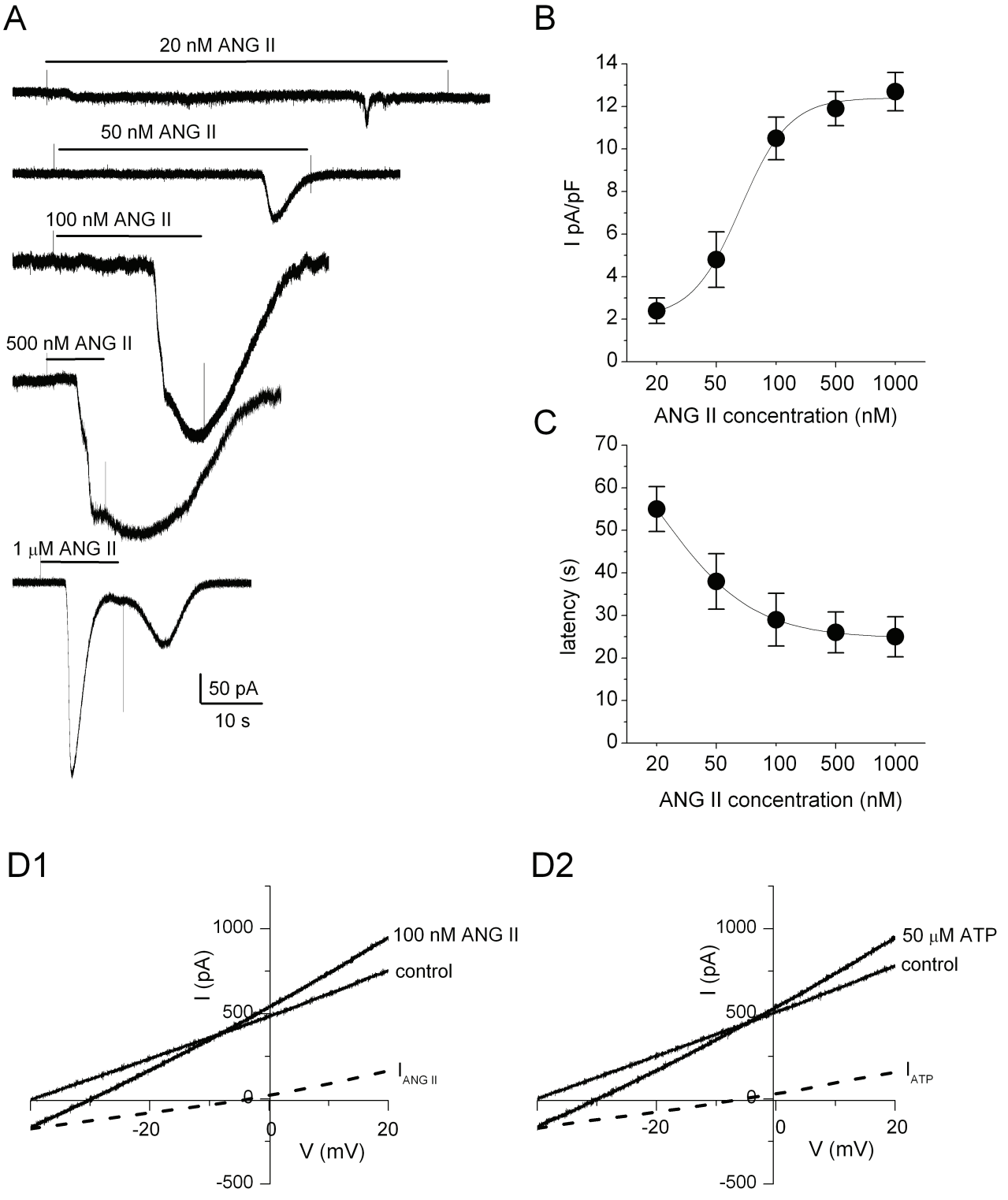
A
20 nM ANG II
50 nM ANG II
100 nM ANG II
500 nM ANG II
1 μM ANG II
50 pA
10 s
B
I pA/pF
ANG II concentration (nM)
C
latency (s)
ANG II concentration (nM)
D1
100 nM ANG II
control
I (pA)
V (mV)
D2
50 μM ATP
control
I (pA)
V (mV)

Figure 5. Blockade of angiotensin II -induced inward currents in type II cells by carbenoxolone and losartan. In A, the inward current elicited by 100 nM ANG II at -60 mV (holding potential) was reversibly inhibited in a type II cell by the Panx-1 channel blocker, carbenoxolone (CBX; 5 µM); pooled current density (pA/pF) data for a group of 5 cells before, during, and after CBX, are summarized in C. In B, the ANG II-induced current was reversibly inhibited by the specific angiotensin AT_1 receptor blocker, losartan (1 µM); pooled current density (pA/pF) data for a group of 4 cells before, during, and after losartan are summarized in D. *** indicates $p < 0.001$.

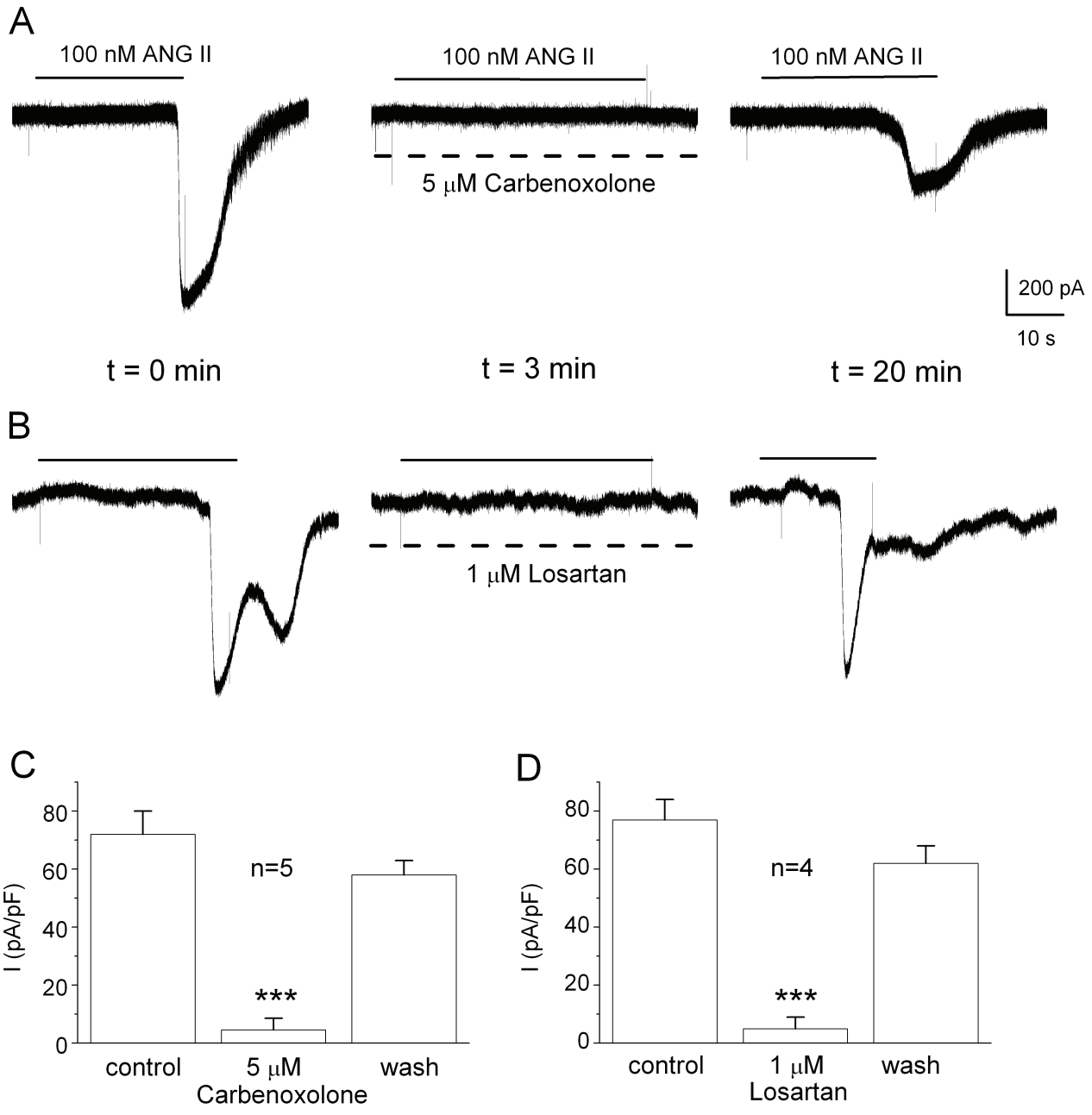
A
100 nM ANG II
100 nM ANG II
100 nM ANG II
5 μM Carbenoxolone
200 pA
10 s
t = 0 min
t = 3 min
t = 20 min
B
1 μM Losartan
C
I (pA/pF)
80
60
40
20
0
n=5
***
control
5 μM Carbenoxolone
wash
D
I (pA/pF)
80
60
40
20
0
n=4
***
control
1 μM Losartan
wash

Figure 6. Comparison of angiotensin II- and ATP-induced Panx-1 current in type II cells during repeated agonist application. In A, repeated application of 100 nM ANG II to the same cell over a 20 min period (t=0 min, left; t=3 min, middle; t=20 min, right) caused a progressive run-down in the peak current (at -60 mV holding potential); summary data from 4 cells are shown in C (black bins). By contrast, when 50 µM ATP was used as the agonist, the current remained relatively stable over the same time period (B,C; white bins). Current run-down in A was attributable to desensitization of the AT_1 receptor, and not loss of Panx-1 channel function, because ATP could readily activate the Panx-1 current soon after (within 2 min) a test with ANG II failed to do so (D); test times with ANG II and ATP indicated above traces. Example in D was typical of n= 4 cells, exposed to 100 nM or 1 µM ANG II; * indicates $p < 0.05$; *** $p< 0.001$.

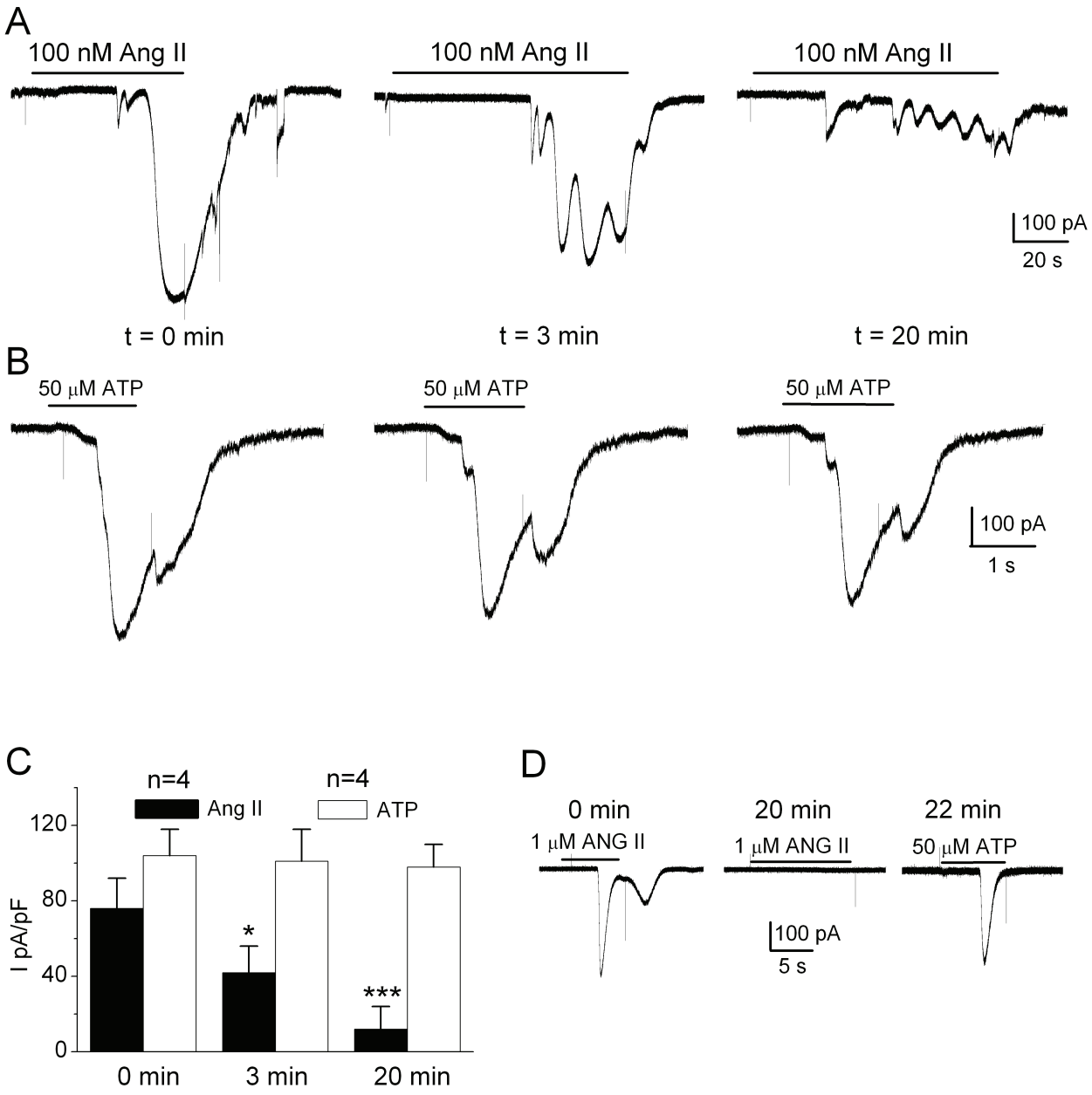
A
100 nM Ang II
100 nM Ang II
100 nM Ang II
100 pA
20 s
t = 0 min
t = 3 min
t = 20 min
B
50 μM ATP
50 μM ATP
50 μM ATP
100 pA
1 s
C
n=4
n=4
Ang II
ATP
120
80
40
0
I pA/pF
*
***
0 min
3 min
20 min
D
0 min
1 μM ANG II
20 min
1 μM ANG II
22 min
50 μM ATP
100 pA
5 s

Figure 7. Synergistic interaction between ATP and angiotensin II on Panx-1 current activation in type II cells. In A, a low dose of ATP (10 µM; left trace) activated the Panx-1 current whereas a 'subthreshold' dose of ANG II (10 nM; middle trace) failed to do so in the same cell; when the two stimuli were combined the current was markedly potentiated relative to that seen with ATP alone (n=3). In B, both ATP (10 µM; left trace) and ANG II (20 nM; middle trace), at doses below their respective EC_{50} values of 34 µM (Zhang et al. 2012) and 76 nM (this study), elicited a detectable Panx-1 current in the same type II cell when applied separately; however, when applied together there was a marked potentiation in the magnitude of the response, as well as a shortening of the response latency (right trace). Summary data in C show that the current density (pA/pF at -60 mV holding potential) elicited when the two agonists were applied together (right bin) exceeded the sum of the separate individual responses (sum of bin a + bin b) by a factor of ~1.6x ($p < 0.05$), indicating a synergistic interaction (n= 5 cells). In D, response latency during combined application was significantly shorter than that seen during separate application of either agonist. Note in B,D, the average latency during ANG II application appeared much shorter (~9 sec) when the agonist was applied after prior activation or 'priming' of the Panx-1 current by ATP (compare with Fig. 4, where latency was ~55 sec for 20 nM ANG II, without prior ATP exposure). * indicates $p < 0.05$; ** $p < 0.01$; *** $p < 0.001$.

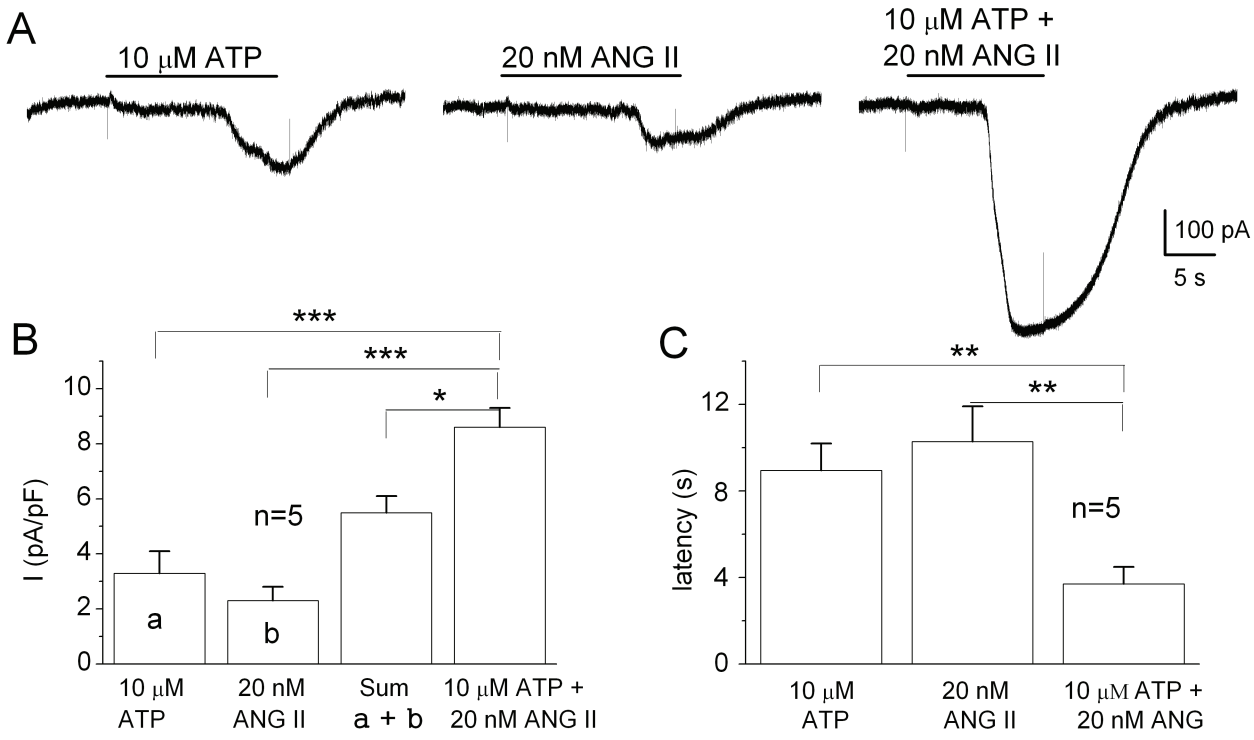
A
10 μM ATP
20 nM ANG II
10 μM ATP +
20 nM ANG II
100 pA
5 s
B
I (pA/pF)
n=5
a
b
10 μM ATP
20 nM ANG II
Sum a + b
10 μM ATP + 20 nM ANG II
C
latency (s)
n=5
10 μM ATP
20 nM ANG II
10 μM ATP + 20 nM ANG

Figure 8. Chelating intracellular Ca^{2+} in type II cells with BAPTA prevents Panx-1 current activation by angiotensin II and ATP. In A, the ANG II-induced Panx-1 current was almost completely and reversibly inhibited during incubation with the membrane permeable Ca^{2+} chelator, BAPTA-AM (1 μM; middle trace). Similarly in B, the same result was obtained when ATP was used as the agonist. Summary data in C,D, show the reversible inhibition of the Panx-1 current evoked by ANG II and ATP respectively, when BAPTA-AM was present (n =4 in C, and 6 in D); *** $p< 0.001$.

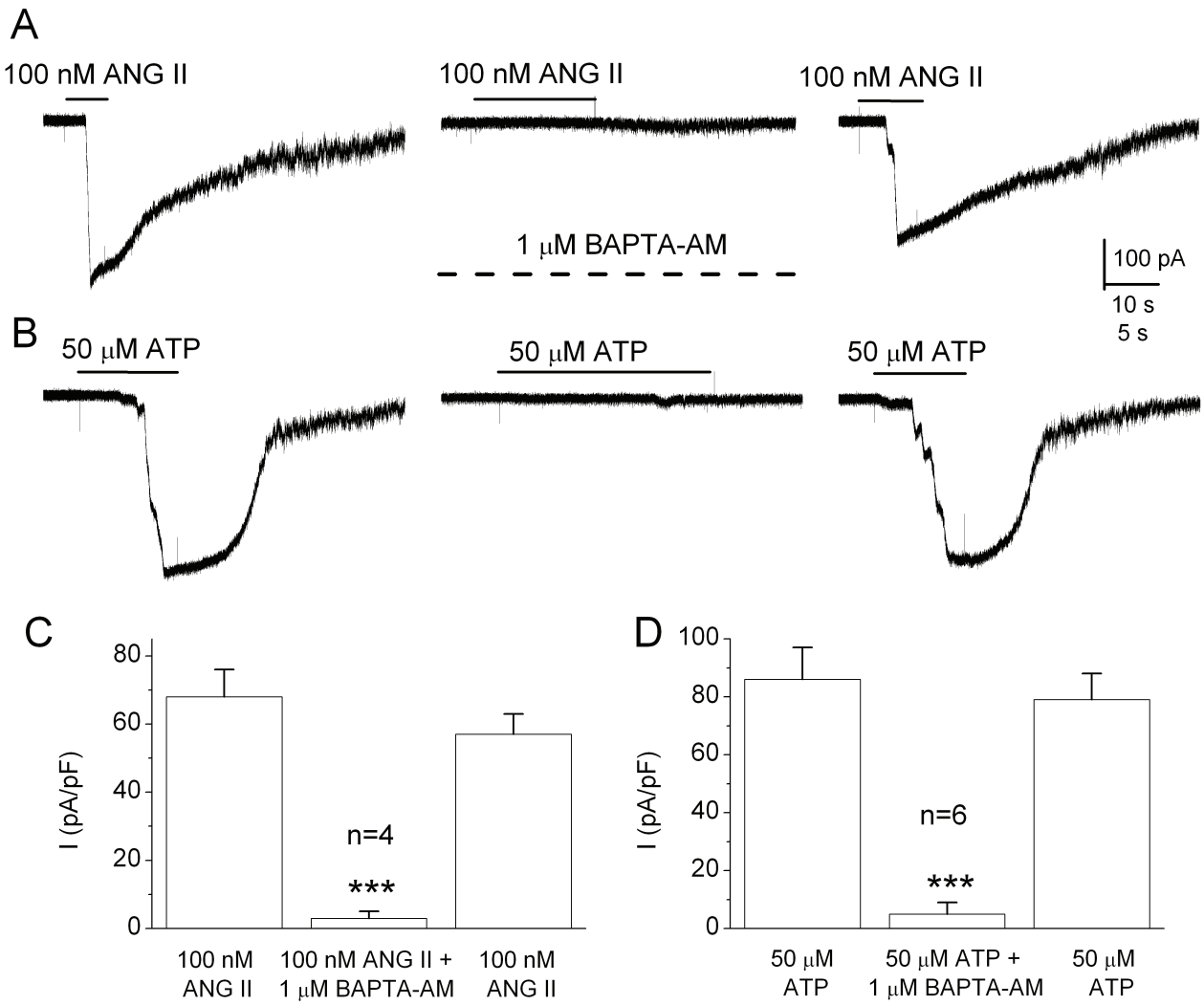
A
100 nM ANG II
100 nM ANG II
100 nM ANG II
1 μM BAPTA-AM
100 pA
10 s
5 s
B
50 μM ATP
50 μM ATP
50 μM ATP
C
I (pA/pF)
80
60
40
20
0
n=4
***
100 nM ANG II
100 nM ANG II + 1 μM BAPTA-AM
100 nM ANG II
D
I (pA/pF)
100
80
60
40
20
0
n=6
***
50 μM ATP
50 μM ATP + 1 μM BAPTA-AM
50 μM ATP

CHAPTER 3

Evidence for paracrine stimulation of glial-like type II cells of the carotid body: Role of 5-HT

Sindy Murali, Min Zhang, and Colin A. Nurse

The work in this chapter is in preparation for submission.

I performed all Ca^{2+} imaging experiments, data analysis, prepared the figures, and wrote the manuscript. M. Zhang performed the patch-clamp electrophysiological experiments. C.A.N was involved in planning and designing of all the experiments, helped to interpret the data, edited and approved the final version of this manuscript.

ABSTRACT

Previous studies have shown that chemoreceptor type I cells of the rat carotid body (CB) synthesize and release 5-hydroxytrptamine (5-HT), and express G-protein coupled 5-HT receptors. Moreover, increased 5-HT signalling contributes to enhanced CB excitation after chronic intermittent hypoxia, attributable to stimulation of 5-HT_{2A} receptors on type I cells. Here, we show that in dissociated rat CB cultures, 5-HT also stimulates glial-like type II cells, identified by the presence of a robust increase in intracellular Ca^{2+} ($\Delta[Ca^{2+}]_i$) during exposure to the selective P2Y2 receptor agonist UTP and/or lack of a Ca^{2+} response to the depolarizing stimulus, high K^+. In the majority (~ 67 %) of type II cells, 5-HT induced a dose-dependent (EC_{50} ~ 183 nM), robust $\Delta[Ca^{2+}]_i$ that was partially inhibited by the 5-HT_{2A} receptor blocker, ketanserin (1 µM). This 5-HT-induced $\Delta[Ca^{2+}]_i$ persisted in Ca^{2+}-free medium and was sensitive to store depletion with thapsigargin (1 µM). As expected, 5-HT also induced $\Delta[Ca^{2+}]_i$ responses in type I cells; however, those responses were partially inhibited by both the 5-HT_{2A} receptor antagonist, ketanserin (1 µM), and the putative 5-HT_{5A} receptor antagonist, SB 69951 (10 µM). Similar to our previous reports on ATP, UTP, and angiotensin II, 5-HT (5 µM) also activated pannexin-1 (Panx-1) current in type II cells that was reversibly abolished by the Panx-1 blocker, carbenoxolone (5 µM). The 5-HT-induced Panx-1 current was reversibly inhibited by ketanserin (1 - 10 nM) and was inhibited by BAPTA (50 µM), suggesting a role for intracellular Ca^{2+} signalling. Since Panx-1 channels act as conduits for the excitatory CB neurotransmitter, ATP, it is plausible that paracrine stimulation of type II cells by 5-HT contributes to enhanced CB excitability, especially in pathophysiological conditions such as sleep apnea.

INTRODUCTION

The carotid bodies (CB) are the main mammalian peripheral O_2-chemoreceptor organs that detect changes in arterial oxygen and mediate reflex hyperventilation during acute hypoxia (Gonzalez et al. 1994). It is well established that type I cells are the CB chemoreceptors which depolarize in response to a fall in arterial partial pressure of O_2 (PO_2). They release neurotransmitters such as ATP, which excite sensory afferent fibers (Gonzalez et al. 1994; Nurse 2005; Buckler 2007; Nurse 2010; Kumar and Prabhakar 2012). Along with ATP, there are several other excitatory and inhibitory neurotransmitter candidates that are thought to play important modulatory roles in afferent signalling via actions at G-protein coupled receptors (Nurse 2005; Nurse 2010; Kumar and Prabhakar 2012).

5-hydroxytryptamine (5-HT), which functions as a neurotransmitter and/or neuromodulator in the nervous system, is expressed in the CB chemoreceptor cells and there is evidence it is released during hypoxia, at least in some studies (Grönblad et al. 1983; Habec et al. 1994; Zhang et al. 2003; Jacono et al. 2005; Ramirez et al. 2012; Yokoyama et al. 2013). Kirby & McQueen (1984) observed that an intracarotid injection of 5-HT resulted in a triphasic response that began with a transient burst of activity, immediately followed by a dose-related chemodepression, and then a delayed longer-lasting chemoexcitation phase. The different phases of the response is attributable to multiple 5-HT receptor subtypes since only the combined actions of 5-HT_2 and 5-HT_3 antagonists eliminated all the effects of 5-HT (Kirby and McQueen 1984). In addition to the metabotropic 5-HT_{2A} receptor and the ligand-gated 5-HT_3 receptor (Zhong et al. 1999), chemoafferent neurones located in the petrosal ganglion may also express the metabotropic 5-HT_{5A} receptor (Wang et al. 2000).

There is evidence that 5-HT may also have paracrine pre-synaptic functions in the CB. For example, in isolated chemoreceptor clusters of rat CB, spontaneous firing was sometimes seen during membrane potential recordings from type I cells (Zhang and Nurse, 2000). Moreover, Zhang et al. (2003) found that 5-HT caused a PKC-mediated inhibition of K^+ channels in type I cells, which enhanced membrane depolarization and the probability of cell firing. The 5-HT receptors involved in this positive feedback loop had the pharmacological profile of 5-HT_{2A} receptors and this was confirmed with RT-PCR and immunocytochemical techniques. Another

role proposed for the 5-HT_{2A} receptor in the CB is to facilitate sensitization during chronic intermittent hypoxia (CIH), a situation that is observed in pathophysiological conditions such as central or obstructive sleep apnea and asthmatic attacks (Peng et al. 2003). CIH results in long-term facilitation (LTF) of the rodent CB sensory discharge (Peng et al. 2003), leading to autonomic imbalances with pathophysiological consequences such as hypertension, myocardial infarcts, and stroke (Nieto et al. 2000; Shahar et al. 2001). During CIH, the intermittent release of 5-HT and subsequent 5-HT_{2A} receptor stimulation induces sensory LTF via PKC-dependent activation of NADPH oxidase (Peng et al. 2006; Peng et al. 2009). In addition to the 5-HT_{2A} receptor, there is a report that CB type I cells also express 5-HT_{5A} receptor (Wang et al. 2000), however its role (if any) in chemoreception has not yet been determined.

Studies on the role of 5-HT in the CB have so far focused on the chemoreceptor type I cell or the sensory petrosal afferents. However, recent studies in this laboratory demonstrated that glial-like type II cells, found in intimate association with receptor type I cells, are also potential targets for CB neuromodulators. For example, we showed that ATP and angiotensin II (ANG II), acting via P2Y2 and AT_1 receptors respectively, could elicit increases in intracellular Ca^{2+} and activation of pannexin-1 channels in type II cells (Zhang et al. 2012; Murali et al. 2014). Because these channels act as conduits for ATP release, paracrine activation of type II cells provides a parallel pathway for increasing the level of excitatory drive at the sensory synapse. In this present study, we tested the hypothesis that 5-HT may exert a similar paracrine function in the CB that includes stimulation of type II cells, leading to Panx1 channel activation.

MATERIALS AND METHODS

Ethical approval

All procedures for animal handling and tissue dissections were carried out according to the guidelines of the Canadian Council on Animal Care (CCAC) and institutional guidelines.

Cell cultures of dissociated rat carotid body

Carotid bifurcations from 9-14 day old rats (Wistar, Charles River, Quebec, Canada) were excised bilaterally, after the animals were first rendered unconscious by a blow to the back of the head, followed immediately by decapitation. The carotid bodies (CBs) were isolated from the surrounding tissue and dissociated cell cultures prepared according to established procedures, described in detail elsewhere (Zhong et al. 1997; Zhang et al. 2000). Briefly, the excised CBs were incubated for 1 h at 37°C in a physiological salt solution containing 0.1% trypsin (Sigma-Aldrich, Oakville, Ontario, Canada) and 0.1% collagenase (Gibco, Grand Isalnd, NY, USA), followed by mechanical dissociation and trituration. The dispersed cell suspension was allowed to adhere to the central wells of modified tissue culture dishes; the wells were pre-coated with a thin layer of Matrigel (BD Biosciences, Mississauga, Ontario, Canada). The cells were cultured in basic growth medium (BGM) consisting of F-12 nutrient medium supplemented with 10% fetal bovine serum, 1% penicillin-streptomycin, 1% glutamine, 0.3% glucose, and 3 μg ml^{-1} insulin, as in previous studies (Zhang et al. 2000; Zhang et al. 2012). To enrich for type II cells and facilitate recordings, the growth medium was switched after 12 hr to Cosmic-BGM containing: 50% BGM plus 50% of modified BGM where 10% fetal bovine serum was replaced with 5% fetal bovine serum and 5% Cosmic calf serum (Hyclone Laboratories Inc. Utah, USA). Our previous study demonstrated that there were no obvious differences in the properties of type II cells cultured in BGM vs. Cosmic-BGM (Zhang et al. 2012). Cultures were grown at 37°C in a humidified atmosphere of 95% air-5% CO_2. Patch clamp recordings were usually carried out in 5-7 day-old CB cultures, which permitted optimal recordings from isolated 'solitary' type II cells; the Ca^{2+} imaging experiments were typically carried out after ~48 h in culture.

Intracellular Ca^{2+} measurements

Intracellular free Ca^{2+} concentration ($[Ca^{2+}]_i$) was monitored using the fluorescent Ca^{2+} indicator fura-2 AM (Molecular Probes, Eugene, OR, USA), as previously described (Piskuric and Nurse 2012; Zhang et al. 2012). Cells were loaded with 2.5 μM fura-2 AM diluted in standard bicarbonate-buffered solution (BBS) for 30 min at 37°C, and subsequently washed for ~15 min to remove free dye. The BBS used in Ca^{2+} imaging experiments had the following composition (in mM): $NaHCO_3$, 24; NaCl, 115; glucose,5; KCl, 5; $CaCl_2$, 2 and $MgCl_2$, 1; the pH was maintained at ~7.4 by bubbling with a 5% CO_2-95% air mixture. Ratiometric Ca^{2+} imaging was performed

using a Nikon Eclipse TE2000-U inverted microscope (Nikon, Mississauga, ON, Canada) equipped with Lambda DG-4 ultra-high-speed wavelength changer (Sutter Instrument CO., Novato, CA, USA), a Hamamatsu OCRCA-ET digital CCD camera (Hamamatsu, Sewickley, PA, USA) and a Nikon S-Fluor 40x oil-immersion objective lens with a numerical aperture of 1.3. Dual images at 340 nm and 380 nm excitation (510 emission) were acquired every 2 s, with an exposure time of 100-200 ms. Pseudocolour ratiometric data were obtained using Simple PCI software version 5.3. All experiments were performed at 35-37°C, and cells were continuously perfused with BBS to maintain an extracellular pH of ~7.4.

The imaging system was calibrated using the Fura-2 Calcium Imaging Calibration Kit from Molecular Probes (Cat. No. F-6774). Photometric data at 340 nm and 380 nm excitation (510 emission) were obtained for 11 buffers of known Ca^{2+} concentrations from Ca^{2+}-free (0 µM) to saturating Ca^{2+} (39 µM). After correcting for background fluorescence, these values were used to calculate the following ratios: 'R' is the 510 nm emission intensity at 340 nm excitation to 510 nm emission intensity at 380 nm excitation; R_{min}, the ratio at zero free Ca^{2+}; R_{max} the ratio at saturating Ca^{2+}; and β, the fluorescence intensity with excitation at 380 nm for zero free Ca^{2+} (F_{380max}), to the fluorescence intensity at saturating free Ca^{2+} (F_{380min}). The intracellular free [Ca^{2+}] was obtained after substituting these ratios into the Grynkiewicz equation (Grynkiewicz et al. 1985) as follows:

$$[Ca^{2+}]_i = K_d \frac{[R - R_{\min}]}{[R_{\max} - R]} \beta$$

where R_{min} = 0.18, R_{max} = 7.81, β = 12.29, K_d = 225 nM and R is the ratio obtained during the experiment for a given cell. For most experiments statistical analysis was performed using Repeated Measures ANOVA with Tukey's Multiple Comparison Test *post hoc* test, as indicated in text.

Electrophysiology

Nystatin perforated-patch whole cell-recording was used to monitor ionic currents in type II cells as previously described (Zhang and Nurse 2000; Zhang et al. 2012). All recordings were carried out at ~35°C and the cells were perfused with standard BBS containing (in mM): $NaHCO_3$, 24; NaCl, 115; KCl, 5; $CaCl_2$, 2; $MgCl_2$, 1; glucose, 10, and sucrose, 12; at pH 7.4 maintained by

bubbling with 5%CO_2-95% air mixture. The pipette solution contained (mM): potassium gluconate, 115; KCl, 25; NaCl, 5; $CaCl_2$, 1; Hepes, 10, and nystatin 200 $\mu g.ml^{-1}$; at pH 7.2. Agonists (e.g. 5-HT) were applied by a 'fast perfusion' system utilizing a double-barreled pipette assembly as previously described (Zhong et al. 1997; Zhang et al. 2000; Zhang et al. 2012). Current measurements under voltage clamp were obtained with the aid of a MultiClamp 700A patch clamp amplifier and a Digidata 1322A analog-to-digital converter (Axon Instruments Inc., Union City, CA, USA), and the data stored on a personal computer. Data acquisition and analysis were performed using pCLAMP software (version 9.0; Axon Instruments Inc.). For multiple comparisons of ionic currents or current density (pA/pF), obtained by dividing peak current by whole cell capacitance), ANOVA was used and the level of significance was set at $p < 0.05$.

Reagents and drugs

The following reagents and drugs obtained from Sigma-Aldrich (Oakville, ON): UTP, 5-hydroxytryptamine (5-HT), ketanserin (Ket), SB 699551, and carbenoxolone (CBX).

RESULTS

In most cases, isolated solitary type II cells were investigated to eliminate or minimize secondary effects from neighbouring type I cells. Intracellular Ca^{2+} responses were recorded from CB cultures ~ 48 hours after plating when type II cells were more easily distinguishable from type I cells morphologically. In addition to their characteristic spindle shape, the identity of type II cells was routinely confirmed by the presence of a rise in intracellular Ca^{2+} following stimulation with the P2Y2R agonist, UTP (Xu et al. 2003; Zhang et al. 2012). As in previous studies (Murali et al. 2014), the absence of cross-talk from type I to type II cells was confirmed by the lack of a $\Delta[Ca^{2+}]_i$ response in type II cells during perfusion with the depolarizing stimulus, high K^+ (30 mM), which stimulates neurosecretion from type I cells. For Ca^{2+} imaging experiments, the 'n' values reported in text refer to the number of cultures dishes sampled, whereas the 'n' value represents number of cells that were tested in voltage-clamp experiments.

5-HT induces an intracellular Ca^{2+} response in type I and type II cells via 5-HT_{2A} receptors

In two day-old CB cultures, perfusion with medium containing 5-HT resulted in a rise in intracellular Ca^{2+} in subpopulations of type I and type II cells, as exemplified in Fig. 1A. In one experimental series, 40.5% (77/190 cells) of type I cells, identified by a Ca^{2+} response to the depolarizing stimulus high K^+, were sensitive to 10 µM 5-HT; this proportion is comparable to that previously reported in electrophysiological studies on 5-HT modulation of K^+ currents in rat type I cells (~40%; (Zhang et al. 2003)). In comparison, a larger proportion (67%; 208/310 cells) of UTP-sensitive type II cells responded to 10 µM 5-HT. In general, the intracellular Ca^{2+} response in type II cells was more robust than that in type I cells. A comparison of the relative magnitude of the mean peak $\Delta[Ca^{2+}]_i$ evoked by 5-HT was ~229 nM in type II cells compared to ~ 54 nM in type I cells (Mann-Whitney t-test; $p < 0.01$; Fig. 1B).

Because the 5-HT_{2A} receptor is commonly linked to the generation of intracellular Ca^{2+} signals in glial cells (Finkbeiner 1993; Verkhratsky and Kettenmann 1996), it was of interest to determine whether or not the 5-HT-induced $\Delta[Ca^{2+}]_i$ responses in type II cells were also mediated by 5-HT_{2A} receptors. First, as exemplified in Fig. 2A, the effects of 5-HT on $\Delta[Ca^{2+}]_i$ responses were dose-dependent. A plot of the dose-response curve for [5-HT] versus $\Delta[Ca^{2+}]_i$ is shown in Fig. 2B; the estimated EC_{50} of 183 nM is slightly higher than that reported for 5-HT acting at 5-HT_{2A} receptors in C6 glioma cells (EC_{50} = 100 nM; (Muraoka et al. 1998). The type II cell receptors displayed slight desensitization on repeated application of 10 µM 5-HT applied ~5 min apart; however, only the first and third responses were significantly different from one another (Friedman Test, $p < 0.001$; n = 10 dishes; Figs. 2C,D).

To confirm the involvement of the 5-HT_{2A} receptor in mediating the 5-HT-evoked Ca^{2+} responses in type II cells, the selective 5-HT_{2A} receptor antagonist ketanserin, was used. The 5-HT-evoked rise in $\Delta[Ca^{2+}]_i$ in the majority of responsive type II cells (180/252; 70%) was reversibly inhibited by ketanserin as illustrated in the exemplar trace in Figure 3A. The mean 5-HT-induced $\Delta[Ca^{2+}]_i$ responses in the absence and presence of ketanserin were 52 nM and 15 nM, respectively, corresponding to ~ 71% inhibition (n = 14 dishes; Friedman test with Dunn's multiple comparison *post hoc* test; $p < 0.01$; Figure 3B). In general, there was only partial recovery of 5-HT-induced responses after washout of ketanserin; the mean $\Delta[Ca^{2+}]_i$ response after ketanserin was 28.5 nM compared to 52 nM before (n =14 dishes; Friedman test with Dunn's multiple

comparison *post hoc* test, $p < 0.001$). This effect may be related to the gradual run-down in 5-HT-evoked responses with repeated 5-HT application as illustrated in Figs. 2 C,D. A similar trend was seen in type I cells. A scatter plot of $\Delta[Ca^{2+}]_i$ responses for type I cells before, during, and after ketanserin is shown in Figure 3C. Ketanserin inhibited the mean $\Delta[Ca^{2+}]_i$ response in type I cells by 54%; the mean (± s.e.m.) $\Delta[Ca^{2+}]_i$ response was 28.4 ± 4.8 nM for 5-HT (10 μM), 13.0 ± 2.26 nM for 5-HT plus ketanserin (1 μM), and 18.0 ± 6.2 nM for 5-HT after washout of ketanserin (Repeated Measures ANOVA, $p < 0.01$, n = 9 dishes). In previous studies, ketanserin blocked the 5-HT-induced inhibition of K^+ currents in rat type I cells (Zhang et al. 2003). However, to our knowledge the present study is the first to show 5-HT-evoked Ca^{2+} responses in type I cells and their inhibition by ketanserin (Fig. 3A & C).

Do 5-HT_{5A} receptors contribute to 5-HT-evoked Ca^{2+} responses?

Since ketanserin did not completely inhibit 5-HT-evoked Ca^{2+} responses in type I and type II cells, we explored the possibility that other 5-HT receptors are involved. Because the expression of 5-HT_{5A} receptors was previously reported in the rat CB (Wang et al. 2000), we tested the effects of the selective 5-HT_{5A} inhibitor, SB 699551 (Thomas et al. 2006). When type I and type II cells were compared, only 5-HT-evoked Ca^{2+} responses in a subpopulation of type I cells were significantly inhibited by 10 μM SB 699551 (Fig. 4A). The presence of SB 699551 abolished Ca^{2+} responses in ~ 62% of 5-HT-responsive type I cells (51/133 cells), however a residual response persisted in the remaining cells; the mean $\Delta[Ca^{2+}]_i$ response before and during SB 699551 was 28.3 ± 3.87 nM vs. 10.4 ± 4.25 nM (n = 9 dishes; Friedman test with Dunn's multiple comparison *post hoc* test; $p < 0.05$), corresponding to an ~ 63% inhibition. In comparison, the mean 5-HT-induced $\Delta[Ca^{2+}]_i$ in type II cells was not significantly affected by 10 μM SB 699551; the mean (± s.e.m.) $\Delta[Ca^{2+}]_i$ response was 51.0 ± 4.91 nM for 5-HT (10 μM), 45.3 ± 5.50 nM for 5-HT + SB 699551, and 34.1 ± 4.59 nM for 5-HT after washout of SB 699551 (Friedman test with Dunn's Multiple Comparison Test, $p > 0.05$; n = 11 dishes). These data raise the possibility that 5-HT_{5A} receptors may contribute to the Ca^{2+} responses in at least a subpopulation of type I cells.

5-HT-induced Ca^{2+} transients in type II cells originate from intracellular stores

To test whether 5-HT-evoked $[Ca^{2+}]_i$ transients in type II cells arose mainly from an intracellular or extracellular source, we monitored type II cell Ca^{2+} responses in a 0 Ca^{2+} solution (+ 1 mM EGTA). In some experiments, the order of presenting normal Ca^{2+} and 0 Ca^{2+} solutions was reversed to account for the desensitization properties of the receptor. A high proportion (86%; n = 133/154) of type II cells that initially responded to 5-HT in normal Ca^{2+} continued to do so in 0 Ca^{2+}. Indeed, as illustrated in Fig. 5A, type II cell Ca^{2+}- transients evoked by 10 µM 5-HT were not significantly altered on switching from normal to 0 Ca^{2+} medium; this suggests that the predominant source of Ca^{2+} is intracellular. Figure 5B illustrates a scatter plot comparison of 5-HT-induced $\Delta[Ca^{2+}]_i$ in normal (2 mM) and zero Ca^{2+} solutions; the mean ± s.e.m. in normal calcium was 77.5 ± 7.15 nM compared to 74.8 ± 13.4 in zero calcium (Unpaired t-test with Welch's correction, p = 0.8644; n = 9 dishes). In order to validate that the source of Ca^{2+} is intracellular, we used an intracellular store depletion agent, thapsigargin (1 µM). Of 431 5-HT-responsive type II cells tested, only 9 cells (i.e. 2.1%) elicited a significant rise in Ca^{2+} in the presence of 5-HT plus thapsigargin; in Fig. 5C, thapsigargin dramatically reduced the mean $\Delta[Ca^{2+}]_i$ from 77.8 ± 6.98 to -16.1 ± 3.61 nM (n = 12 dishes; Friedman test with Dunn's multiple comparison *post hoc* test, p < 0.001). In these experiments the effects of thapsigargin were not reversible (Fig. 5C).

5-HT-induced signaling activates pannexin-1 currents in type II cells

We previously demonstrated that ATP acting via P2Y2 receptors (Zhang et al. 2012), and angiotensin II (ANG II) acting via AT_1 receptors (Murali et al. 2014), activated pannexin-1 (Panx-1) currents in type II cells. To determine whether 5-HT acts similarly, we carried out voltage clamp studies on type II cells. As exemplified in Figs. 6A,B, 5 µM 5-HT activated an inward current at negative holding potentials and the current reversed direction near 0 mV (n = 5 cells); the mean reversal potential was ~ -11 mV (n = 5 cells), consistent with activation of a non-selective cation current.

To confirm that 5-HT signaling leads to the opening of Panx-1 channels in type II cells, we used the selective Panx-1 inhibitor, carbenoxolone (CBX) (Ma et al. 2009). As exemplified in Fig. 7A, the 5-HT-induced inward current (at -60 mV holding potential) was reversibly inhibited by 5 µM CBX, as observed in our previous studies where ATP and ANG II were used to activate the Panx-1 current (Zhang et al. 2012; Murali et al. 2014); summary data for a group of 3 cells are

shown in Fig. 7B. The onset of the blockade was slow as it developed gradually over a period of 6 min as illustrated in Fig. 7A.

Evidence that 5-HT$_{2A}$ receptors mediate the 5-HT activation of pannexin-1 channels in type II cells

Given the sensitivity of the 5-HT-induced Ca^{2+} transients to the 5-HT$_{2A}$ blocker ketanserin (Fig. 3), we tested the effects of ketanserin on the 5-HT-induced Panx-1 current in type II cells. As illustrated in Fig. 8A, low doses of ketanserin (1-10 nM) reversibly inhibited 5-HT-induced Panx-1 current; a histogram of the concentration-dependent inhibition of the 5-HT-induced Panx-1 current density (pA/pF; at -60 mV holding potential) for a group of 5 cells is shown in Figure 8B. The concentrations of ketanserin used within this experiment conformed to the IC_{50} value for ketanserin at 5-HT$_{2A}$ receptors in a previous study (IC_{50} = 1.58 nM; (Barnes and Sharp 1999). Interestingly, when similar experiments were conducted with the 5-HT$_{5A}$ receptor antagonist, SB 699551, a concentration (10 µM) that was 10 times higher than the IC_{50} for the 5-HT$_{5A}$R (I_{50} = 1 µM; (Thomas 2006)) was required to inhibit 5-HT-induced Panx-1 currents in type II cells (data not shown). The significance of these data is uncertain as 10 µM SB 699551 appears to cause a non-specific block of Panx-1 channels when the latter are activated by ATP (M. Zhang; unpublished observations).

A rise in intracellular Ca^{2+} is required for 5-HT-evoked pannexin-1 currents in type II cells

Our previous studies with ATP and ANG II demonstrated that a rise in cystolic Ca^{2+} provided a link between metabotropic receptor activation and the opening of Panx-1 channels (Zhang et al. 2012; Murali et al. 2014). We therefore investigated whether 5-HT-evoked Panx-1 currents required a rise in cytoplasmic Ca^{2+} using the Ca^{2+} chelator, BAPTA (50 µM). In contrast to our observations on 5-HT- induced Ca^{2+} responses, repeated, but rapid short-duration applications of 5-HT to the same type II cell evoked similar current responses with negligible desensitization (Fig. 9A1). In Fig. 9A2, the same cell was studied with a second pipette containing 50 µM BAPTA resulting in a time-dependent decline of the 5-HT-induced Panx-1 current at 3 min. The preliminary data suggests that Ca^{2+} is required for Panx-1 channel activation by 5-HT.

DISCUSSION

Characterizing the 5-HT receptors responsible for mediating 5-HT evoked Ca^{2+} responses in type I & type II cells

Previous studies have demonstrated that type II cells of rat carotid body (CB) are capable of eliciting Ca^{2+} transients in response to ATP, UTP, ANG II, and muscarine (Xu et al. 2003; Tse et al. 2012; Zhang et al. 2012; Murali et al. 2014). The present study has highlighted for the first time that a proportion of rat CB type II cells are capable of 5-HT-induced intracellular Ca^{2+} responses. Perforated-patch clamp recordings are consistent with ratiometric calcium imaging studies in that a subpopulation of type II cells are 5-HT sensitive leading to the opening of pannexin-1 (Panx-1) channels, which has recently been shown to act as conduits for ATP release (Zhang et al. 2012). The role of 5-HT in CB response to acute hypoxia is uncertain, however, previous studies have focused on type I cells because they express 5-HT_{2A} receptors and 5-HT biosynthetic enzymes and transporters (Zhang et al. 2003; Peng et al. 2006; Yokoyama et al. 2013). To our knowledge, there are no studies demonstrating 5-HT-evoked Ca^{2+} responses in either type I or type II cells. Although type I cells did not have as large of a peak Ca^{2+} response in comparison to type II cells, they responded to the 5-HT stimulus with Ca^{2+} oscillations for a longer period of time (unpublished observations). In contrast, type II cells responded with a large peak Ca^{2+} that was sometimes repeated in an oscillatory manner but, for a much shorter duration in comparison with type I cells (unpublished observations). Usually, Ca^{2+} oscillations are observed during activation of inositol triphosphate (IP_3) triggered intracellular Ca^{2+} release via activation phospholipase C (PLC) coupled to metabotropic receptors. The initial Ca^{2+} peak is the result of the IP_3-induced Ca^{2+} release, while the oscillations are a result of plasmalemmal Ca^{2+} entry or Ca^{2+}-induced Ca^{2+} release from ryanodine receptors or IP_3-gated receptors (Finkbeiner 1993). Type I cell Ca^{2+} oscillations may be the result of 5-HT_{2A} receptor activation, leading to closure of K^+ channels, membrane depolarization (Zhang et al. 2003), and voltage-gated Ca^{2+} entry (Peers and Buckler 1995; Nurse 2005; Nurse 2010). Type II cell Ca^{2+} oscillations are likely the result of Ca^{2+}-induced Ca^{2+} release via IP_3-gated receptors since these oscillations persisted in Ca^{2+}-free media and were sensitive to intracellular store depletion with thapsigargin.

We hypothesized that members of the 5-HT_2 family were likely candidates for the receptor(s) responsible for 5-HT- evoked Ca^{2+} transients seen in both type I and type II cells because these receptors preferentially couple to $G_{q/11}$ to increase cytosolic Ca^{2+} via the IP_3 pathway (Hoyer et al. 2002). Ketanserin, a selective 5-HT_{2A} blocker, reduced the proportion of 5-HT - sensitive type I and type II cells and significantly attenuated the mean Ca^{2+} response. It is well established that ketanserin is a competitive antagonist with an extremely high affinity ($10^{-8.8}$ M) for the 5-HT_{2A} receptor (Hoyer et al. 2002). However, a fairly large concentration of ketanserin (1 μM) did not completely abolish the 5-HT-evoked Ca^{2+} responses in some type I and type II cells, suggesting involvement of other 5-HT receptors. Interestingly the estimated EC_{50} for 5-HT-induced Ca^{2+} responses in type II cells was ~ 183 nM, a value between the EC_{50} values for 5-HT_{2A} and 5-HT_{5A} receptors (EC_{50} for 5-HT_{2A} = 100 nM (Muraoka et al. 1998); EC_{50} for 5-HT_{5A} = 560 nM (Noda et al. 2003). Given a previous report that 5-HT_{5A} receptors are expressed in the rat carotid body (Wang et al. 2000), and can signal via IP_3-sensitive Ca^{2+} stores (Noda et al. 2003), we tested for their possible involvement. Interestingly, the 5-HT_{5A} antagonist, SB 699551 (10 μM), significantly blocked 5-HT-evoked Ca^{2+} responses in type I but had no effect on type II cells. These data suggested that the predominant receptor responsible for 5-HT-evoked Ca^{2+} responses in type II cells is the 5-HT_{2A} receptor. Additional experiments, including immunofluorescence labeling, are required to elucidate the 5-HT receptor profile in type I and type II cells.

5-HT-evoked Ca^{2+} transients in type II cells activate pannexin-1 channels

The 5-HT-induced Ca^{2+} transients in type II cells persisted in Ca^{2+}-free saline and were abolished in the presence of the intracellular store depletion agent, thapsigargin. This suggested that the predominant source of calcium is intracellular. There was a progressive decrease in the intracellular Ca^{2+} response seen with repeated exposures to high doses of 5-HT. However, such run-down was not observed during perforated-patch whole-cell recordings of 5-HT-activated Panx-1 currents. A difference in the application of the agonist may account for the divergent responses observed with the two techniques. During ratiometric calcium imaging the agonist was applied continuously for a minute and this may have favored receptor desensitization. On the other hand, during electrophysiology recordings 'puffs' of the agonist were applied rapidly and only for a few seconds. The 5-HT-activated, non-selective cation current observed was due to the opening

of Panx-1 channels since low doses of the Panx-1 blocker, carbenoxolone (5 µM) (Ma et al. 2009), inhibited the current. 5-HT-evoked Panx-1 activation requires a rise in intracellular Ca^{2+} as demonstrated in experiments where Panx-1 currents were almost completely blocked in the presence of the Ca^{2+} chelator, BAPTA (50 µM). This result is reminiscent of that seen when ATP and ANG II triggered Panx-1 activation in type II cells (Murali et al. 2014). It is unknown whether the link between Ca^{2+} and Panx-1 activation requires binding of the divalent cation directly to the channel or via a secondary mechanism such as PKC. Further electrophysiology studies utilizing specific inhibitors are required to resolve this issue.

In contrast with calcium imaging observations, both the 5-HT_{2A} and 5-HT_{5A} antagonists inhibited 5-HT-activated Panx-1 currents in type II cells. Interestingly, low doses of ketanserin, within the IC_{50} range of the 5-HT_{2A} receptor, was able to completely and reversibly block the Panx-1 current activated by 5-HT. On the other hand, SB 699551 inhibited Panx-1 currents at a concentration 10x the IC_{50} dose of the 5-HT_{5A} receptor; this effect may result from a non-specific block of the Panx-1 channel by the drug (M. Zhang; unpublished observations) Despite the fact that the 5-HT_{5A} receptor is capable of IP_3-Ca^{2+} signaling (Noda et al. 2003), it does not significantly contribute to the 5-HT-evoked Ca^{2+} transients seen in type II cells. However, the 5-HT_{5A} receptor is capable of signaling through multiple pathways, and it may activate a secondary signaling pathway (e.g. PKA, Src kinase) that may be necessary for Panx-1 activation (Adayev et al. 2005; Weilinger et al. 2012). Further studies are required to clarify whether the 5-HT_{5A} receptor has a physiological role in type II cells.

Physiological significance and clinical significance

The observations in this study suggest that 5-HT signaling in type II cells occurs via a G-protein coupled 5-HT_{2A} (and/or 5-HT_{5A}) receptor, coupled to the phosphatidyl inositol-IP_3 pathway, leading Panx-1 channel activation. Previous studies have demonstrated that open Panx-1 channels in type II cells act as conduits for release of the CB excitatory neurotransmitter, ATP (Nurse 2010; Zhang et al. 2012; Nurse and Piskuric 2013). Thus, paracrine activation of 5-HT receptors on type II cells may serve to enhance CB excitation by promoting further ATP release. While the role of 5-HT signaling during acute hypoxia is questionable, 5-HT is a critical neuromodulator during chronic intermittent hypoxia (CIH), a situation that mediates long-lasting

activation or long-term facilitation (LTF) of the CB chemoreflex. Acute hypoxia releases 5-HT from CIH- treated CBs and this response involves the mobilization of intracellular Ca^{2+} stores (Peng et al. 2009). Furthermore, repetitive applications of 5-HT for short periods of time evoked sensory LTF in control CBs and the effect was inhibited by the 5-HT_{2A} antagonist, ketanserin (Peng et al. 2006). Pathophysiological conditions that mimic CIH, such as central or obstructive sleep apnea and asthmatic attacks, elicit a progressive increase in respiratory motor output and autonomic dysfunction that result in elevated blood pressure, myocardial infarcts, and stroke (Nieto et al. 2000; Shahar et al. 2001). It is plausible that during these pathophysiological conditions, 5-HT released by type I cells activate Panx-1 channels on type II cells to boost CB chemosensory drive and thereby contribute to exacerbation of the disease progression.

Figure 1. Comparison of type I and type II 5-HT-evoked Ca^{2+} responses. In A, 5-HT (10 µM) causes a rise in intracellular Ca^{2+} ($[Ca^{2+}]_i$) in both a type II cell and a type I cell in the same culture; note that the type II cell (indicated by the yellow arrow), which responds to UTP but not high K^+, elicits a more robust Ca^{2+} response than the type I cell (indicated by the red arrow); the type I cell responds to high K^+ but not UTP. Comparison of the peak ± s.e.m $[Ca^{2+}]_i$ responses in type II versus type I cells after exposure to 10 µM 5-HT is shown in B (n = 12 dishes; 20-30 cells sampled per dish).

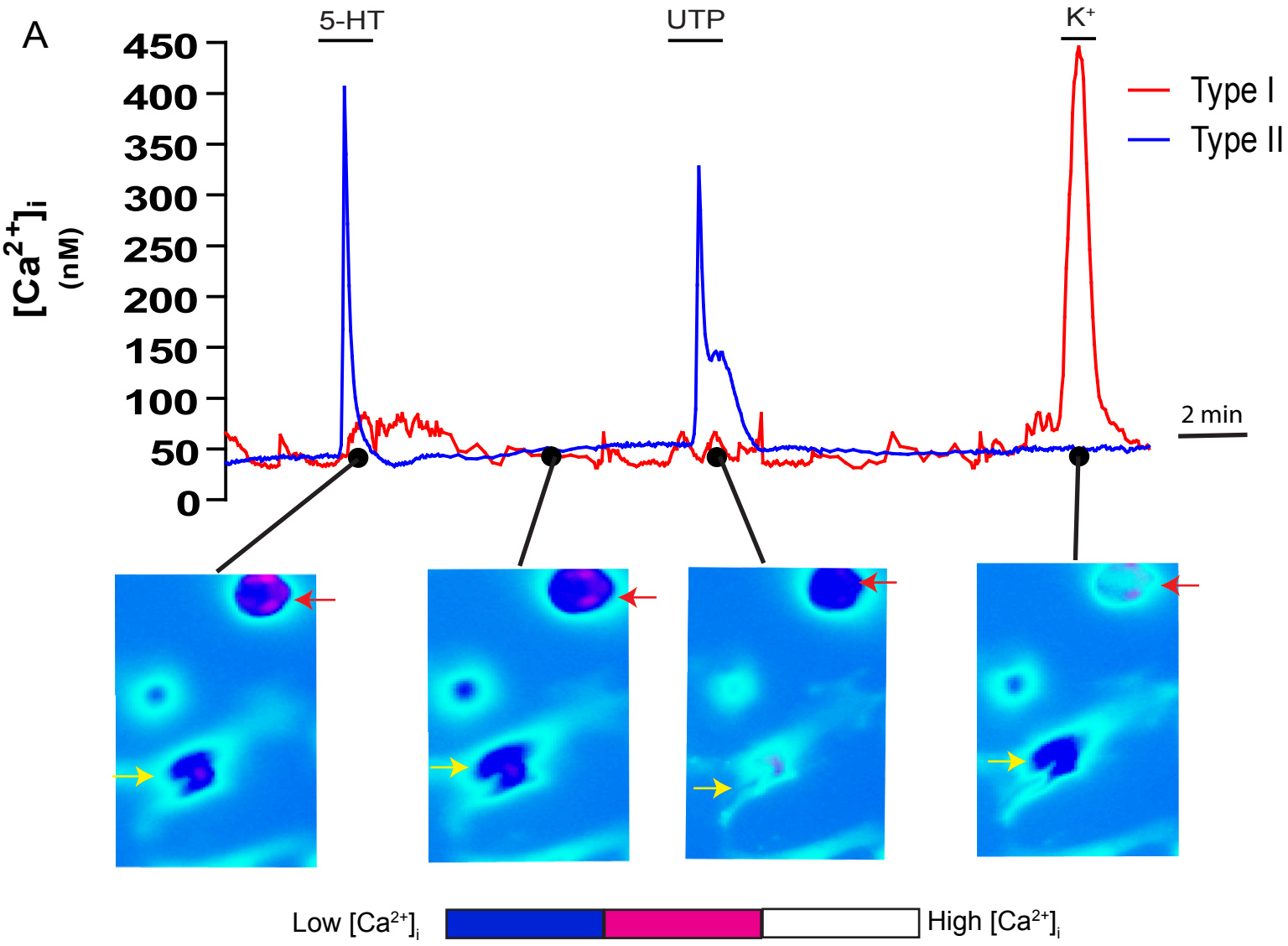
A
5-HT
UTP
K+
Type I
Type II
[Ca2+]i (nM)
450
400
350
300
250
200
150
100
50
0
2 min
Low [Ca2+]i
High [Ca2+]i

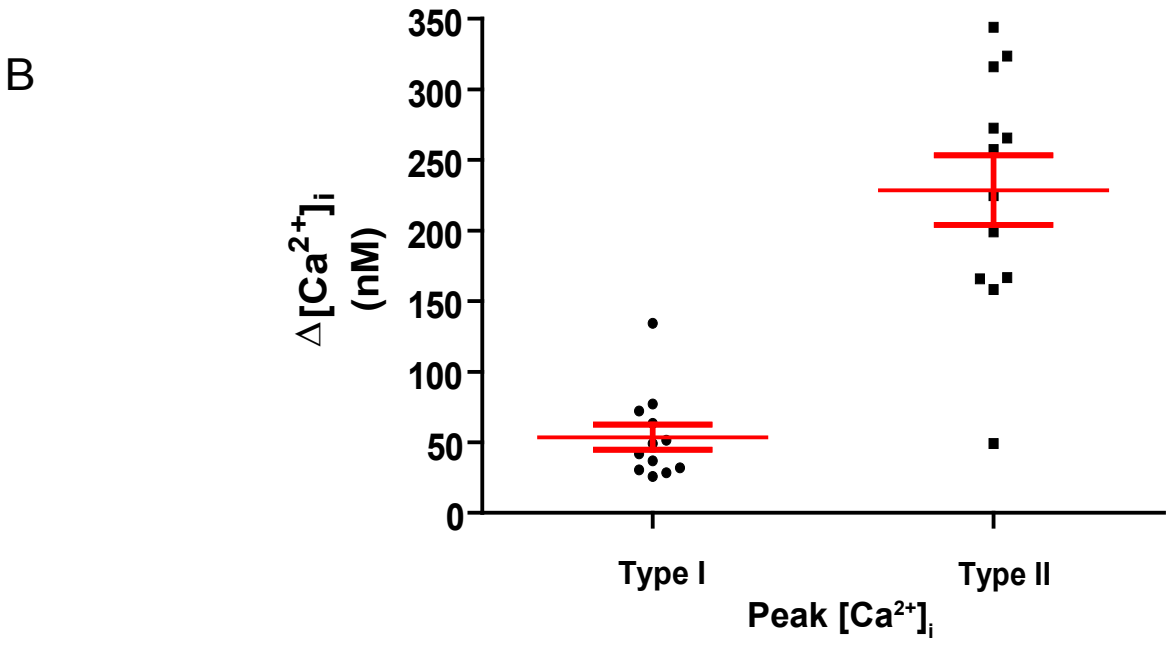
B
Δ[Ca2+]i (nM)
350
300
250
200
150
100
50
0
Type I
Type II
Peak [Ca2+]i

Figure 2. Effects of 5-HT on intracellular calcium transients in type II cells. The effects of increases doses of 5-HT (10 nM, 100 nM, 1 µM, 5 µM, 10 µM) on intracellular Ca^{2+} concentration ($[Ca^{2+}]_i$) in a type II cell is shown in A. B. Dose-response relation for 5-HT-induced $\Delta[Ca^{2+}]_i$ in type II cells; a fit of the dose-response curve with the Hill equation yielded an EC_{50} = 183 nM (n = 15 dishes). C. Decrease in $[Ca^{2+}]_i$ responses in type II cells with repeated exposures to 10 µM 5-HT, attributable to receptor desensitization. D. Time-course of the reduction in $\Delta[Ca^{2+}]_i$ responses in type II cells after 1, 6, and 11 min exposure to 10 µM 5-HT; *** $p < 0.001$, Friedman Test with Dunn's Multiple Comparison *post hoc* test.

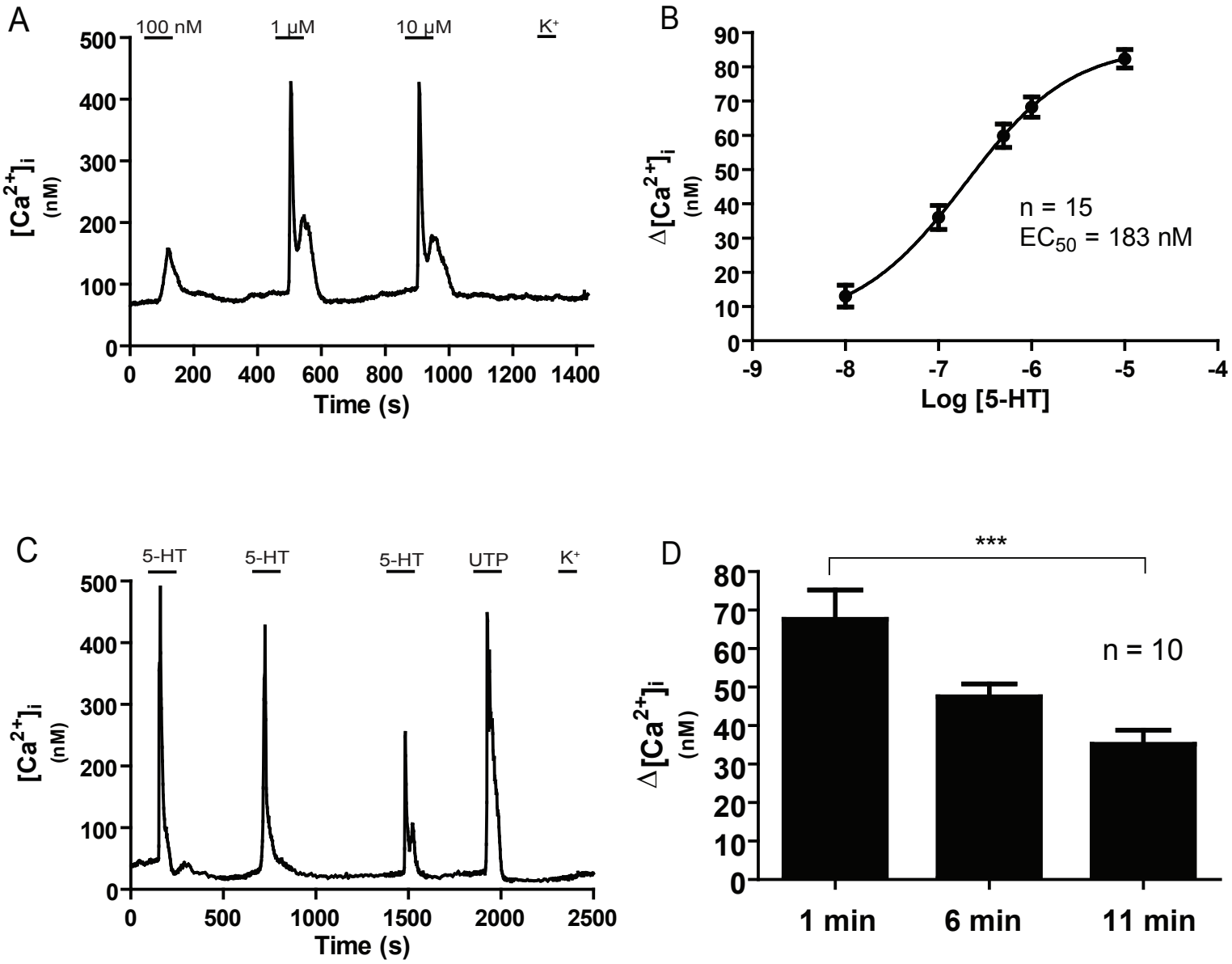
A
100 nM
1 µM
10 µM
K+
[Ca2+]i (nM)
Time (s)
B
Δ[Ca2+]i (nM)
n = 15
EC50 = 183 nM
Log [5-HT]
C
5-HT
5-HT
5-HT
UTP
K+
[Ca2+]i (nM)
Time (s)
D
***
Δ[Ca2+]i (nM)
n = 10
1 min
6 min
11 min

Figure 3. 5-HT evoked Ca^{2+} responses in both type I and type II cells are partially inhibited by ketanserin.. A, an exemplar Ca^{2+}-imaging trace demonstrating that ketanserin (1μM), a selective 5-HT_{2A} antagonist, completely blocked 5-HT-induced Ca^{2+} transients in this particular type I and type II cell from the same cluster. A complete inhibition of the Ca^{2+} response in both type I and type II cells was not always the case as seen in the cumulative data in B and C. The 5-HT-evoked Ca^{2+} responses in type II and type I cells are significantly inhibited by ketanserin; summary data are shown in B & C. * indicates $p < 0.05$; ** $p < 0.01$; *** $p < 0.001$.

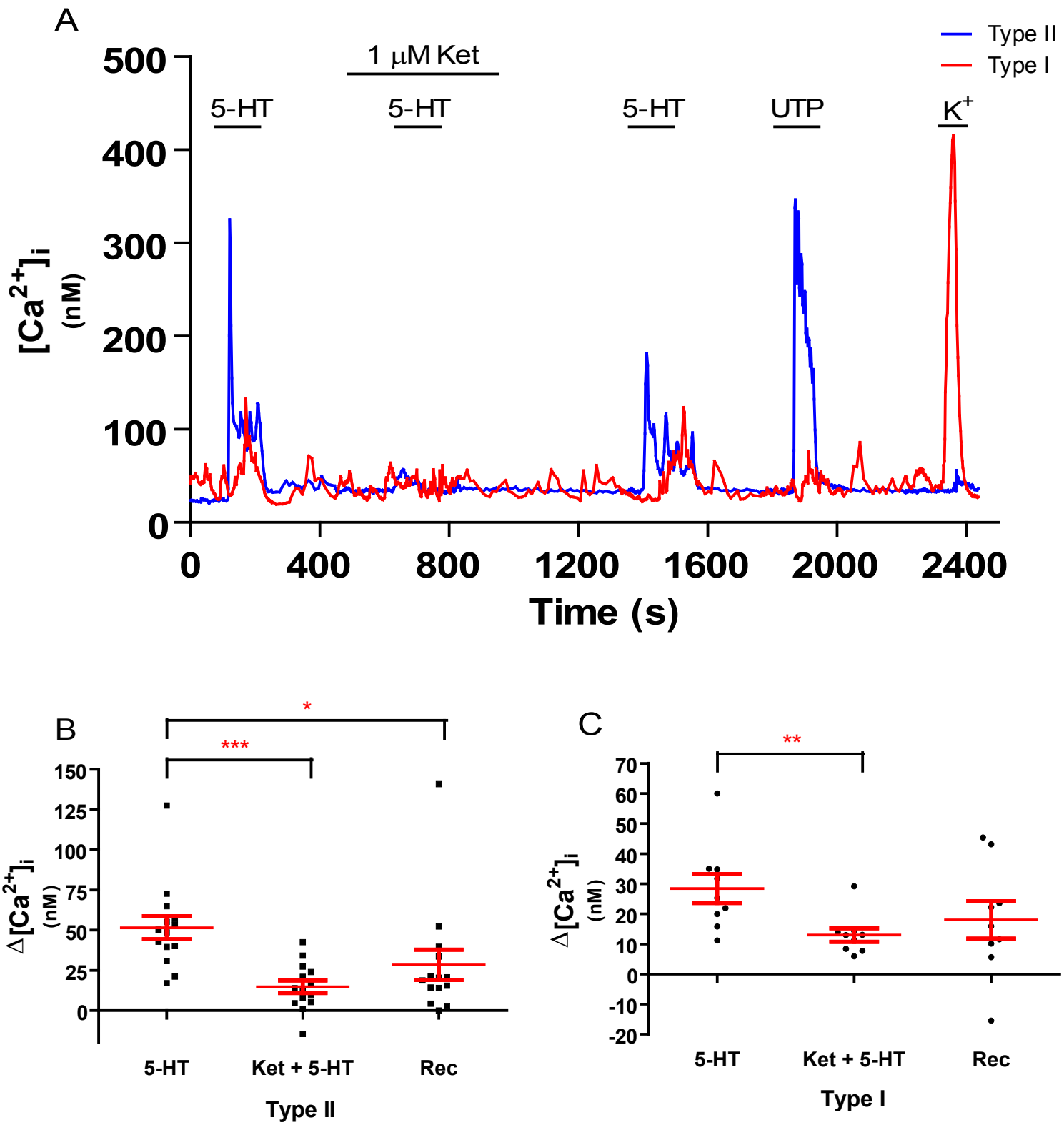
A
Type II
Type I
1 μM Ket
5-HT
5-HT
5-HT
UTP
K+
500
400
300
200
100
0
[Ca2+]i (nM)
0
400
800
1200
1600
2000
2400
Time (s)
B
*
***
150
125
100
75
50
25
0
Δ[Ca2+]i (nM)
5-HT
Ket + 5-HT
Rec
Type II
C
**
70
60
50
40
30
20
10
0
-10
-20
Δ[Ca2+]i (nM)
5-HT
Ket + 5-HT
Rec
Type I

Figure 4. SB 699551, a selective 5-HT_{5A} receptor antagonist, inhibits 5-HT-evoked Ca^{2+} responses in type I cells, but not type II cells. A, an exemplar Ca^{2+}-imaging trace demonstrating that 10 μM SB 699551, a selective 5-HT_{5A} antagonist, completely blocked 5-HT-induced Ca^{2+} transients in the type I cell but not the type II cell. In B, the 5-HT-induced rise in $[Ca^{2+}]_i$ in type I cells was reversibly inhibited by SB 699551; * indicates $p < 0.05$. C, a comparison of the mean ± s.e.m. of the $[Ca^{2+}]_i$ response in type II cells in the presence and absence of SB 699551 were significantly similar ($p > 0.05$).

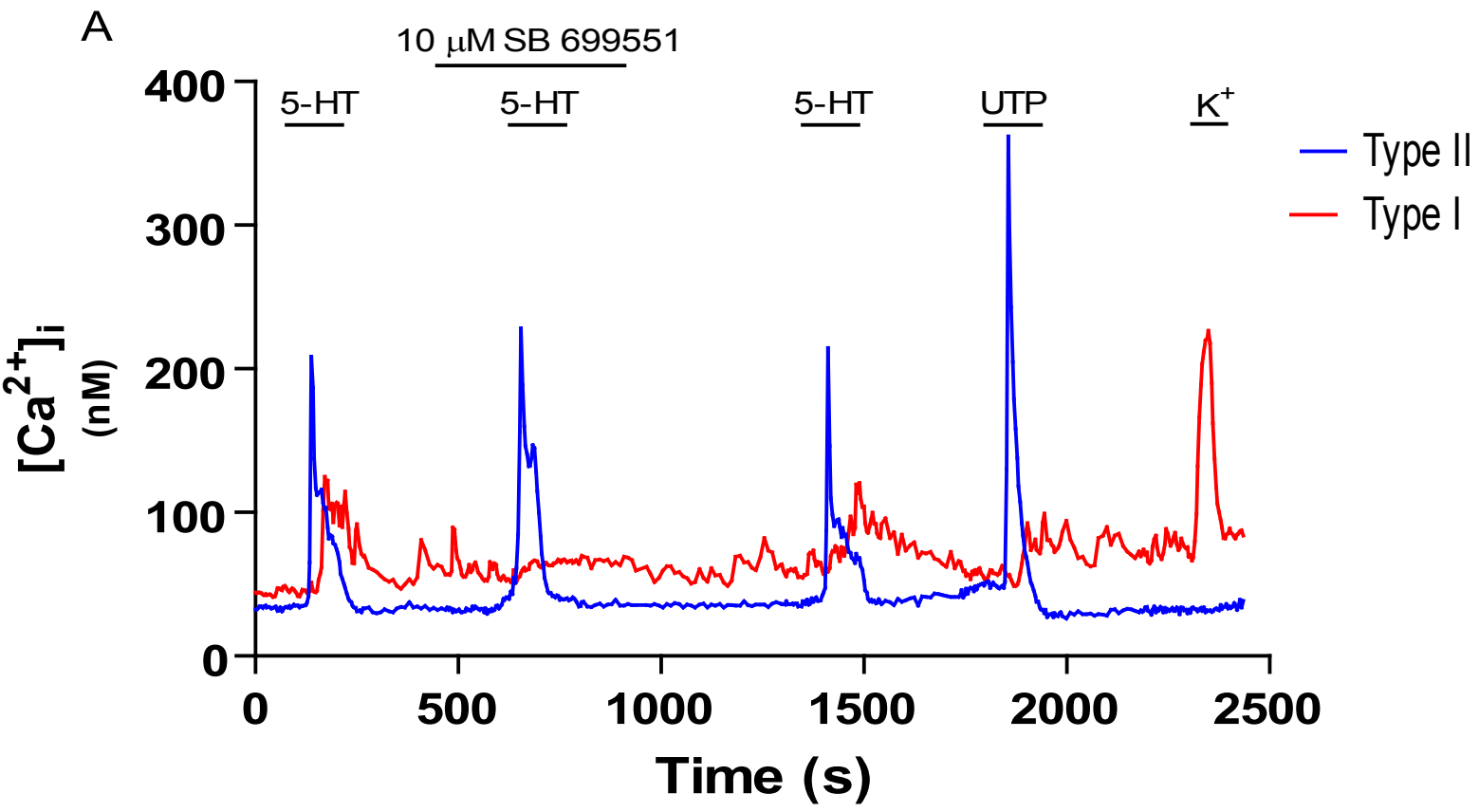
A
10 μM SB 699551
5-HT
5-HT
5-HT
UTP
K+
Type II
Type I
400
300
200
100
0
[Ca2+]i (nM)
0
500
1000
1500
2000
2500
Time (s)

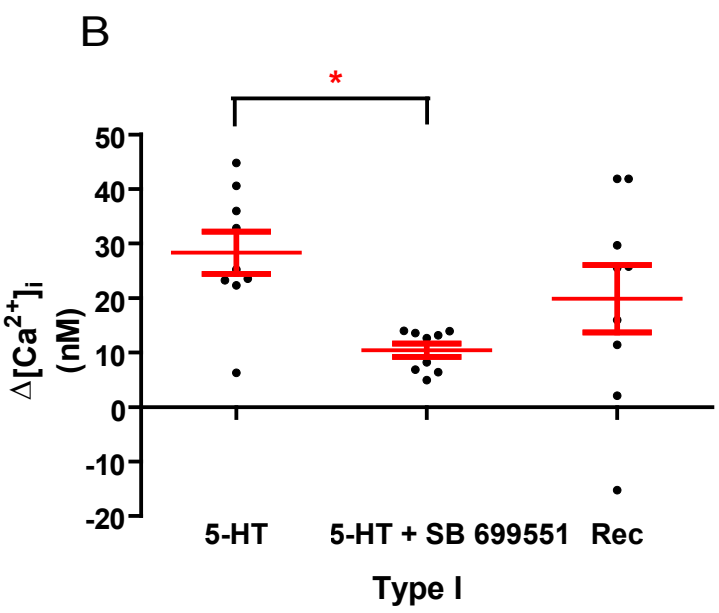
B
*
50
40
30
20
10
0
-10
-20
Δ[Ca2+]i (nM)
5-HT
5-HT + SB 699551
Rec
Type I

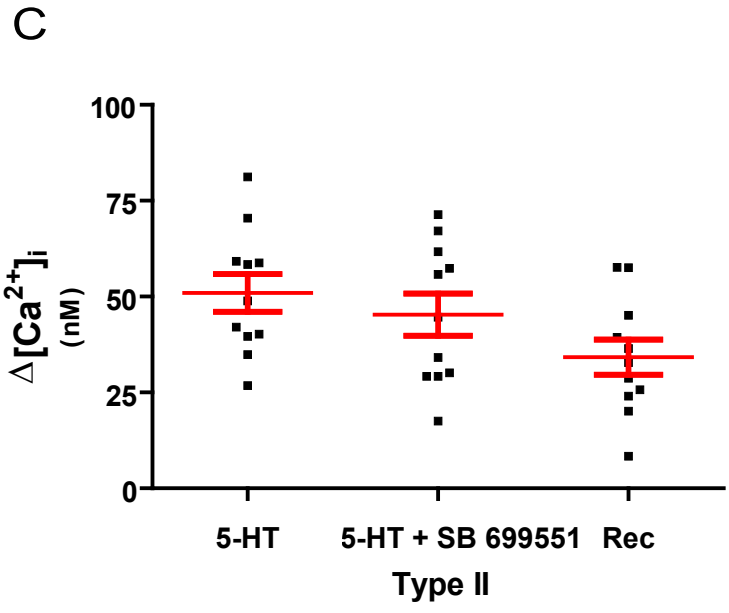
C
100
75
50
25
0
Δ[Ca2+]i (nM)
5-HT
5-HT + SB 699551
Rec
Type II

Figure 5. Role of intracellular stores in 5-HT-induced rise in $[Ca^{2+}]_i$ in type II cells. In A, the 5-HT-induced rise in $[Ca^{2+}]_i$ persists in solution containing nominally-free extracellular Ca^{2+} (0 Ca^{2+}); summary data of mean ± s.e.m. Ca^{2+} responses from 9 dishes are shown in B. In C, the 5-HT-induced rise in $[Ca^{2+}]_I$ is inhibited by thapsigargin (Thaps; 1 μM); summary data was obtained from 12 dishes. ** indicates $p < 0.01$; *** $p < 0.001$.

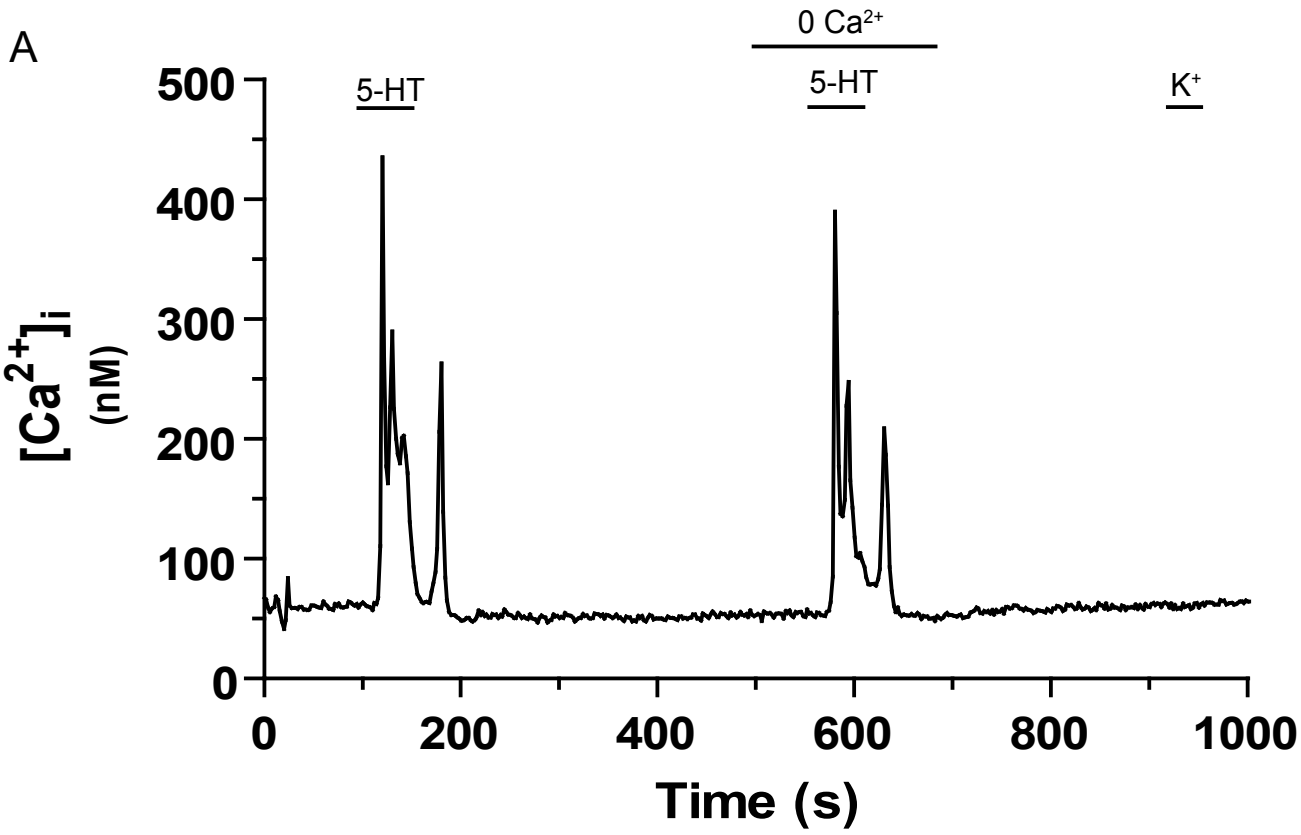
A
0 Ca2+
5-HT
5-HT
K+
500
400
300
200
100
0
[Ca2+]i
(nM)
0
200
400
600
800
1000
Time (s)

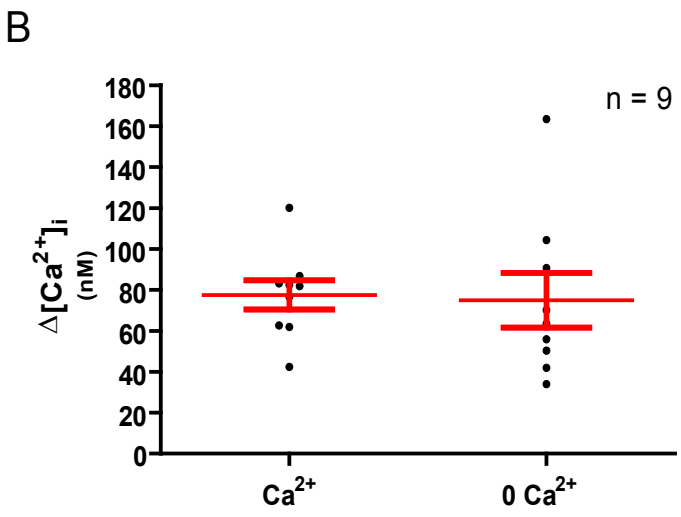
B
n = 9
180
160
140
120
100
80
60
40
20
0
Δ[Ca2+]i
(nM)
Ca2+
0 Ca2+

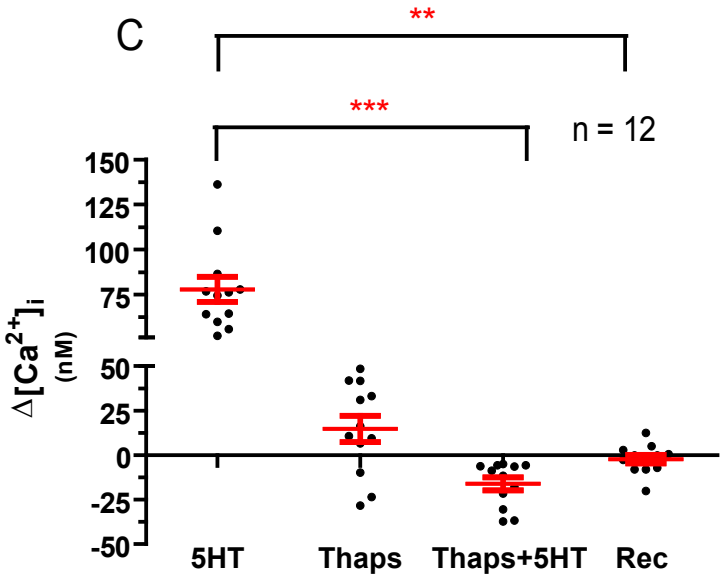
C
**
***
n = 12
150
125
100
75
50
25
0
-25
-50
Δ[Ca2+]i
(nM)
5HT
Thaps
Thaps+5HT
Rec

Figure 6. Reversal potential of 5-HT-induced current in type II cells. A, exemplar traces of whole-cell currents evoked by 5 µM 5-HT at different membrane potentials. B, current-voltage (I-V) plot of 5-HT-evoked currents for a group of 5 type II cells showing a mean reversal potential at -11 mV, consistent with the opening of non-selective ion channels.

A

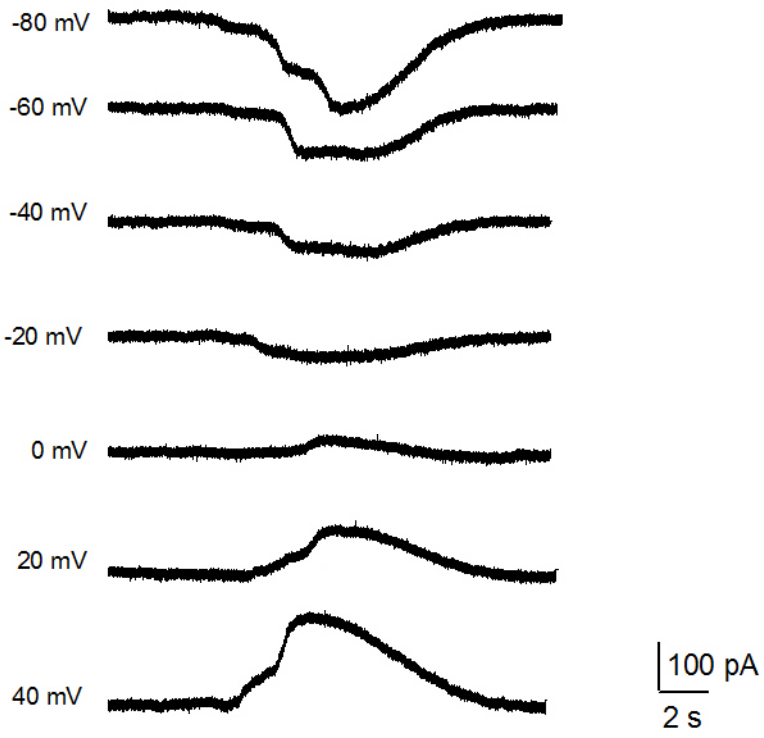
-80 mV
-60 mV
-40 mV
-20 mV
0 mV
20 mV
40 mV
100 pA
2 s

B

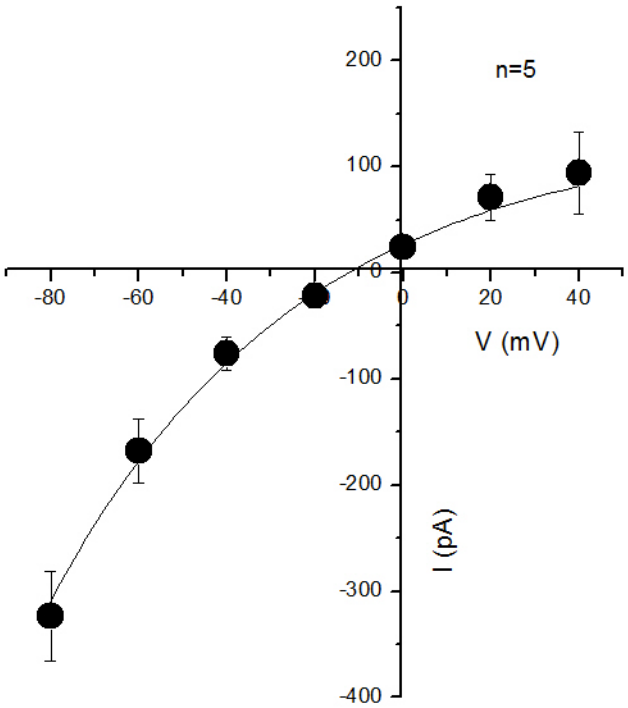
n=5
200
100
0
-100
-200
-300
-400
-80
-60
-40
0
20
40
V (mV)
I (pA)

Figure 7. Effect of pharmacological blocker of Panx-1 channels on 5-HT-evoked whole-cell currents in type II cells. The selective Panx-1 inhibitor carbenoxolone (CBX; 5 µM) caused a slowly developing blockade of the inward current induced by 5 µM 5-HT (at -60 mV holding potential) in A. Note the blockade was readily reversible and developed gradually over a period of 6 min. A histogram of the pooled current density (pA/pF) data for a group for 3 cells before, during, and after CBX is summarized in B. *** indicates $p < 0.001$.

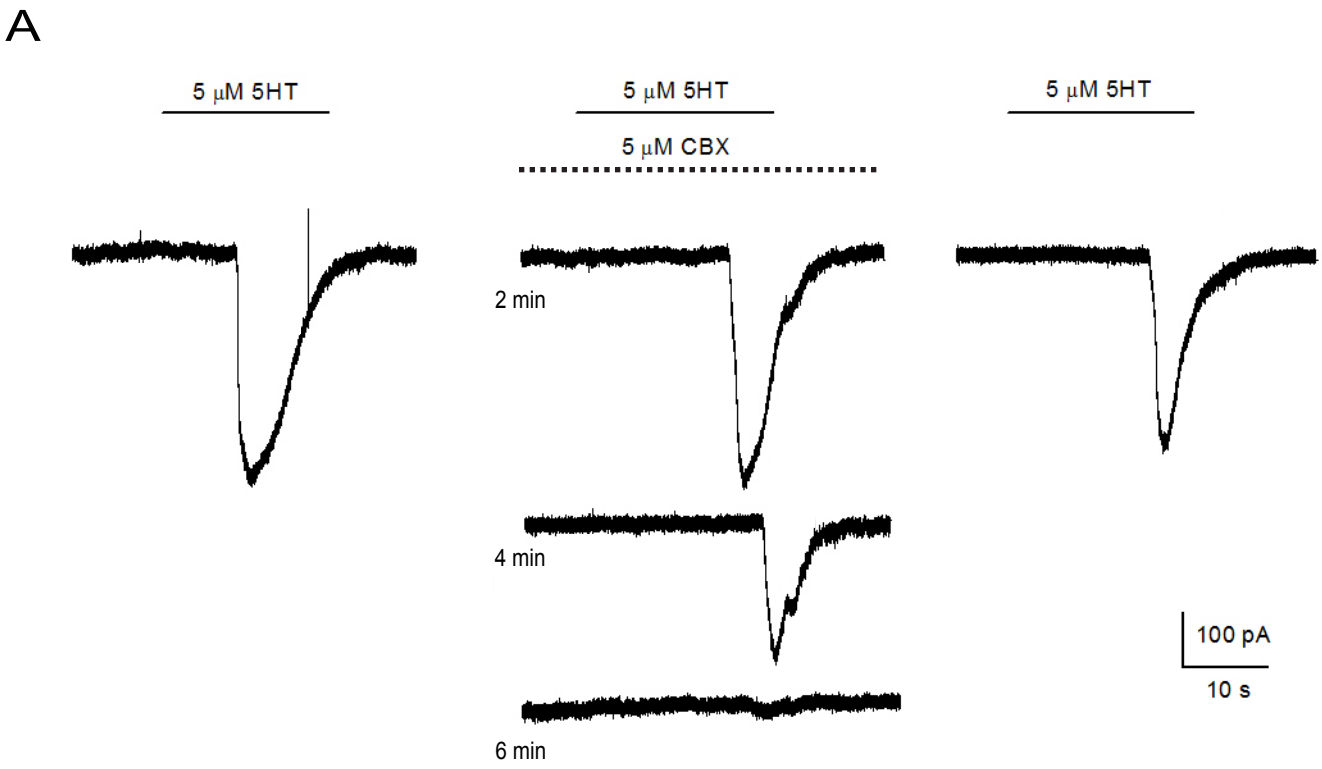
A
5 μM 5HT
5 μM 5HT
5 μM CBX
5 μM 5HT
2 min
4 min
6 min
100 pA
10 s

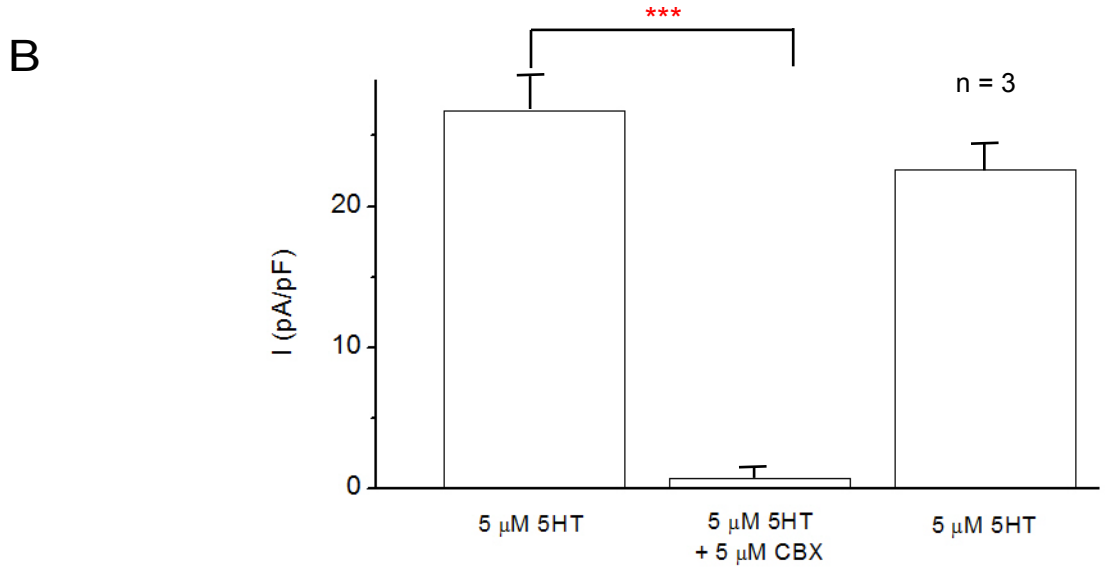
B
***
n = 3
I (pA/pF)
20
10
0
5 μM 5HT
5 μM 5HT
+ 5 μM CBX
5 μM 5HT

Figure 8. Blockade of 5-HT-induced inward currents in type II cells by ketanserin. In A, the inward current elicited by 5 μM 5-HT at -60 mV (holding potential) was reversibly inhibited in a type II cell by increasing doses of ketanserin; a complete block was obtained at 10 nM ketanserin. Pooled current density (pA/pF) data for a group of 5 cells before, during 1 nM, 5 nM, and 10 nM ketanserin, are summarized in B. *** indicates $p < 0.001$.

A

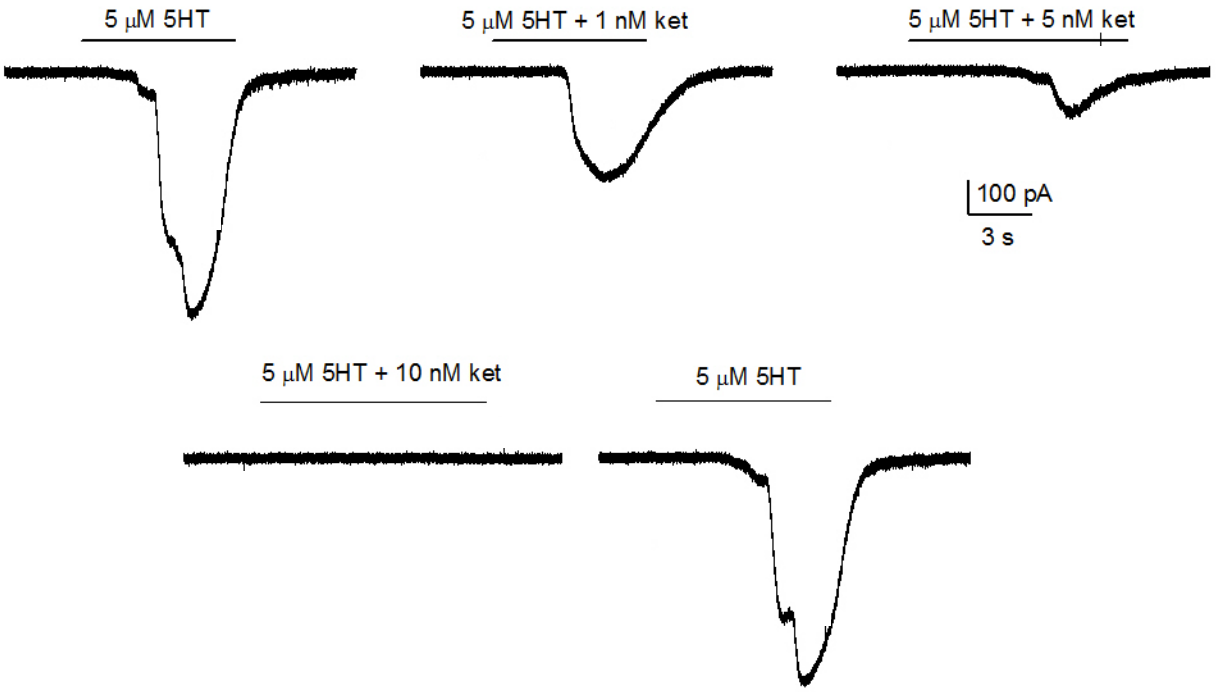
5 μM 5HT
5 μM 5HT + 1 nM ket
5 μM 5HT + 5 nM ket
100 pA
3 s
5 μM 5HT + 10 nM ket
5 μM 5HT

B

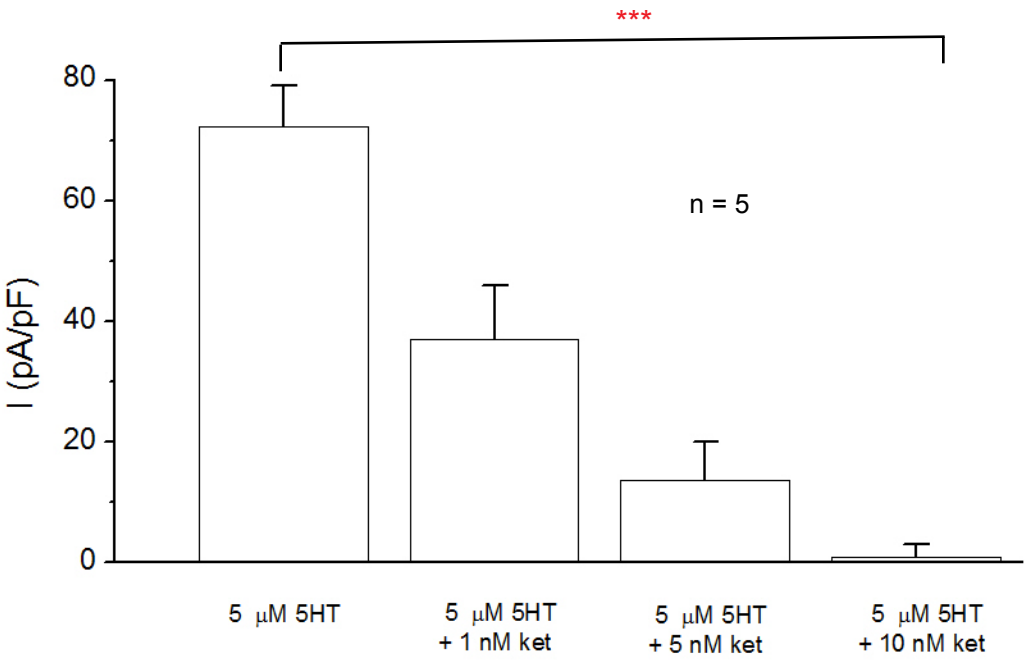
***
80
60
40
20
0
I (pA/pF)
n = 5
5 μM 5HT
5 μM 5HT + 1 nM ket
5 μM 5HT + 5 nM ket
5 μM 5HT + 10 nM ket

Figure 9. Chelating intracellular Ca^{2+} in type II cells with BAPTA prevents Panx-1 current activation by 5-HT. In A1, repeated application of 10 µM 5-HT to the same cell over a 10 min period (t = 1 min, left, t = 3 min, middle; t = 10 min, right) produced similar peak currents (at – 60 mV holding potential). In A2, the pipette was withdrawn, and the *same* cell was studied with a second pipette containing 50 µM BAPTA; note the progressive, time-dependent decline of 5-HT-induced Panx-1 current at 3 min (n = 1).

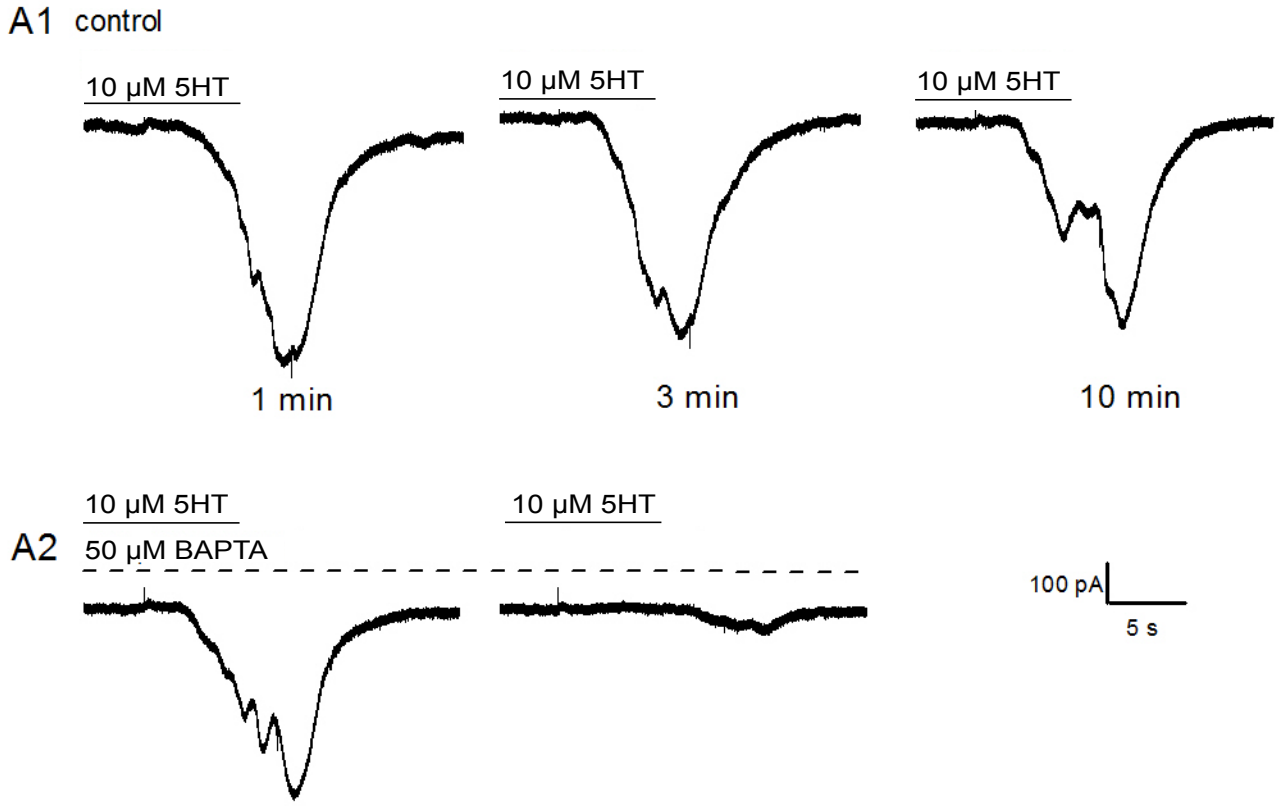
A1 control
10 μM 5HT
10 μM 5HT
10 μM 5HT
1 min
3 min
10 min
A2
10 μM 5HT
50 μM BAPTA
10 μM 5HT
100 pA
5 s

CHAPTER 4

Purinergic mechanisms contribute to bidirectional cross-talk between chemoreceptor and glial cells of rat carotid body

Sindy Murali & Colin A. Nurse

The work in this chapter is in preparation for submission.

I performed all Ca^{2+} imaging experiments, data analysis, preparation of figures, and wrote the manuscript. C.A.N. was involved in the planning and designing of the all the experiments, helped interpret the data, edited and approved the final version of this manuscript.

ABSTRACT

The mammalian carotid body (CB) is an arterial chemoreceptor organ consisting of chemoreceptor type I cells in intimate association with glial-like type II cells. The processes of type II cells ensheath type I cell clusters, raising the possibility of paracrine cell-to-cell interactions. Though type II cells selectively express metabotropic P2Y2 receptors that can be activated by a key CB neurotransmitter ATP, leading to 'ATP-induced ATP release' via pannexin-1 (Panx-1) channels (Zhang et al. 2012), there is no direct evidence that type I and type II cells actually communicate during chemotransduction. In the present study, we first examined whether type I cells of the rat CB can signal type II cells during sensory transduction, and second, whether type II cells may in turn reciprocate and signal type I cells via Panx-1 channels. Within chemoreceptor clusters, stimulation of type I cells using the chemostimulus isohydric hypercapnia, or the depolarizing stimulus high K^+, led to a rise in intracellular Ca^{2+} ($\Delta[Ca^{2+}]_i$) in type I cells, and a delayed, secondary rise in $\Delta[Ca^{2+}]_i$ in contiguous type II cells. Application of the P2Y2R antagonist suramin (100 µM) reversibly inhibited or abolished the delayed response in type II cells and reduced type I cell Ca^{2+} responses. Likewise, selective stimulation of type II cells with the P2Y2R agonist UTP (100 µM) sometimes led to a delayed, secondary $\Delta[Ca^{2+}]_i$ response in nearby type I cells. As expected, the Panx-1 channel blocker, carbenoxolone (5 µM) reversibly inhibited the UTP-evoked secondary Ca^{2+} responses in type I cells, but was without effect on type II cells. Interestingly, this secondary type I cell response could also be reversibly inhibited by a combination of selective adenosine A_{2A} and A_{2B} receptor antagonists. Taken together, these data strongly support the notion that reciprocal cross-talk involving purinergic signaling can occur between type I and type II cells, and that type I cells communicate with type II cells during sensory transduction.

INTRODUCTION

Peripheral chemoreceptors within mammalian carotid bodies (CBs) sense the chemical composition of arterial blood, i.e. O_2, CO_2/H^+, and glucose levels, and maintain homeostasis via afferent pathways that mediate respiratory and cardiovascular reflexes (Gonzalez et al. 1994; López-Barneo et al. 2001; Kumar and Prabhakar 2012). The bilaterally-paired CBs are located at the bifurcation of the common carotid arteries and receive sensory innervation from the petrosal ganglion via the carotid sinus nerve (McDonald 1981). Within the CB, clusters of chemoreceptor type I cells are found in intimate association with glia-like type II cells in a ratio of approximately 4:1 (McDonald and Mitchell 1975; McDonald 1981). Chemostimuli such as hypoxia (low PO_2) and acid hypercapnia (high CO_2/H^+) depolarize type I cells, leading to Ca^{2+}-dependent release of a variety of neurotransmitters and neuromodulators that help shape the afferent sensory discharge (Gonzalez et al. 1994; Nurse 2005; Nurse 2010). Among these neurochemicals is the key excitatory neurotransmitter, ATP, which activates ionotropic P2X2/3 receptors on petrosal afferent terminals (Nurse 2005; Nurse 2010). Adenosine, generated via breakdown of extracellular ATP or released from type I cells via equilibrative transporters (Conde & Monteiro, 2004), contributes further to CB excitation by activating adenosine A_2 receptors located on type I cells and/or petrosal terminals.

It has been hypothesized that glial-like type II cells may also participate in paracrine signaling in the CB, in part because they express G-protein-coupled receptors for several neuromodulators expressed in type I cells. These neuromodulators include ATP, ACh, angiotensin II (Xu et al. 2003; Tse et al. 2012; Zhang et al. 2012; Murali et al. 2014), and 5-HT (this thesis, Chapter 3). Thus, during exogenous application of agonists for purinergic P2Y2 receptors (e.g. ATP or UTP) or angiotensin AT1 receptors (e.g. angiotensin II), type II cells respond with a rise in intracellular Ca^{2+} (Xu et al. 2003; Zhang et al. 2012; Murali et al. 2014). In both instances, activation of the signaling cascade leads to the opening of large-pore pannexin-1 (Panx-1) channels, which act as conduits for the further release of ATP (Zhang et al. 2012; Murali et al. 2014). While these data raise the attractive possibility that paracrine stimulation of type II cells

may contribute to CB excitation via ATP efflux through Panx-1 channels, there is no direct evidence that type I cells actually communicate with type II cells during sensory transduction.

In the present study, we explore the possibility of cross-talk between receptor type I and glial-like type II cells in the rat CB. As a first step, we investigated whether direct stimulation of type I cells with chemostimuli such as high CO_2 (hypercapnia), or the depolarizing agent high K^+, might *indirectly* stimulate adjacent type II cells as a result of 'purinergic' cross-talk. Secondly, we asked whether selective stimulation of type II cells with P2Y2R agonists could result in reciprocal cross-talk, leading to *indirect* responses in type I cells via Panx-1 channels. To address these questions, we applied ratiometric calcium imaging techniques using an *in vitro* preparation of dissociated rat CB containing clusters of type I and contiguous type II cells. In summary, we obtained compelling evidence for paracrine signaling and cross-talk between type I and type II cells involving purinergic mechanisms.

METHODS

Ethical approval

All procedures for animal handling and tissue dissections were carried out according to the guidelines of the Canadian Council on Animal Care (CCAC) and institutional guidelines.

Cell cultures of dissociated rat carotid body

Carotid bifurcations from 9-14 day old rats (Wistar, Charles River, Quebec, Canada) were excised bilaterally, after the animals were first rendered unconscious by a blow to the back of the head, followed immediately by decapitation. The carotid bodies (CBs) were isolated from the surrounding tissue and dissociated cell cultures prepared according to established procedures, described in detail elsewhere (Zhong et al. 1997; Zhang et al. 2000). Briefly, the excised CBs were incubated for 1 h at 37°C in a physiological salt solution containing 0.1% trypsin (Sigma-Aldrich, Oakville, Ontario, Canada) and 0.1% collagenase (Gibco, Grand Isalnd, NY, USA), followed by mechanical dissociation and trituration. The dispersed cell suspension was allowed to adhere to the central wells of modified tissue culture dishes; the wells were pre-coated with a thin layer of

Matrigel (BD Biosciences, Mississauga, Ontario, Canada). The cells were cultured in basic growth medium (BGM) consisting of F-12 nutrient medium supplemented with 10% fetal bovine serum, 1% penicillin-streptomycin, 1% glutamine, 0.3% glucose, and 3 µg ml^{-1} insulin, as in previous studies (Zhang et al. 2000; Zhang et al. 2012).

Intracellular Ca^{2+} measurements

Intracellular free Ca^{2+} concentration ($[Ca^{2+}]_i$) was monitored using the fluorescent Ca^{2+} indicator fura-2 AM (Molecular Probes, Eugene, OR, USA), as previously described (Piskuric and Nurse 2012; Zhang et al. 2012). Cells were loaded with 2.5 µM fura-2 AM diluted in standard bicarbonate-buffered solution (BBS) for 30 min at 37°C, and subsequently washed for ~15 min to remove free dye. The BBS used in Ca^{2+} imaging experiments had the following composition (in mM): $NaHCO_3$, 24; NaCl, 115; glucose,5; KCl, 5; $CaCl_2$, 2 and $MgCl_2$, 1; the pH was maintained at ~7.4 by bubbling with a 5% CO_2-95% air mixture. Ratiometric Ca^{2+} imaging was performed using a Nikon Eclipse TE2000-U inverted microscope (Nikon, Mississauga, ON, Canada) equipped with Lambda DG-4 ultra-high-speed wavelength changer (Sutter Instrument CO., Novato, CA, USA), a Hamamatsu OCRCA-ET digital CCD camera (Hamamatsu, Sewickley, PA, USA) and a Nikon S-Fluor 40x oil-immersion objective lens with a numerical aperture of 1.3. Dual images at 340 nm and 380 nm excitation (510 emission) were acquired every 2 s, with an exposure time of 100-200 ms. Pseudocolour ratiometric data were obtained using Simple PCI software version 5.3. All experiments were performed at 35-37°C, and cells were continuously perfused with BBS to maintain an extracellular pH of ~7.4.

The imaging system was calibrated using the Fura-2 Calcium Imaging Calibration Kit from Molecular Probes (Cat. No. F-6774). Photometric data at 340 nm and 380 nm excitation (510 emission) were obtained for 11 buffers of known Ca^{2+} concentrations from Ca^{2+}-free (0 µM) to saturating Ca^{2+} (39 µM). After correcting for background fluorescence, these values were used to calculate the following ratios as follows: 'R' is the 510 nm emission intensity at 340 nm excitation to 510 nm emission intensity at 380 nm excitation; R_{min}, the ratio at zero free Ca^{2+}; R_{max} the ratio at saturating Ca^{2+}; and β, the fluorescence intensity with excitation at 380 nm for zero free Ca^{2+} (F_{380max}), to the fluorescence intensity at saturating free Ca^{2+} (F_{380min}). The intracellular free $[Ca^{2+}]$

was obtained after substituting these ratios into the Grynkiewicz equation (Grynkiewicz et al. 1985) as follows:

$$[Ca^{2+}]_i = K_d \frac{[R - R_{\min}]}{[R_{\max} - R]} \beta$$

where R_{min} = 0.18, R_{max} = 7.81, β = 12.29, K_d = 225 nM and R is the ratio obtained during the experiment for a given cell. For most experiments statistical analysis was performed using Repeated Measures ANOVA with Tukey's Multiple Comparison Test *post hoc* test, as indicated in text. The n values indicated within the figures represents the number of dishes; 20-30 cells were imaged per a dish.

Reagents and drugs

Cells were perfused with standard BBS containing (in mM): 24 $NaHCO_3$, 115 NaCl, 5 glucose, 5 KCl, 2 $CaCl_2$, and 1 $MgCl_2$, and pH was maintained at ~ 7.4 by bubbling 5% CO_2 – 95% air mixture. Isohydric hypercapnia was generated by doubling the concentration of $NaHCO_3$ to 48 mM (maintaining osmolarity by reducing NaCl to 91 mM) and aerating with 10% CO_2 – 90% air (pH ~ 7.4). The following reagents and drugs obtained from Sigma-Aldrich (Oakville, ON): UTP, carbenoxolone (CBX), and suramin, SCH58261, and MRS 1754.

RESULTS

Chemostimulation or depolarization of type I cells can elicit indirect 'secondary' responses in contiguous type II cells

Solitary type II cells, well isolated from receptor clusters, do not normally respond *directly* to chemostimuli such as hypoxia and acid hypercapnia (Piskuric & Nurse, 2012), or the depolarization agent high K^+ (30 mM) (Fig. 1A & B). However, in general, type II cells can be uniquely identified by the presence of a rapid and robust rise in intracellular Ca^{2+} ($\Delta[Ca^{2+}]_i$) during application of the P2Y2R agonist, UTP (100 µM) (Xu et al. 2003; Zhang et al. 2012). To determine

whether type I cells can communicate with contiguous type II cells during sensory transduction, we *simultaneously* imaged several cells within receptor clusters while applying the chemostimulus, isohydric hypercapnia (10% CO_2; pH=7.4). As expected from previous studies (Buckler and Vaughan-Jones 1994; Piskuric and Nurse 2012), and exemplified in Fig. 1C & D, type I cells frequently responded to isohydric hypercapnia with a robust rise in intracellular Ca^{2+} ($\Delta[Ca^{2+}]_i$). Figure 1C & D also illustrates that, in contrast to their 'solitary' counterparts, a UTP-sensitive type II cell near the cell cluster responded to the *same* chemostimulus with a smaller, but significant $\Delta[Ca^{2+}]_i$. Data pooled from many similar examples revealed that the mean $\Delta[Ca^{2+}]_i$ response (73 nM) of type I cells was significantly greater than that (33 nM) of type II cells (Mann-Whitney test, $p < 0.001$; Figure 1E). Notably, the type II cell response was always delayed relative to that in the type I cell, consistent with cross-talk from type I to type II cells. A comparison of the relative latencies of type I versus type II cell responses to isohydric hypercapnia is shown in Fig. 2B; the positive value of the mean latency difference indicates that the '*follower*' type II cell responses were delayed by 10.5 ± 2.7 sec relative to the '*driver*' type I cell responses (n = 17 dishes; Kruskal-Wallis Test with Dunn's Multiple Comparison *post hoc* test, $p < 0.05$). Taken together, these data are consistent with the notion that chemostimulation of CB receptor type I cells can lead to the secondary activation of neighboring type II cells via paracrine mechanisms. As discussed later, direct stimulation of type II cells with UTP, as illustrated in Fig. 1D, may also lead to paracrine secondary activation of type I cells.

We next determined whether depolarization of type I cells with high K^+ (30 mM) could similarly elicit delayed intracellular $\Delta[Ca^{2+}]_I$ responses in contiguous type II cells within cell clusters. Unlike type I cells, 'solitary' type II cells do not respond directly to high K^+ (Xu et al. 2003; Piskuric and Nurse 2012; Zhang et al. 2012). As exemplified in Fig. 1D, high K^+ elicited robust $\Delta[Ca^{2+}]_i$ responses in type I cells as expected and, in the *same* cluster, smaller but delayed $\Delta[Ca^{2+}]_i$ responses were frequently observed in neighboring type II cells. A scatterplot of $\Delta[Ca^{2+}]_i$ in type II cells during high K^+ is shown in Fig. 2A, which combines pooled data from many similar experiments (n=17). The mean (~55 nM) type II cell $\Delta[Ca^{2+}]_i$ response to high K^+ was comparable to that (~33 nM) seen during isohydric hypercapnia (Fig. 2A; Paired t-test, $p = 0.0518$; n = 54 responsive cells). Comparison of response latencies revealed that for high K^+ the '*follower*' type II cell responses were delayed by 8.8 ± 1.8 sec relative to the '*driver*' type I cell responses; this

was significantly shorter than the delay seen with isohydric hypercapnia (n = 17 dishes; Kruskal-Wallis Test with Dunn's Multiple Comparison *post hoc* test, $p < 0.05$).

Suramin, a P2Y2R antagonist, inhibits indirect Ca^{2+} responses in type II cells evoked by isohydric hypercapnia or high K^+

The indirect Ca^{2+} responses seen in type II cells following stimulation of type I cells in Fig. 1 could be due to paracrine activation of P2Y2R on type II cells by ATP released from nearby type I cells. To test this, we investigated whether these indirect Ca^{2+} responses, triggered by isohydric hypercapnia or high K^+, could be inhibited by suramin, a blocker of P2Y2R. As exemplified in Fig. 3A, the indirect type II cell $\Delta[Ca^{2+}]_i$ response due to isohydric hypercapnia was completely inhibited by 100 µM suramin in most cases; ~ 90% (122/136) of type II cells that initially responded to the stimulus failed to do so in the presence of suramin. The mean $\Delta[Ca^{2+}]_i$ was 42.3 ± 4.1 nM before and 7.0 ± 4.6 nM after suramin, corresponding to ~84% reduction ($p < 0.001$; n = 12 dishes; Friedman test with Dunn's multiple comparison *post hoc* test). The recovery of the isohydric hypercapnic Ca^{2+} responses after washout of suramin was 33.9 ± 4.7 nM. Similarly, as illustrated in Fig. 4, suramin reversibly inhibited the high K^+-induced secondary Ca^{2+} responses in type II cells; the mean $\Delta[Ca^{2+}]_i$ was 76.0 ± 10.0 nM before, 20.0 ± 4.1 nM during, and 66.4 ± 10.4 nM after wash-out of suramin (n = 13 dishes; Friedman test with Dunn's multiple comparison *post hoc* test, $p < 0.05$; Fig. 4B). Taken together, these data suggest that the rise in $\Delta[Ca^{2+}]_i$ seen in type II cells during isohydric hypercapnia and high K^+ is due largely to the paracrine action of ATP, released from type I cells.

Evidence for cross-talk from type II to type I cells: Role of pannexin-1 channels?

During the course of these studies we routinely applied the selective P2Y2R agonist UTP to confirm the identity of type II cells within receptor clusters (Xu et al. 2003; Zhang et al. 2012). Interestingly, in these experiments a delayed Ca^{2+} response was often seen in nearby type I cells, consistent with cross-talk from type II to type I cells (see Figs. 1 & 5). A scatterplot showing a comparison of $\Delta[Ca^{2+}]_i$ responses in type II versus type I cells from many experiments (n=15) is shown in Fig. 5B; the mean $\Delta[Ca^{2+}]_i$ response for the '*driver*' type II cells was ~175 nM compared

to ~43 nM for the '*follower*' type I cells during exposure to 100 µM UTP. Figure 2B indicates the mean latency difference between type I and type II cell responses to UTP was -11.5 ± 1.7 sec, where the negative value reflects the delay in the type I cell response relative to the type II cell (n = 17 dishes; Kruskal-Wallis Test with Dunn's Multiple Comparison *post hoc* test, $p < 0.05$).

Because activation of P2Y2 receptors on type II cells leads to the opening of large-pore, pannexin-1 (Panx-1) channels (Zhang et al. 2012), we tested whether cross-talk from type II to type I cells involved release of factor(s) via Panx-1 channels. As shown in Fig. 5A & B, addition of the selective Panx-1 channel blocker carbenoxolone (CBX; 5 µM) resulted in the inhibition of the UTP-evoked secondary response in type I cells, and the effect was reversible. Data from a total of 160 type I cells that initially responded to UTP revealed that only 18 (~11%) showed any detectable $\Delta[Ca^{2+}]_i$ responses in the presence of UTP plus CBX. Summary data from this experimental series are shown in Fig. 5B; the mean $\Delta[Ca^{2+}]_i$ for type I cells in the presence of UTP was 48.1 ± 6.0 nM, -2.6 ± 3.2 nM in the presence of UTP plus CBX, and 39.8 ± 6.1 nM in the presence of UTP after washout of CBX (n= 15 dishes; Friedman test with Dunn's multiple comparison *post hoc* test, $p < 0.001$). Notably, CBX had no significant effect on UTP-evoked Ca^{2+} responses in type II cells; the mean $\Delta[Ca^{2+}]_i$ responses for control UTP, UTP plus CBX, and recovery with UTP alone were 171.5 ± 14.7 nM, 115.9 ± 11.2 nM, and 110.0 ± 8.2 nM respectively (Friedman Test with Dunn's Multiple Comparison *post hoc* test , $p > 0.05$). These data are consistent with the notion that type II cells may communicate with type I cells via open Panx-1 channels.

Adenosine A_2 antagonists inhibit UTP-evoked secondary Ca^{2+} responses in type I cells

Panx-1 channels have pores large enough to allow release of molecules <1 kDa such as ATP and glutamate from a variety of cell types (Locovei et al. 2006; Huang et al. 2007; Dubyak 2009; Iglesias et al. 2009; MacVicar and Thompson 2010; Sridharan et al. 2010). We previously showed that Panx-1 channels in rat CB type II cells act as conduits for ATP release (Zhang et al. 2012). However, it was unlikely that ATP was the *direct* mediator of the secondary type I cell responses following UTP stimulation of type II cells because ATP is known to inhibit type I cells via P2Y1 receptors (Xu et al. 2005). Because the ATP break-down product adenosine (Ado) can elicit $\Delta[Ca^{2+}]_i$ responses in type I cells via Ado A_{2A} and/or A_{2B} receptors (Xu et al. 2006), we tested

the effects of A_2 antagonists on secondary UTP-evoked Ca^{2+} responses in type I cells. As illustrated in Fig. 6A & B, combined application of an A_{2A} selective antagonist (SCH58261; 5 μM) and an A_{2B} antagonist (MRS 1754; 100 nM) led to a significant reduction in the proportion of type I cells that responded to UTP; only ~30% (84/279) of type I cells that initially responded to UTP did so in the presence of the Ado receptor blockers. Also, the mean $\Delta[Ca^{2+}]_i$ was depressed by 73% (mean $\Delta[Ca^{2+}]_i$ before and during suramin was 53.5 ± 4.3 vs. 14.6 ± 3.5 nM; Friedman test with Dunn's multiple comparison *post hoc* test, $p < 0.01$; n = 13 dishes). As expected, Ado blockers did not affect the UTP-evoked Ca^{2+} responses in type II cells; the mean (± s.e.m.) $\Delta[Ca^{2+}]_i$ response was 95.8 ± 8.1 for UTP and 63.3 ± 7.3 for UTP plus Ado blockers (Friedman test with Dunn's multiple comparison *post hoc* test, $p > 0.05$; n = 13 dishes). The above data suggest that Ado is at least partially responsible for cross-talk from type II to type I cells.

Contrasting effects of suramin on high CO_2 vs. high K^+-evoked Ca^{2+} responses in type I cells

In order to assess the importance of type II cell purinergic cross-talk with type I cells, we investigated whether suramin, the general P2 receptor antagonist, affected the magnitude of the type I cell Ca^{2+} responses during isohydric hypercapnic and high K^+ application. Interestingly, suramin partially inhibited the Ca^{2+} responses induced by isohydric hypercapnia in type I cells; the mean (± s.e.m.) $\Delta[Ca^{2+}]_i$ response was 69.2 ± 5.5 nM for isohydric hypercapnia, 40.9 ± 8.7 nM for isohydric hypercapnia plus suramin (100 μM), and 59.2 ± 9.1 nM for isohydric hypercapnia after washout of suramin (Repeated Measures ANOVA with Tukey's multiple comparison *post hoc* test; $p < 0.05$, n = 12 dishes). Suramin also inhibited the proportion of type I cells that was responsive to isohydric hypercapnia by ~30%. However, during the high K^+ stimulus, suramin had no significant effect on the Ca^{2+} responses in type I cells; the mean $\Delta[Ca^{2+}]_i$ response to high K^+ was 311.1 ± 20.4 nM vs 280.6 ± 40.4 nM in high K^+ plus suramin ($p > 0.05$; n = 13 dishes; Friedman test with Dunn's multiple comparison *post hoc* test). Given that suramin would block inhibitory P2Y1 receptors on type I cells, one would expect a facilitation of the type I cell Ca^{2+} response in the presence of suramin. The fact that we observed an inhibition of type I Ca^{2+} responses to isohydric hypercapnia in the presence of suramin alludes to the importance of P2Y2R activation and Panx-1 signaling by type II cells. The communication between type I and type II cells is reciprocal and type II purinergic signalling with type I cells is significant during the

transduction of a chemical stimulus (isohydric hypercapnia), but not during a general depolarizing stimulus (high K^+).

DISCUSSION

The present study has provided direct evidence for communication between carotid body (CB) type I and type II cells and more importantly, we show for the first time that this cross-talk can be elicited by a chemostimulus, i.e. elevated CO_2. Type II cells have been described as glia-like, sheath, and/or sustenacular cells that form intimate associations with chemoreceptor type I cells (McDonald and Mitchell 1975; Kondo 2002). However, until now there has been no direct evidence that they play an active role during chemotransduction. Previous studies in this laboratory have demonstrated that type II cells express gap junction-like pannexin-1 (Panx-1) channels which act as conduits for ATP release following P2Y2 receptor activation and intracellular Ca^{2+} mobilization (Zhang et al. 2012). That study led the authors to propose that release of the primary excitatory neurotransmitter ATP from type I cells during chemostimulation resulted in paracrine activation of type II cells and amplification of the ATP signal via the mechanism of ATP-induced ATP release. In the present study, depolarization of type I cells by high CO_2 (isohydric hypercapnia) or high K^+ caused a delayed rise in intracellular Ca^{2+} in type II cells, attributable to P2Y2R activation by ATP released from type I cells. We also provide evidence that communication between type I and type II cells is bi-directional, as direct stimulation of P2Y2 receptors on type II cells with UTP led to a delayed activation of type I cells by factors(s) released via Panx-1 channels. These data add further support to the notion that type II cells participate in a 'tripartite synapse' with type I cells and petrosal nerve endings and contribute to sensory integration in the CB by releasing 'gliotransmitters' (Nurse and Piskuric 2013; Nurse 2014).

An *in vitro* model of rat CB chemoreceptor clusters in monolayer culture, combined with ratiometric calcium imaging allowed us to uncover evidence for cross-talk between type I and type II cells. When imaging from a cluster, the predominant response was usually the type I cell which outnumber contiguous type II cells by a ratio at least 4 to 1 (McDonald 1981). Nevertheless, the two second delay between every image taken by the calcium imaging system was sufficient for detection of the slow paracrine signaling mechanisms involving G-protein coupled receptors. We

observed several cases of successful type I and type II cell cross-talk where selective activation of one cell type resulted in delayed, secondary Ca^{2+} responses in the other cell type. The delayed UTP-evoked Ca^{2+} responses in type I cells were slower in comparison with high K^+- and isohydric hypercapnia-induced delayed Ca^{2+} responses in type II cells. This difference likely reflects the longer signal transduction pathway leading up to Panx-1 channel opening following stimulation of G-protein coupled P2Y2 receptors on type II cells.

Type I cells communicate with type II cells using ATP as a paracrine signal

Isohydric hypercapnia (10% CO_2/pH = 7.4) is a potent chemostimulus that depolarizes and raises intracellular Ca^{2+} in type I cells (Buckler and Vaughan-Jones 1993; Buckler and Vaughan-Jones 1994), thereby stimulating neurosecretion (Rigual et al. 1984; Rigual et al. 1991; Zhang and Nurse 2004). Because type I cells display variable sensitivities to high CO_2 we also used high K^+ to evoke a robust and more widespread type I cell depolarization so as to optimize cross-talk. The predominant neurotransmitter responsible for this type I to type II cell cross-talk was ATP since suramin, a purinergic P2Y2R antagonist, partially or completely inhibited the delayed hypercapnia- and high K^+-induced Ca^{2+} transients in type II cells. In addition to ATP, other excitatory neuromodulators released from type I cells that could potentially contribute to the indirect Ca^{2+} responses evoked by high K^+ and/or isohydric hypercapnia in type II cells include ACh (Zhang et al. 2000; Shirahata et al. 2007), 5-HT (Zhang et al. 2003), and angiotensin II (Fung et al. 2001; Schultz 2011). Indeed, Tse et al. (2012) demonstrated that stimulating type II cells with the muscarinic ACh receptor agonist (i.e. musarine) or angiotensin II led to a rise in intracellular Ca^{2+}. Moreover, we recently showed that angiotensin II, acting via AT1 receptors, induced a rise in intracellular Ca^{2+} leading to the opening of Panx-1 channels in type II cells (Murali et al. 2014). It was also demonstrated in this thesis (Chapter 3) that 5-HT similarly mobilizes intracellular Ca^{2+} and opens Panx-1 channels in type II cells via $5HT_{2a}$-like receptors.

Interestingly, in the case of isohydric hypercapnia, suramin also reversibly inhibited type I cell Ca^{2+} responses. Because any autocrine-paracrine actions of ATP on type I cells are thought to involve inhibitory P2Y1 receptors (Xu et al. 2005), it is likely that suramin blocked the excitatory effects of a paracrine signal derived from P2Y2R stimulation of type II cells (see below).

Type II cells communicate with type I cells via Panx-1 channels and the neuromodulator adenosine

Ratiometric fura-2 imaging experiments revealed that the P2Y2R agonist UTP first elicited direct intracellular Ca^{2+} responses in type II cells followed by a delayed rise in intracellular Ca^{2+} in type I cells. As expected for the involvement of Panx-1 channels in this cross-talk, the secondary Ca^{2+} responses seen in type I cells were completely inhibited by 5 μM carbenoxolone, a selective Panx-1 channel blocker. The principal neuromodulator responsible for type II to type I cell cross-talk appeared to be adenosine because the indirect $\Delta[Ca^{2+}]_i$ responses in type I cells were reversibly abolished by a combination of the specific A_{2A} and A_{2B} adenosine receptor antagonists, SCH58261 and MRS 1754, respectively. We propose that ATP released from type II cells via Panx-1 channels is catabolized extracellularly by ectonucleotidases into adenosine, which then stimulates A_2 receptors on type I cells leading to a rise in intracellular Ca^{2+} (Xu et al. 2006). However, we cannot presently rule out the possibility that adenosine may be released directly from type II cells via Panx-1 channels. A small proportion of type I cells that indirectly responded to the UTP stimulus was unaffected by the A_2R blockers suggesting that multiple 'gliotransmitters' may be released by type II cells. One possible candidate is glutamate, an excitatory neurotransmitter, released via Panx-1 channels from astrocytes that participate in the long-range transfer of physiological signals in the brain (Barbe et al. 2006; Malarkey and Parpura 2008; Thompson and MacVicar 2008). A previous study in rat CB using RT-PCR, Western blot analysis, and immunohistochemical techniques revealed that ionotropic N-methyl-D-aspartate (NMDA) glutamate receptors are strongly expressed in the rat carotid body and are localized predominantly to type I cells. The infusion of NMDA augmented carotid sinus nerve activity, which could be inhibited by the selective NMDA receptor blocker, MK-801, suggesting that glutamate has an excitatory role in chemoreception (Liu et al. 2009).

In summary, we demonstrate for the first time that rat CB type II cells can respond indirectly to the chemostimulus isohydric hypercapnia with an increase in cytosoloic $[Ca^{2+}]$. Moreover, we have contributed novel information on the role of purinergic signaling mechanisms at the CB chemosensory 'tripartite synapse'. Further studies are required to identify other

neuromodulators that are likely to be involved in the bi-directional communication between receptor type I and glial-lke type II cells in the CB.

Figure 1. Isohydric hypercapnia elicits secondary Ca^{2+} responses in type II cells that are in close proximity to type I clusters. A, B. Solitary type II cell (well isolated from type I cluster) responds to P2Y2R agonist, UTP, but not to isohydric hypercapnia or the depolarizing stimulus high K^+ (n = 17). C, D. In contrast, when type II cells are near type I cells there can be cross-talk: thus, type II cells (blue trace) can respond after a delay when type I cells (red trace) are stimulated with isohydric hypercapnia (D); also type I cells can respond with a delay when type II cells are stimulated with UTP (n = 17). F. A comparison of the relative magnitude of the peak $\Delta[Ca^{2+}]_i$-evoked by 10% CO_2 revealed that there is a statistical difference between the mean Ca^{2+} response of type I (~ 73 nM; n = 203 cells) and type II (~33 nM; n = 36 cells) responsive cells (Mann-Whitney Test, $p < 0.001$).

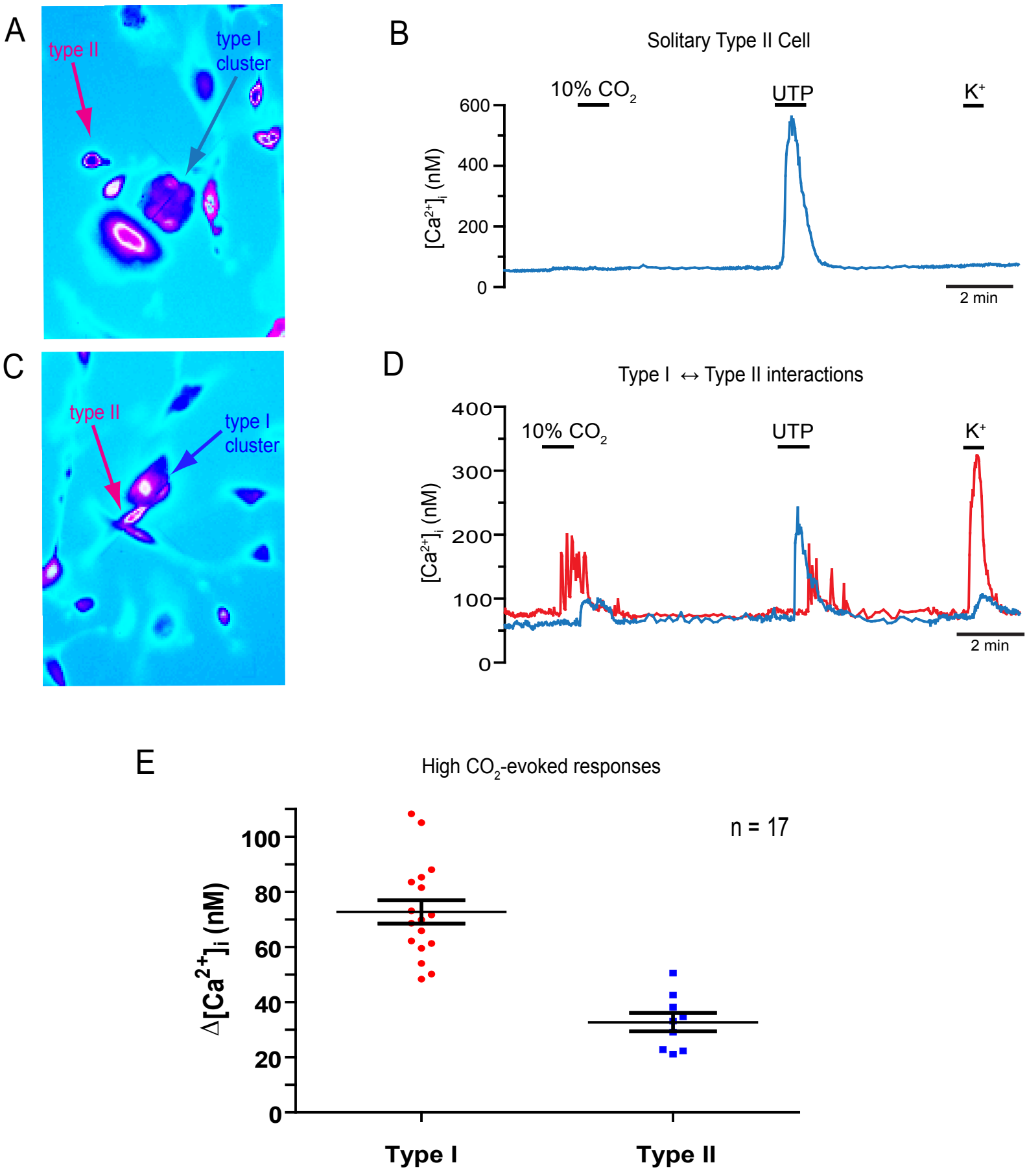
A
type II
type I cluster
B
Solitary Type II Cell
10% CO2
UTP
K+
600
400
200
0
[Ca2+]i (nM)
2 min
C
type II
type I cluster
D
Type I ↔ Type II interactions
400
300
200
100
0
10% CO2
UTP
K+
[Ca2+]i (nM)
2 min
E
High CO2-evoked responses
n = 17
100
80
60
40
20
0
Δ[Ca2+]i (nM)
Type I
Type II

Figure 2. A comparison of mean secondary Ca^{2+} response in type II cells and mean latency responses between all three stimuli. High K^+ (30 mM), a stimuli used to identify type I cells, elicited a statistically larger Ca^{2+} response in responsive type II cells in comparison with the isohydric hypercapnic stimuli (Paired t-test; $p < 0.05$), the mean Ca^{2+} response of the responsive subpopulation of type II cells was ~ 55 nM (n= 54 responsive cells) (A). The latencies of the Ca^{2+} response in type I vs. type II cells were compared among all three stimuli. Positive latency values denote that type I cells responded first followed by the type II response whereas negative values indicate that type II cells were the first to respond. The order of fastest difference in latencies in triggering a Ca^{2+} response in type I and then type II cells were Hi K^+ > 10 % CO_2 > UTP; the respective mean difference in latencies are: 8.8 ± 1.8 s, 10.5 ± 2.7 s, and -11.5 ± 1.7 s (n = 10 dishes; Kruskal-Wallis Test, $p < 0.05$)(B).

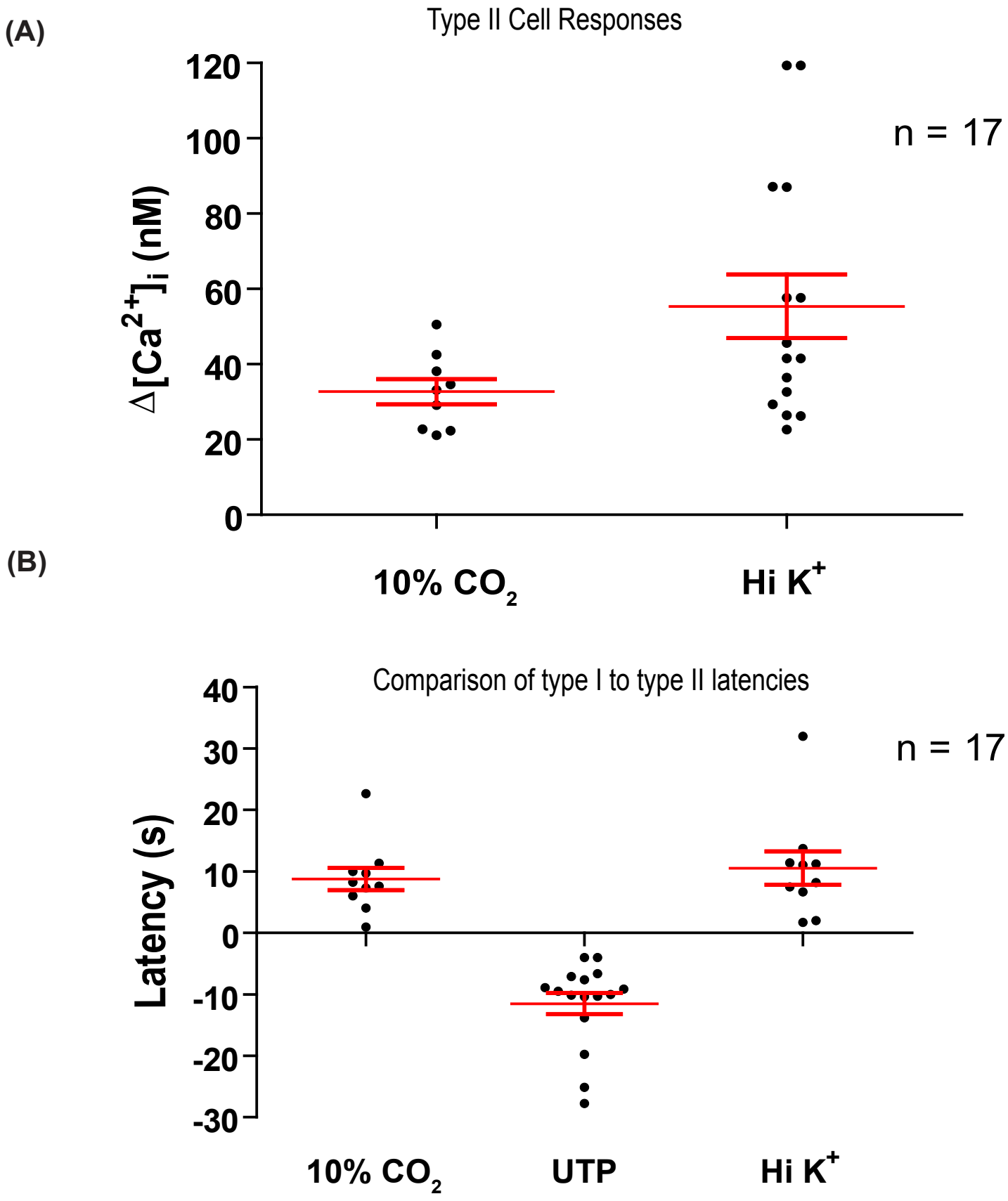
(A)
Type II Cell Responses
120
100
80
60
40
20
0
Δ[Ca2+]i (nM)
n = 17
10% CO2
Hi K+
(B)
Comparison of type I to type II latencies
40
30
20
10
0
-10
-20
-30
Latency (s)
n = 17
10% CO2
UTP
Hi K+

Figure 3. Suramin inhibits indirect Ca^{2+} responses evoked by isohydric hypercapnia in type II cells. Suramin reversibly abolished the isohydric hypercapnic (10% CO_2)-induced secondary Ca^{2+} response in type II cells (A). The mean $\Delta[Ca^{2+}]_i$ before and during suramin was 42.3 ± 4.1 vs. 6.95 ± 4.6 nM and the recovery was 33.9 ± 4.7 (n = 12 dishes; Friedman test with Dunn's multiple comparison *post hoc* test, $p < 0.001$). Isohydric hypercapnic-evoked Ca^{2+} responses in type I cells were affected by suramin since there was a decrease in the mean $\Delta[Ca^{2+}]_i$ response in the presence of suramin (control 69.2 ± 5.5 nM vs. suramin-containing solution 40.9 ± 8.7 nM; n= 12 dishes; Friedman test with Dunn's multiple comparison *post hoc* test, $p < 0.05$). (B)

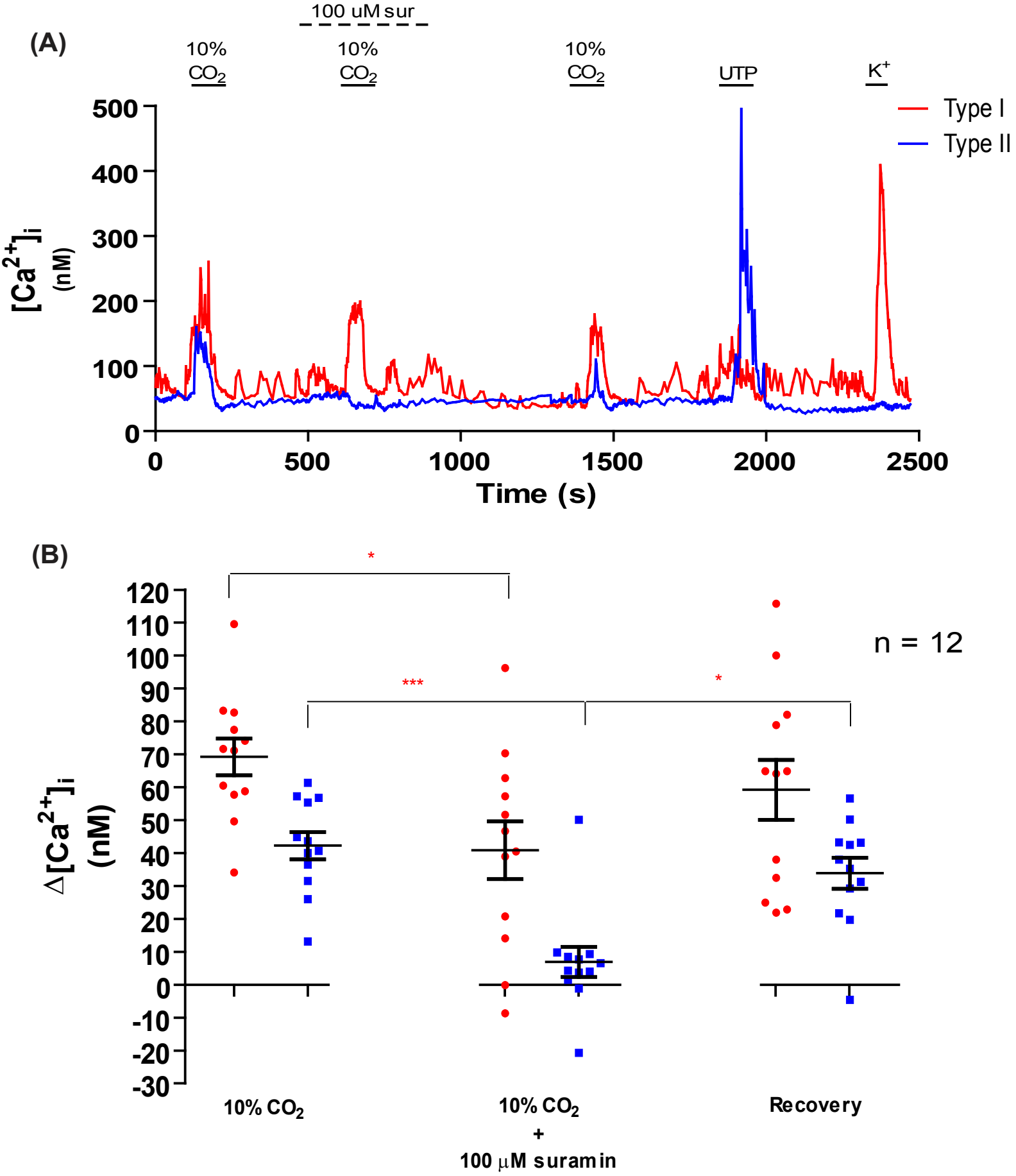
(A)
100 uM sur
10% CO2
10% CO2
10% CO2
UTP
K+
Type I
Type II
[Ca2+]i (nM)
Time (s)
(B)
n = 12
Δ[Ca2+]i (nM)
10% CO2
10% CO2 + 100 μM suramin
Recovery

Figure 4. Suramin inhibits indirect Ca^{2+} responses evoked by High K^+ in type II cells. Suramin reversibly abolished the Hi K^+-induced Ca^{2+} response in type II cells (A). The mean $\Delta[Ca^{2+}]_i$ before and during suramin was 76.0 ± 10.0 vs. 20.0 ± 4.1 nM and the recovery was 66.4 ± 10.4 (n = 12 dishes; Friedman test with Dunn's multiple comparison *post hoc* test, $p < 0.001$). Hi K^+ - evoked Ca^{2+} responses in type I cells were not affected by suramin since there was no statistical difference in the mean $\Delta[Ca^{2+}]_i$ in the presence or absence of suramin (control 311.1 ± 20.4 nM vs. suramin-containing solution 280.6 ± 40.4 nM; n= 13 dishes; Friedman test with Dunn's multiple comparison *post hoc* test, $p > 0.05$). (B)

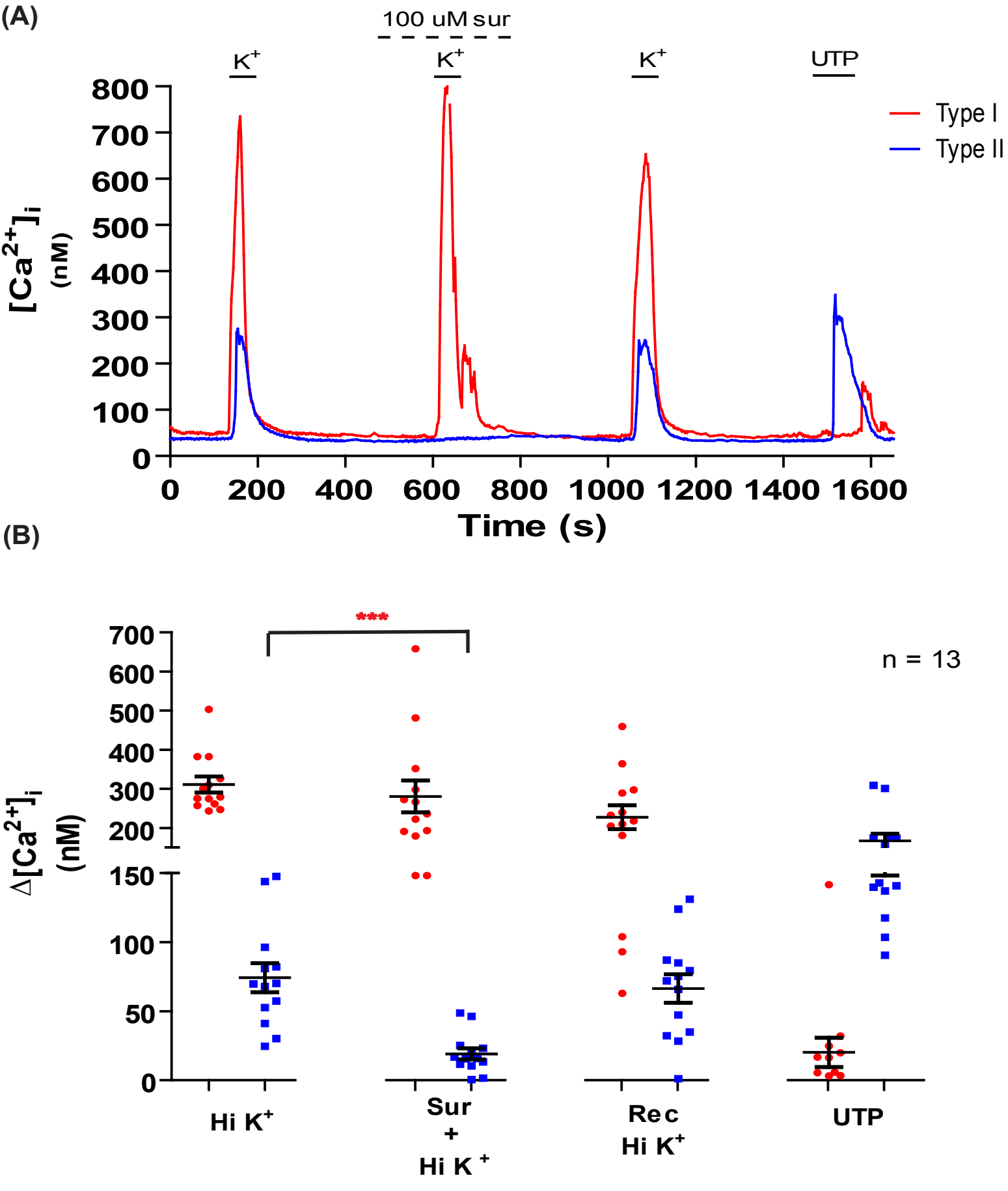
(A)
100 uM sur
K+
K+
K+
UTP
Type I
Type II
[Ca2+]i (nM)
800
700
600
500
400
300
200
100
0
0
200
400
600
800
1000
1200
1400
1600
Time (s)
(B)
***
n = 13
Δ[Ca2+]i (nM)
700
600
500
400
300
200
150
100
50
0
Hi K+
Sur + Hi K+
Rec Hi K+
UTP

Figure 5. Type II cells require pannexin-1 (Panx-1) channels in order to communicate with type I cells. UTP-evoked Ca^{2+} response in type I cells was markedly inhibited by carbenoxolone (CBX), suggesting that gliotransmission from type II cells requires Panx-1 channels (A). The mean ± s.e.m. $\Delta[Ca^{2+}]_i$ in control, CBX-containing solutions, and recovery respectively was 48.1 ± 6.0 vs. -2.6 ± 3.2 vs. 39.8 ± 6.1 nM (n = 15 dishes; Friedman test with Dunn's multiple comparison *post hoc* test, $p < 0.001$). CBX had no effect on UTP-evoked Ca^{2+} responses in type II cells since the mean ± s.e.m. $\Delta[Ca^{2+}]i$ in control, CBX-containing solutions, and recovery were statistically similar (171.5 ± 14.7 vs. 115.9 ± 11.2 vs. 110.0 ± 8.2; Friedman Test, $p > 0.05$). (B)

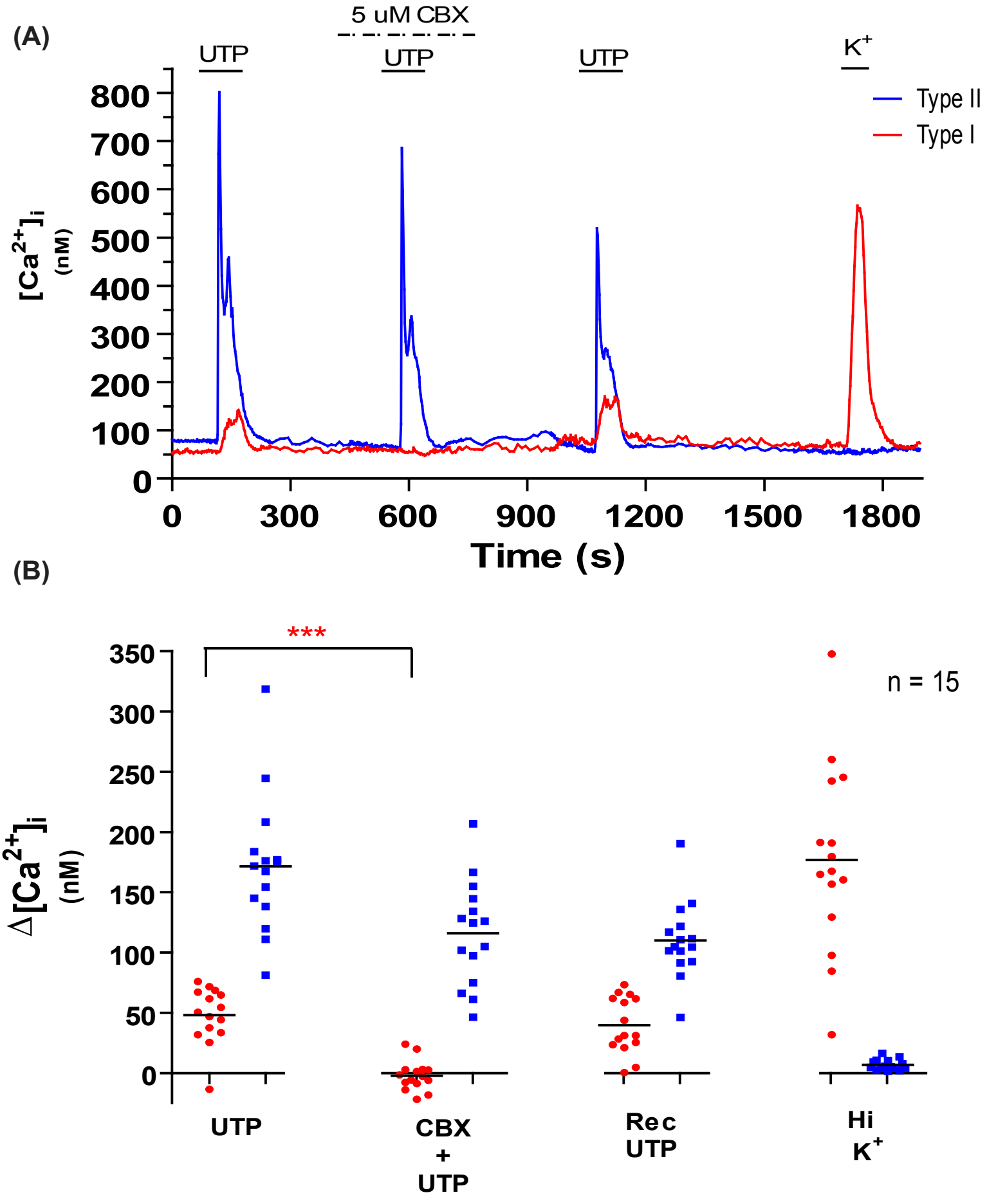
(A)
5 uM CBX
UTP
UTP
UTP
K+
Type II
Type I
[Ca2+]i (nM)
800
700
600
500
400
300
200
100
0
0
300
600
900
1200
1500
1800
Time (s)
(B)
***
n = 15
Δ[Ca2+]i (nM)
350
300
250
200
150
100
50
0
UTP
CBX + UTP
Rec UTP
Hi K+

Figure 6. Type II cells communicate with type I cells via the neuromodulator adenosine (Ado). UTP-evoked Ca^{2+} response in type I cells was markedly inhibited by the combination of the adenosine A2A, SCH 58261(5 μM), and A2B, MRS 1754 (100 nM), receptor antagonists suggesting that type II gliotransmission of ATP gets broken down into adenosine (Ado) facilitating type II to type I crosstalk (A). The mean ± s.e.m. $\Delta[Ca^{2+}]_i$ in UTP, UTP + Ado antagonists-containing solutions, and recovery respectively was 53.5 ± 4.3 vs. 14.6 ± 3.5 vs. 46.2 ± 5.1 nM (n = 13 dishes; Friedman test with Dunn's multiple comparison *post hoc* test, $p < 0.01$)(B).

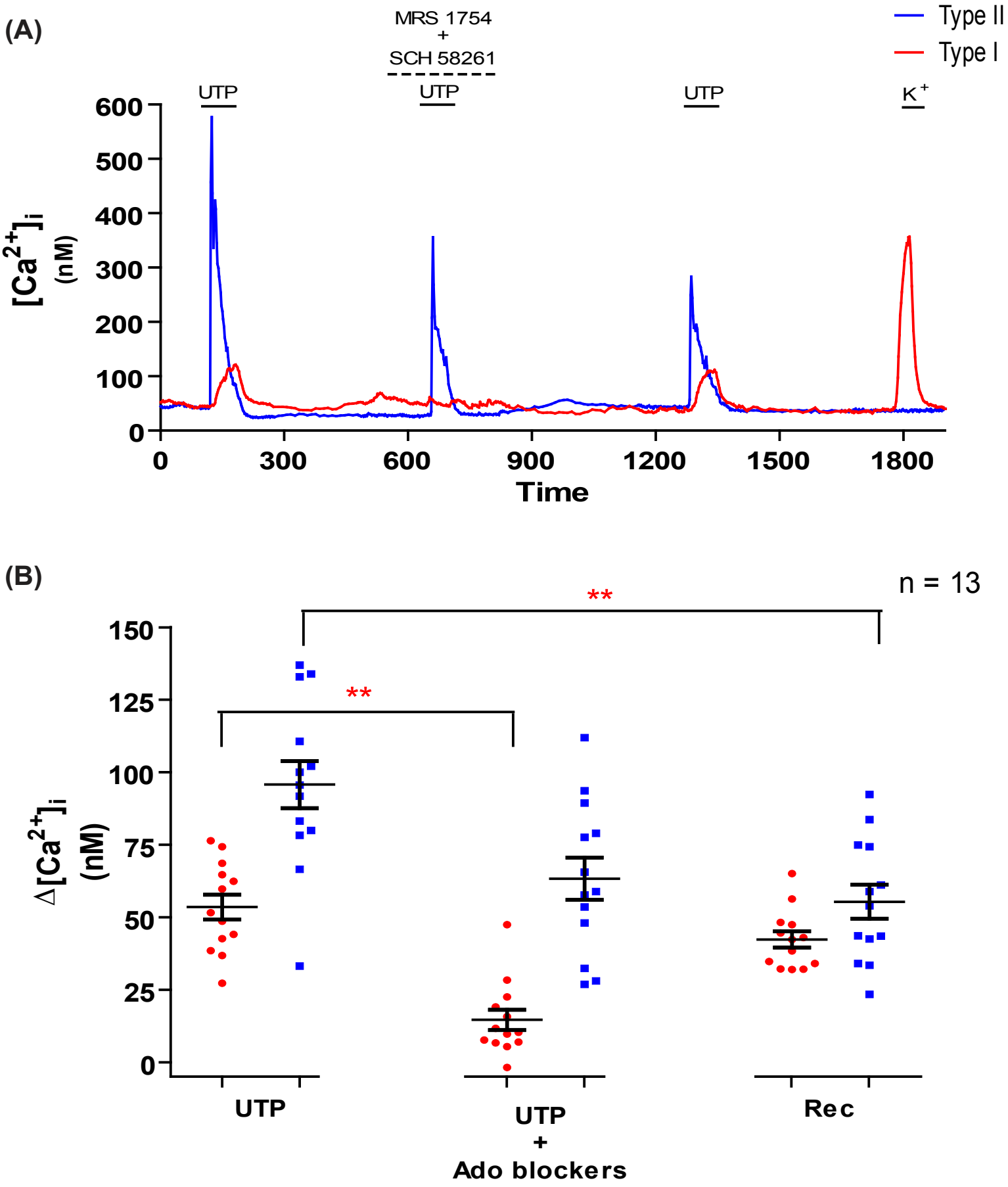
(A)
MRS 1754
+
SCH 58261
Type II
Type I
UTP
UTP
UTP
K+
600
500
400
300
200
100
0
[Ca2+]i
(nM)
0
300
600
900
1200
1500
1800
Time
(B)
n = 13
**
**
150
125
100
75
50
25
0
Δ[Ca2+]i
(nM)
UTP
UTP
+
Ado blockers
Rec

CHAPTER 5

General Discussion

Although the presence of type II cells in the carotid body (CB) has been known for ~ 35 years, it is only recently that their functional significance to carotid body chemoreception has emerged. In addition to their role in chemotransduction, type II cells occupy a stem cell niche; they give rise to type I cells under chronic hypoxic conditions (Pardal et al. 2007). In the past, CB literature has described type II cells as sheath or sustentacular cells. They are considered to be "glial-like" due to similarities shared with Schwann and satellite cells of the nervous system (McDonald 1981). Since type II cell cytoplasmic processes interdigitate glomus cell clusters, it has been suggested that they form paracrine cell-cell interactions. Such interactions provide a mechanism by which type II cells may modulate synaptic activity in the CB and contribute to the final chemoreceptor response. This physiological role was uncovered with the aid of ratiometric calcium imaging and electrophysiological experiments demonstrating that type II cells expressed purinergic P2Y2 receptors (Xu et al. 2003; Zhang et al. 2012). Stimulation of these receptors led to a rise in intracellular Ca^{2+} ($\Delta[Ca^{2+}]_i$) and the opening of pannexin-1 (Panx-1) channels (Zhang et al. 2012). Because opening of Panx-1 channels resulted in the release of ATP, a CB excitatory neurotransmitter, it was concluded that type II cells acted as ATP amplifiers. Nonetheless, there were many unanswered questions about type II cell physiology. Importantly, it was unknown whether other CB neurotransmitters and neuromodulators elicited paracrine activation of type II cells and/or whether activation would lead to the opening of Panx-1 channels. Moreover, the mechanisms by which type II and type I cells communicated with one another were unclear. This thesis has contributed novel insights to these two areas.

To answer the above questions, I first tested the responsiveness of type II cells to two neuromodulators that have been implicated in CB pathophysiologies, i.e. angiotensin II (ANG II) and 5-HT. Using ratiometric calcium imaging, I found that ANG II and 5-HT elicited some of the largest and most frequent $\Delta[Ca^{2+}]_i$ in type II cells. Both ANG II and 5-HT may act via their respective G-protein coupled AT_1 (AT_1R) and 5-HT_2 (5-HT_2R) receptors respectively, to activate phosphatidyl ionositol-IP_3 pathway. This involves the activation of phospholipase C, leading to the generation of IP_3 which in turn triggers Ca^{2+} release from the endoplasmic reticulum (GUO et al. 2001; Hoyer et al. 2002). These Ca^{2+} responses were necessary for the opening of Panx-1 channels as demonstrated by perforated-patch, whole cell experiments where Panx-1 currents were almost completely and reversibly blocked in the presence of the membrane permeable Ca^{2+} chelator, BAPTA-AM (Murali et al. 2014). Interestingly, ANG II and 5-HT are neuromodulators that are involved in alterations in CB physiology during several pathophysiological conditions. These include conditions associated with exposures to chronic hypoxia and/or chronic intermittent hypoxia such as chronic heart failure, sleep-disordered breathing, and hypertension (Prabhakar and Peng 2004; Li et al. 2007; Prabhakar 2011; Schultz 2011). During these disease pathologies, CB chemosensitivity becomes exaggerated leading to an augmentation of the sensory discharge resulting in hypertension (Peng et al. 2003; Prabhakar and Peng 2004; Prabhakar 2011; Schultz 2011). It is plausible that type II cells may contribute to sensitization of the CB sensory discharge via ANG II-AT_1Rs and/or 5-HT-5-HT_2R signaling, which results in the Ca^{2+}-dependent activation of Panx-1 channels and release of ATP.

A novel contribution from my studies was the demonstration that purinergic signaling contributes significantly to bi-directional communication between type I and type II cells during chemotransduction. There is ample evidence that glial cells in the central nervous system (CNS) play an active role in synapse integration via "gliotransmission" at tripartite synapses (Eroglu and Barres 2010; Parpura et al. 2012). Importantly, ATP and other purine signals, such as adenosine, serve as a common currency for glia-neuron communication during initiation of a variety of CNS processes (Fields and Burnstock 2006). Activity-dependent release of ATP from synapses, axons, and glia activates purinergic membrane receptors that modulate intracellular calcium. This enables glia to detect neural activity and communicate among other glial cells by releasing ATP through membrane channels and vesicles (Barbe et al. 2006; Fields and Burnstock 2006). Similar to neuron-glial communication in the CNS, it appeared likely that the same might apply to CB type

I-type II cell communication since ATP is the main excitatory sensory neurotransmitter (Zhang et al. 2000; Zhang and Nurse 2004).

Ratiometric calcium imaging was a relatively non-invasive technique that allowed us to explore multiple concurrent interactions between type I and type II cells. Importantly, we demonstrated for the first time that type II cells were capable of *indirectly* responding to a chemical stimulus, isohydric hypercapnia, when the cells are present in close proximity to a type I cell cluster. ATP was the predominant neurotransmitter responsible for this paracrine type I-type II cell cross-talk since the latter was inhibited by suramin, a general purinergic P2Y2 receptor antagonist. Further studies are required to determine whether or not ATP can also mediate cross-talk from type I to type II cells in response to other chemostimuli such as hypoxia and acid hypercapnia.

On the other hand, cross-talk from type II to type I cells was dependent on Panx-1 channel opening because the *indirect* UTP-evoked Ca^{2+} responses in type I cells were inhibited by low concentrations of carbenoxolone, a Panx-I channel blocker. Moreover, because UTP- induced Ca^{2+} responses in type I cells were reversibly abolished by a combination adenosine A_{2A} and A_{2B} receptor antagonists, adenosine was likely the key mediator. The combined data taken together highlight the significance of purinergic signaling between type I and type II cells during sensory transduction. Thus, this thesis provides a novel interpretation and a broader view of the role played by type II cells in the CB chemoreceptor complex and their function during the transduction of chemostimuli (Figure 1).

Future Directions

The work presented in this thesis has raised several questions that require further investigation.

1. What is the source of adenosine for type II to type I cell cross-talk?

   There are two possible sources of adenosine for type II to type I cross-talk: one possibility is the direct release of adenosine via Panx-1 channels and the other is the hydrolysis of ATP, released via Panx-1 channels, into adenosine by 5'-ectonucleotidases (Conde and Monteiro 2004). Latency data from ratiometric calcium imaging are insufficient to determine the source

of adenosine due to the limitations of this technique (see Chapter 4). One way to determine the source adenosine is by using ecto-5'-nucleotidase inhibitors such as, α, β-methylene ADP, to test whether they can inhibit UTP-evoked Ca^{2+} responses in type I cells.

2. Do type II cells release 'gliotransmitters' other than ATP?

   As discussed in Chapter 4, a proportion of UTP-induced type I cell Ca^{2+} responses was unaffected by adenosine blockers suggesting that multiple gliotransmitters may be released from type II cells. A prominent excitatory neurotransmitter in the CNS is glutamate, which can be released from astrocytes via Panx-1 channels (Barbe et al. 2006; Malarkey and Parpura 2008; Thompson and MacVicar 2008). A previous study revealed that ionotropic N-methyl-D-aspartate (NMDA) glutamate receptors are strongly expressed in the carotid body and are localized predominantly in type I cells (Liu et al. 2009). Because ATP and adenosine receptor activation can modulate glutamate release from CNS neurons and/or astrocytes (Fields and Burnstock 2006), it is plausible that a similar mechanism may operate in the CB.

3. Does chronic hypoxia (CH) and/or chronic intermittent hypoxia (CIH) affect type II cell signaling?

   The upregulation of ANG II and 5-HT signaling pathways in the CB has been seen in animals that have been exposed to chronic or intermittent hypoxia (Leung et al. 2000; Lam and Leung 2003; Peng et al. 2003; Peng et al. 2006; Lam et al. 2014). The upregulation of these signaling pathways results in an enhanced CB excitation and it is possible that ANG II-AT_1R and 5-HT-5-HT_2R signaling within type II cells may contribute via Panx-1 mediated ATP release (Chapter 2 & 3). It is known that type I cells show augmented ANG II-evoked Ca^{2+} responses after exposure to CIH (Lam et al. 2014). The question arises whether ANG II or 5-HT- evoked Ca^{2+} responses are also enhanced in type II cells after exposure to CH or CIH. Another question to explore is whether type I to type II cell cross-talk, which under normal conditions is mediated mainly by ATP (Chapter 4), might involve greater contributions from ANG II or 5-HT signaling pathways after exposure to CH or CIH.

Figure 1. Contributions of this thesis to the carotid body 'triparite model'. During various circumstances, receptor type I cells can release neurotransmitters/modulators such as: ATP, angiotensin II (ANG II), and 5-HT, which have paracrine effects on type II cells by activating their respective G-protein coupled receptors, P2Y2R, AT_1R, and $5\text{-}HT_{2A}R$. This thesis demonstrated that AT_1R and $5\text{-}HT_{2A}R$ signaling resulted in IP_3-mediated Ca^{2+} release from intracellular stores that lead to the opening of pannexin-1 (Panx-1) channels (Chapters 2 & 3). Previous studies have shown that these channels are conduits for ATP that directly excites petrosal afferents via P2X2/X3 receptors (Zhang et al. 2012). This thesis highlights the importance of Panx-1 channels in glial-like type II cell communication with receptor type I cells. The excitatory neuromodulator, adenosine (Ado), participates in type II to type I cell crosstalk. Another significant contribution of this thesis was the demonstration of type I to type II cell communication during transduction of isohydric hypercapnic. Type I to type II cell crosstalk was predominantly mediated by the excitatory neurotransmitter, ATP (Chapter 4).

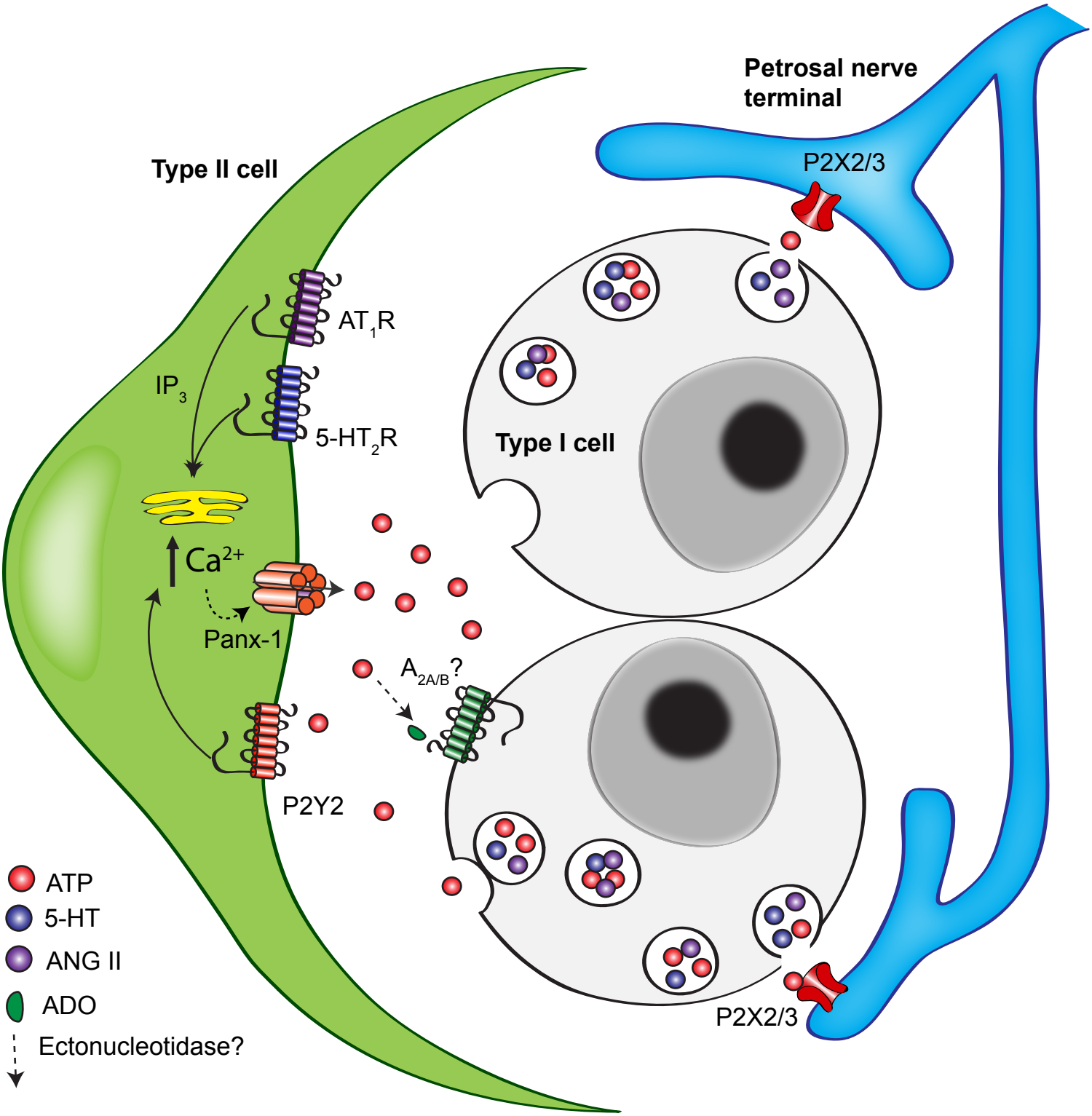
Petrosal nerve terminal
P2X2/3
Type II cell
AT1R
IP3
5-HT2R
Type I cell
Ca2+
Panx-1
A2A/B?
P2Y2
P2X2/3
ATP
5-HT
ANG II
ADO
Ectonucleotidase?

REFERENCES

Adayev, T., Ranasinghe, B., & Banerjee, P. (2005). Transmembrane signaling in the brain by serotonin, a key regulator of physiology and emotion. *Bioscience reports,* **25**, 363-385.

Alcayaga, J., Barrios, M., Bustos, F., Miranda, G., Molina, M. a. J., & Iturriaga, R. (1999). Modulatory effect of nitric oxide on acetylcholine-induced activation of cat petrosal ganglion neurons in vitro. *Brain research,* **825**, 194-198.

Alcayaga, J., Cerpa, V., Retamal, M., Arroyo, J., Iturriaga, R., & Zapata, P. (2000). Adenosine triphosphate-induced peripheral nerve discharges generated from the cat petrosal ganglion in vitro. *Neuroscience letters,* **282**, 185-188.

Allen, A. (1998). Angiotensin AT1 receptor-mediated excitation of rat carotid body chemoreceptor afferent activity. *The Journal of physiology,* **510**, 773-781.

Baldwin, S. A., Mackey, J. R., Cass, C. E., & Young, J. D. (1999). Nucleoside transporters: molecular biology and implications for therapeutic development. *Molecular medicine today,* **5**, 216-224.

Balla, T., Baukal, A. J., Eng, S., & Catt, K. J. (1991). Angiotensin II receptor subtypes and biological responses in the adrenal cortex and medulla. *Molecular pharmacology,* **40**, 401-406.

Balla, T., Varnai, P., Tian, Y., & Smith, R. D. (1998). Signaling events activated by angiotensin II receptors: what goes before and after the calcium signals. *Endocrine research,* **24**, 335-344.

Bao, L., Locovei, S., & Dahl, G. (2004). Pannexin membrane channels are mechanosensitive conduits for ATP. *FEBS letters,* **572**, 65-68.

Barbe, M. T., Monyer, H., & Bruzzone, R. (2006). Cell-cell communication beyond connexins: the pannexin channels. *Physiology,* **21**, 103-114.

Barnes, N. M., & Sharp, T. (1999). A review of central 5-HT receptors and their function. *Neuropharmacology,* **38**, 1083-1152.

Benicky, J., Hafko, R., Sanchez-Lemus, E., Aguilera, G., & Saavedra, J. M. (2012). Six commercially available angiotensin II AT1 receptor antibodies are non-specific. *Cellular and molecular neurobiology,* **32**, 1353-1365.

Bennett, M. V., Contreras, J. E., Bukauskas, F. F., & Sáez, J. C. (2003). < i> New roles for astrocytes</i>: Gap junction hemichannels have something to communicate. *Trends in neurosciences,* **26**, 610-617.

Bosnyak, S., Jones, E. S., Christopoulos, A., Aguilar, M.-I., Thomas, W. G., & Widdop, R. E. (2011). Relative affinity of angiotensin peptides and novel ligands at AT1 and AT2 receptors. *Clinical science*, **121**, 297-303.

Bruzzone, R., Hormuzdi, S. G., Barbe, M. T., Herb, A., & Monyer, H. (2003). Pannexins, a family of gap junction proteins expressed in brain. *Proceedings of the National Academy of Sciences*, **100**, 13644-13649.

Buckler, K. (1997). A novel oxygen-sensitive potassium current in rat carotid body type I cells. *The Journal of Physiology*, **498**, 649-662.

Buckler, K., & Vaughan-Jones, R. (1993). Effects of acidic stimuli on intracellular calcium in isolated type I cells of the neonatal rat carotid body. *Pflügers Archiv*, **425**, 22-27.

Buckler, K., & Vaughan-Jones, R. (1994). Effects of hypoxia on membrane potential and intracellular calcium in rat neonatal carotid body type I cells. *The Journal of Physiology*, **476**, 423-428.

Buckler, K. J. (2007). TASK-like potassium channels and oxygen sensing in the carotid body. *Respiratory physiology & neurobiology*, **157**, 55-64.

Buckler, K. J. (2012). Effects of exogenous hydrogen sulphide on calcium signalling, background (TASK) K channel activity and mitochondrial function in chemoreceptor cells. *Pflügers Archiv-European Journal of Physiology*, **463**, 743-754.

Buckler, K. J., & Vaughan-Jones, R. D. (1994). Effects of hypercapnia on membrane potential and intracellular calcium in rat carotid body type I cells. *The Journal of Physiology*, **478**, 157-171.

Buckler, K. J., Williams, B. A., & Honore, E. (2000). An oxygen-, acid-and anaesthetic-sensitive TASK-like background potassium channel in rat arterial chemoreceptor cells. *The Journal of Physiology*, **525**, 135-142.

Bureau, M., Lamarche, J., Foulon, P., & Dalle, D. (1985). Postnatal maturation of respiration in intact and carotid body-chemodenervated lambs. *J. Appl. Physiol*, **59**, 869-874.

Buttigieg, J., & Nurse, C. A. (2004). Detection of hypoxia-evoked ATP release from chemoreceptor cells of the rat carotid body. *Biochemical and biophysical research communications*, **322**, 82-87.

Campanucci, V. A., Dookhoo, L., Vollmer, C., & Nurse, C. A. (2012). Modulation of the carotid body sensory discharge by NO: an up-dated hypothesis. *Respiratory physiology & neurobiology*, **184**, 149-157.

Chen, J., Dinger, B., & Fidone, S. (1997). cAMP production in rabbit carotid body: role of adenosine. *Journal of Applied Physiology*, **82**, 1771-1775.

Conde, S., Obeso, A., Vicario, I., Rigual, R., Rocher, A., & Gonzalez, C. (2006). Caffeine inhibition of rat carotid body chemoreceptors is mediated by A2A and A2B adenosine receptors. *Journal of neurochemistry*, **98**, 616-628.

Conde, S. V., Gonzalez, C., Batuca, J. R., Monteiro, E. C., & Obeso, A. (2008). An antagonistic interaction between A2B adenosine and D2 dopamine receptors modulates the function of rat carotid body chemoreceptor cells. *Journal of neurochemistry*, **107**, 1369-1381.

Conde, S. V., & Monteiro, E. C. (2004). Hypoxia induces adenosine release from the rat carotid body. *Journal of neurochemistry*, **89**, 1148-1156.

Conde, S. V., & Monteiro, E. C. (2006). Profiles for ATP and adenosine release at the carotid body in response to O2 concentrations *The Arterial Chemoreceptors* **(pp. 179-184)**: Springer.

De Castro, F., & Rubio, M. (1968). The anatomy and innervation of the blood vessels of the carotid body and the role of chemoreceptive reactions in the autoregulation of the blood flow. *Arterial Chemoreceptors*, **267**, 77.

De Gasparo, M., Catt, K., Inagami, T., Wright, J., & Unger, T. (2000). International union of pharmacology. XXIII. The angiotensin II receptors. *Pharmacological reviews*, **52**, 415-472.

Ding, Y., Li, Y. L., & Schultz, H. D. (2011). Role of blood flow in carotid body chemoreflex function in heart failure. *The Journal of physiology*, **589**, 245-258.

Dubyak, G. R. (2009). Both sides now: multiple interactions of ATP with pannexin-1 hemichannels. Focus on "A permeant regulating its permeation pore: inhibition of pannexin 1 channels by ATP". *American Journal of Physiology-Cell Physiology*, **296**, C235-C241.

Duchen, M., Caddy, K., Kirby, G., Patterson, D., Ponte, J., & Biscoe, T. (1988). Biophysical studies of the cellular elements of the rabbit carotid body. *Neuroscience*, **26**, 291-311.

Dunwiddie, T. V., Diao, L., & Proctor, W. R. (1997). Adenine nucleotides undergo rapid, quantitative conversion to adenosine in the extracellular space in rat hippocampus. *The Journal of neuroscience*, **17**, 7673-7682.

Eroglu, C., & Barres, B. A. (2010). Regulation of synaptic connectivity by glia. *Nature*, **468**, 223-231.

Eyzaguirre, C. (2007). Electric synapses in the carotid body–nerve complex. *Respiratory*

physiology & neurobiology, **157**, 116-122.

Fields, R. D., & Burnstock, G. (2006). Purinergic signalling in neuron–glia interactions. *Nature Reviews Neuroscience,* **7**, 423-436.

Finkbeiner, S. M. (1993). Glial calcium. *Glia,* **9**, 83-104.

Fung, M., Lam, S., Dong, X., Chen, Y., & Leung, P. (2002). Postnatal hypoxemia increases angiotensin II sensitivity and up-regulates AT1a angiotensin receptors in rat carotid body chemoreceptors. *Journal of endocrinology,* **173**, 305-313.

Fung, M. L. (2014). The role of local renin-angiotensin system in arterial chemoreceptors in sleep-breathing disorders. *Frontiers in physiology,* **5**.

Fung, M.-L., Lam, S.-Y., Chen, Y., Dong, X., & Leung, P. S. (2001). Functional expression of angiotensin II receptors in type-I cells of the rat carotid body. *Pflügers Archiv,* **441**, 474-480.

Ganfornina, M. D., & López-Barneo, J. (1992). Potassium channel types in arterial chemoreceptor cells and their selective modulation by oxygen. *The Journal of general physiology,* **100**, 401-426.

Goette, A., & Lendeckel, U. (2008). Electrophysiological effects of angiotensin II. Part I: signal transduction and basic electrophysiological mechanisms. *Europace,* **10**, 238-241.

Gonzalez, C., Almaraz, L., Obeso, A., & Rigual, R. (1994). Carotid body chemoreceptors: from natural stimuli to sensory discharges. *Physiological reviews,* **74**, 829-898.

Grönblad, M., Liesi, P., & Rechardt, L. (1983). Serotonin-like immunoreactivity in rat carotid body. *Brain research,* **276**, 348-350.

Grynkiewicz, G., Poenie, M., & Tsien, R. Y. (1985). A new generation of Ca2+ indicators with greatly improved fluorescence properties. *Journal of Biological Chemistry,* **260**, 3440-3450.

GUO, D. F., Sun, Y. L., Hamet, P., & Inagami, T. (2001). The angiotensin II type 1 receptor and receptor-associated proteins. *Cell research,* **11**, 165-180.

Guthrie, P. B., Knappenberger, J., Segal, M., Bennett, M. V., Charles, A. C., & Kater, S. (1999). ATP released from astrocytes mediates glial calcium waves. *The Journal of neuroscience,* **19**, 520-528.

Habec, J., Pallot, D., & Kummer, W. (1994). Serotonin immunoreacmtivitiyn the carotid body of adult humans.

Hanson, M., Nye, P., & Torrance, R. (1981). *The exodus of an extracellular bicarbonate theory of chemoreception and the genesis of an intracellular one.* Paper presented at the Arterial Chemoreceptors. Proceedings of Sixth International Meeting.

He, L., Chen, J., Dinger, B., Stensaas, L., & Fidone, S. (2006). Effect of chronic hypoxia on purinergic synaptic transmission in rat carotid body. *Journal of Applied Physiology*, **100**, 157-162.

He, L., Dinger, B., & Fidone, S. (2005). Effect of chronic hypoxia on cholinergic chemotransmission in rat carotid body. *Journal of Applied Physiology*, **98**, 614-619.

Henger, Anna, Huber, Tobias, Fischer, Karl-Georg, Nitschke, Roland, Mundel, Peter, Schollmeyer, Peter, . . . Pavenstadt, Hermann. (1997). Angiotensin II increases the cytosolic calcium activity in rat podocytes in culture. *Kidney international*, **52**, 687-693.

Hoyer, D., Hannon, J. P., & Martin, G. R. (2002). Molecular, pharmacological and functional diversity of 5-HT receptors. *Pharmacology Biochemistry and Behavior*, **71**, 533-554.

Huang, Y., Grinspan, J. B., Abrams, C. K., & Scherer, S. S. (2007). Pannexin1 is expressed by neurons and glia but does not form functional gap junctions. *Glia*, **55**, 46-56.

Huang, Y.-J., Maruyama, Y., Dvoryanchikov, G., Pereira, E., Chaudhari, N., & Roper, S. D. (2007). The role of pannexin 1 hemichannels in ATP release and cell–cell communication in mouse taste buds. *Proceedings of the National Academy of Sciences*, **104**, 6436-6441.

Iglesias, R., Dahl, G., Qiu, F., Spray, D. C., & Scemes, E. (2009). Pannexin 1: the molecular substrate of astrocyte "hemichannels". *The Journal of Neuroscience*, **29**, 7092-7097.

Iturriaga, R., Mokashi, A., & Lahiri, S. (1993). Dynamics of carotid body responses in vitro in the presence of CO~ 2-HCO^-~ 3: role of carbonic anhydrase. *Journal of Applied Physiology*, **75**, 1587-1587.

Jacono, F., Peng, Y.-J., Kumar, G., & Prabhakar, N. (2005). Modulation of the hypoxic sensory response of the carotid body by 5-hydroxytryptamine: role of the 5-HT 2 receptor. *Respiratory physiology & neurobiology*, **145**, 135-142.

Jennings, D. B. (1993). Breathing for protein function and [H< sup>+</sup>] homeostasis. *Respiration physiology*, **93**, 1-12.

Jiang, R., & Eyzaguirre, C. (2003). Dye and electric coupling between carotid nerve terminals and glomus cells *Chemoreception* **(pp. 247-253)**: Springer.

Katz, D. M., & Black, I. B. (1986). Expression and regulation of catecholaminergic traits in primary sensory neurons: relationship to target innervation in vivo. *The Journal of*

neuroscience, **6**, 983-989.

Kawamura, M., Ruskin, D. N., & Masino, S. A. (2010). Metabolic autocrine regulation of neurons involves cooperation among pannexin hemichannels, adenosine receptors, and KATP channels. *The Journal of Neuroscience,* **30**, 3886-3895.

Kemp, P. J. (2006). Detecting acute changes in oxygen: will the real sensor please stand up? *Experimental physiology,* **91**, 829-834.

Kienitz, M.-C., Bender, K., Dermietzel, R., Pott, L., & Zoidl, G. (2011). Pannexin 1 constitutes the large conductance cation channel of cardiac myocytes. *Journal of Biological Chemistry,* **286**, 290-298.

Kim, D., Cavanaugh, E. J., Kim, I., & Carroll, J. L. (2009). Heteromeric TASK-1/TASK-3 is the major oxygen-sensitive background K+ channel in rat carotid body glomus cells. *The Journal of physiology,* **587**, 2963-2975.

Kimura, H., Nagai, Y., Umemura, K., & Kimura, Y. (2005). Physiological roles of hydrogen sulfide: synaptic modulation, neuroprotection, and smooth muscle relaxation. *Antioxidants & redox signaling,* **7**, 795-803.

Kirby, G., & McQueen, D. (1984). Effects of the antagonists MDL 72222 and ketanserin on responses of cat carotid body chemoreceptors to 5-hydroxytiyptamine. *British journal of pharmacology,* **83**, 259-269.

Kobayashi, S., Conforti, L., & Millhorn, D. E. (2000). Gene expression and function of adenosine A2A receptor in the rat carotid body. *American Journal of Physiology-Lung Cellular and Molecular Physiology,* **279**, L273-L282.

Kondo, H. (2002). Are there gap junctions between chief (glomus, type I) cells in the carotid body chemoreceptor? A review. *Microscopy research and technique,* **59**, 227-233.

Kumar, P., & Bin-Jaliah, I. (2007). Adequate stimuli of the carotid body: more than an oxygen sensor? *Respiratory physiology & neurobiology,* **157**, 12-21.

Kumar, P., & Prabhakar, N. R. (2012). Peripheral chemoreceptors: function and plasticity of the carotid body. *Comprehensive Physiology*.

Lam, S. Y., Fung, M.-L., & Leung, P. S. (2004). Regulation of the angiotensin-converting enzyme activity by a time-course hypoxia in the carotid body. *Journal of Applied Physiology,* **96**, 809-813.

Lam, S. Y., & Leung, P. S. (2002). A locally generated angiotensin system in rat carotid body. *Regulatory peptides,* **107**, 97-103.

Lam, S. Y., & Leung, P. S. (2003). Chronic hypoxia activates a local angiotensin-generating system in rat carotid body. *Molecular and cellular endocrinology,* **203**, 147-153.

Lam, S. Y., Liu, Y., Ng, K. M., Liong, E. C., Tipoe, G. L., Leung, P. S., & Fung, M. L. (2014). Upregulation of a local renin–angiotensin system in the rat carotid body during chronic intermittent hypoxia. *Experimental physiology,* **99**, 220-231.

Leung, P., Lam, S., & Fung, M. (2000). Chronic hypoxia upregulates the expression and function of AT (1) receptor in rat carotid body. *Journal of Endocrinology,* **167**, 517-524.

Leung, P. S. (2004). The peptide hormone angiotensin II: its new functions in tissues and organs. *Current Protein and Peptide Science,* **5**, 267-273.

Li, Q., Sun, B., Wang, X., Jin, Z., Zhou, Y., Dong, L., Jiang, L.-H., & Rong, W. (2010). A crucial role for hydrogen sulfide in oxygen sensing via modulating large conductance calcium-activated potassium channels. *Antioxidants & redox signaling,* **12**, 1179-1189.

Li, Y.-L., Gao, L., Zucker, I. H., & Schultz, H. D. (2007). NADPH oxidase-derived superoxide anion mediates angiotensin II-enhanced carotid body chemoreceptor sensitivity in heart failure rabbits. *Cardiovascular research,* **75**, 546-554.

Li, Y.-L., Xia, X.-H., Zheng, H., Gao, L., Li, Y.-F., Liu, D., Patel, K. P., Wang, W., & Schultz, H. D. (2006). Angiotensin II enhances carotid body chemoreflex control of sympathetic outflow in chronic heart failure rabbits. *Cardiovascular research,* **71**, 129-138.

Liu, Y., Ji, E.-S., Xiang, S., Tamisier, R., Tong, J., Huang, J., & Weiss, J. W. (2009). Exposure to cyclic intermittent hypoxia increases expression of functional NMDA receptors in the rat carotid body. *Journal of Applied Physiology,* **106**, 259-267.

Livermore, S., & Nurse, C. A. (2013). Enhanced adenosine A2b receptor signaling facilitates stimulus-induced catecholamine secretion in chronically hypoxic carotid body type I cells. *American Journal of Physiology-Cell Physiology,* **305**, C739-C750.

Locovei, S., Wang, J., & Dahl, G. (2006). Activation of pannexin 1 channels by ATP through P2Y receptors and by cytoplasmic calcium. *FEBS letters,* **580**, 239-244.

Lohman, A. W., & Isakson, B. E. (2014). Differentiating connexin hemichannels and pannexin channels in cellular ATP release. *FEBS letters,* **588**, 1379-1388.

López-Barneo, J. (1996). Oxygen-sensing by ion channels and the regulation of cellular functions. *Trends in neurosciences,* **19**, 435-440.

López-Barneo, J. (2003). Oxygen and glucose sensing by carotid body glomus cells. *Current opinion in neurobiology,* **13**, 493-499.

Lopez-Barneo, J., Lopez-Lopez, J. R., Urena, J., & Gonzalez, C. (1988). Chemotransduction in the carotid body: K+ current modulated by PO2 in type I chemoreceptor cells. *Science*, **241**, 580-582.

López-Barneo, J., Pardal, R., & Ortega-Sáenz, P. (2001). Cellular mechanism of oxygen sensing. *Annual Review of Physiology*, **63**, 259-287.

Lugliani, R., Whipp, B. J., Seard, C., & Wasserman, K. (1971). Effect of bilateral carotid-body resection on ventilatory control at rest and during exercise in man. *New England Journal of Medicine*, **285**, 1105-1111.

Ma, W., Hui, H., Pelegrin, P., & Surprenant, A. (2009). Pharmacological characterization of pannexin-1 currents expressed in mammalian cells. *Journal of Pharmacology and Experimental Therapeutics*, **328**, 409-418.

MacVicar, B. A., & Thompson, R. J. (2010). Non-junction functions of pannexin-1 channels. *Trends in neurosciences*, **33**, 93-102.

Makarenko, V. V., Nanduri, J., Raghuraman, G., Fox, A. P., Gadalla, M. M., Kumar, G. K., . . . Prabhakar, N. R. (2012). Endogenous H2S is required for hypoxic sensing by carotid body glomus cells. *American Journal of Physiology-Cell Physiology*, **303**, C916-C923.

Malarkey, E. B., & Parpura, V. (2008). Mechanisms of glutamate release from astrocytes. *Neurochemistry international*, **52**, 142-154.

Marshall, J. M. (1994). Peripheral chemoreceptors and cardiovascular regulation. *Physiological Reviews*, **74**, 543-594.

McDonald, D. M. (1981). Peripheral chemoreceptors: structure-function relationships of the carotid body. *Regulation of Breathing*, **17**, 105-319.

McDonald, D. M., & Mitchell, R. A. (1975). The innervation of glomus cells, ganglion cells and blood vessels in the rat carotid body: a quantitative ultrastructural analysis. *Journal of Neurocytology*, **4**, 177-230.

McQueen, D., & Ribeiro, J. (1981). Effect of adenosine on carotid chemoreceptor activity in the cat. *British journal of pharmacology*, **74**, 129-136.

McQueen, D., & Ribeiro, J. (1983). On the specificity and type of receptor involved in carotid body chemoreceptor activation by adenosine in the cat. *British journal of pharmacology*, **80**, 347-354.

McQueen, D., & Ribeiro, J. (1986). Pharmacological characterization of the receptor involved in chemoexcitation induced by adenosine. *British journal of pharmacology*, **88**, 615-620.

Monteiro, E., & Ribeiro, J. (1987). Ventilatory effects of adenosine mediated by carotid body chemoreceptors in the rat. *Naunyn-Schmiedeberg's archives of pharmacology,* **335**, 143-148.

Monteiro, E., & Ribeiro, J. (1989). Adenosine deaminase and adenosine uptake inhibitions facilitate ventilation in rats. *Naunyn-Schmiedeberg's archives of pharmacology,* **340**, 230-238.

Monti-Bloch, L., & Eyzaguirre, C. (1990). Effects of different stimuli and transmitters on glomus cell membranes and intercellular communications *Arterial Chemoreception* **(pp. 157-167)**: Springer.

Morgan, M., Pack, R., & Howe, A. (1975). Nerve endings in rat carotid body. *Cell and tissue research,* **157**, 255-272.

Murali, S., Zhang, M., & Nurse, C. A. (2014). Angiotensin II mobilizes intracellular calcium and activates pannexin-1 channels in rat carotid body type II cells via AT1 receptors. *The Journal of physiology,* **592**, 4747-4762.

Muraoka, S., Kamei, K., Muneoka, K., & Takigawa, M. (1998). Chronic Imipramine Administration Amplifies the Serotonin2A Receptor-Induced Intracellular Ca2+ Mobilization in C6 Glioma Cells Through a Calmodulin-Dependent Pathway. *Journal of neurochemistry*, **71**, 1709-1718.

Neubauer, J. A., & Sunderram, J. (2004). Oxygen-sensing neurons in the central nervous system. *Journal of Applied Physiology,* **96**, 367-374.

Nieto, F. J., Young, T. B., Lind, B. K., Shahar, E., Samet, J. M., Redline, S., D'Agostino, R. B., Newman, A. B., Lebowitz, M. D., & Pickering, T. G. (2000). Association of sleep-disordered breathing, sleep apnea, and hypertension in a large community-based study. *Jama,* **283**, 1829-1836.

Noda, M., Yasuda, S., Okada, M., Higashida, H., Shimada, A., Iwata, N., . . . Uchida, M. (2003). Recombinant human serotonin 5A receptors stably expressed in C6 glioma cells couple to multiple signal transduction pathways. *Journal of neurochemistry,* **84**, 222-232.

Nurse, C. A. (2005). Neurotransmission and neuromodulation in the chemosensory carotid body. *Autonomic Neuroscience,* **120**, 1-9.

Nurse, C. A. (2010). Neurotransmitter and neuromodulatory mechanisms at peripheral arterial chemoreceptors. *Experimental physiology,* **95**, 657-667.

Nurse, C. A. (2014). Synaptic and paracrine mechanisms at carotid body arterial chemoreceptors. *The Journal of physiology,* **592**, 3419-3426.

Nurse, C. A., & Piskuric, N. A. (2013). *Signal processing at mammalian carotid body chemoreceptors.* Paper presented at the Seminars in cell & developmental biology.

Nurse, C. A., & Zhang, M. (1999). Acetylcholine contributes to hypoxic chemotransmission in co-cultures of rat type 1 cells and petrosal neurons. *Respiration physiology,* **115**, 189-199.

Obeso, A., Rocher, A., Fidone, S., & Gonzalez, C. (1992). The role of dihydropyridine-sensitive Ca< sup> 2+</sup> channels in stimulus-evoked catecholamine release from chemoreceptor cells of the carotid body. *Neuroscience,* **47**, 463-472.

Ohtake, P. J., & Jennings, D. B. (1993). Angiotensin II stimulates respiration in awake dogs and antagonizes baroreceptor inhibition. *Respiration physiology,* **91**, 335-351.

Pardal, R., Ortega-Sáenz, P., Durán, R., & López-Barneo, J. (2007). Glia-like stem cells sustain physiologic neurogenesis in the adult mammalian carotid body. *Cell,* **131**, 364-377.

Parpura, V., Heneka, M. T., Montana, V., Oliet, S. H., Schousboe, A., Haydon, P. G., Stout, R. F., Spray, D. C., Reichenbach, A., & Pannicke, T. (2012). Glial cells in (patho) physiology. *Journal of neurochemistry,* **121**, 4-27.

Pearse, A., Polak, J., Rost, F., Fontaine, J., Le Lievre, C., & Le Douarin, N. (1973). Demonstration of the neural crest origin of type I (APUD) cells in the avian carotid body, using a cytochemical marker system. *Histochemie,* **34**, 191-203.

Peers, C. (1990). Hypoxic suppression of K< sup>+</sup> currents in type I carotid body cells: Selective effect on the Ca< sup> 2+</sup>-activated K< sup>+</sup> current. *Neuroscience letters,* **119**, 253-256.

Peers, C., & Buckler, K. (1995). Transduction of chemostimuli by the type I carotid body cell. *The Journal of membrane biology*, **144**, 1-9.

Peers, C., & Wyatt, C. N. (2007). The role of maxiK channels in carotid body chemotransduction. *Respiratory physiology & neurobiology,* **157**, 75-82.

Peng, Y. J., Yuan, G., Jacono, F. J., Kumar, G. K., & Prabhakar, N. R. (2006). 5-HT evokes sensory long-term facilitation of rodent carotid body via activation of NADPH oxidase. *The Journal of physiology,* **576**, 289-295.

Peng, Y.-J., Nanduri, J., Raghuraman, G., Souvannakitti, D., Gadalla, M. M., Kumar, G. K., Snyder, S. H., & Prabhakar, N. R. (2010). H2S mediates O2 sensing in the carotid body. *Proceedings of the National Academy of Sciences*, **107**, 10719-10724.

Peng, Y.-J., Overholt, J. L., Kline, D., Kumar, G. K., & Prabhakar, N. R. (2003). Induction of sensory long-term facilitation in the carotid body by intermittent hypoxia: implications for recurrent apneas. *Proceedings of the National Academy of Sciences*, **100**, 10073-

10078.

Peng, Y.-J., Raghuraman, G., Khan, S. A., Kumar, G. K., & Prabhakar, N. R. (2011). Angiotensin II evokes sensory long-term facilitation of the carotid body via NADPH oxidase. *Journal of Applied Physiology*, **111**, 964-970.

Pérez-García, M., Almaraz, L., & Gonzalez, C. (1991). Cyclic AMP modulates differentially the release of dopamine induced by hypoxia and other stimuli and increases dopamine synthesis in the rabbit carotid body. *Journal of neurochemistry*, **57**, 1992-2000.

Piskuric, N. A., & Nurse, C. A. (2012). Effects of chemostimuli on [Ca2+] i responses of rat aortic body type I cells and endogenous local neurons: comparison with carotid body cells. *The Journal of physiology*, **590**, 2121-2135.

Prabhakar, N. R. (2011). Sensory plasticity of the carotid body: role of reactive oxygen species and physiological significance. *Respiratory physiology & neurobiology*, **178**, 375-380.

Prabhakar, N. R., & Peers, C. (2014). Gasotransmitter regulation of ion channels: a key step in o2 sensing by the carotid body. *Physiology*, **29**, 49-57.

Prabhakar, N. R., & Peng, Y.-J. (2004). Peripheral chemoreceptors in health and disease. *Journal of Applied Physiology*, **96**, 359-366.

Ramirez, M., Gallego-Martin, T., Olea, E., Rocher, A., Obeso, A., & Gonzalez, C. (2012). Serotonin Dynamics and Actions in the Rat Carotid Body: Preliminary Findings *Arterial Chemoreception* **(pp. 255-263)**: Springer.

Rigual, R., Gonzalez, E., Fidone, S., & Gonzalez, C. (1984). Effects of low pH on synthesis and release of catecholamines in the cat carotid body in vitro. *Brain research*, **309**, 178-181.

Rigual, R., Lopez-Lopez, J., & Gonzalez, C. (1991). Release of dopamine and chemoreceptor discharge induced by low pH and high PCO2 stimulation of the cat carotid body. *The Journal of physiology*, **433**, 519-531.

Rocher, A., Geijo-Barrientos, E., Cáceres, A. I., Rigual, R., González, C., & Almaraz, L. (2005). Role of voltage-dependent calcium channels in stimulus–secretion coupling in rabbit carotid body chemoreceptor cells. *The Journal of physiology*, **562**, 407-420.

Rocher, A., Obeso, A., Gonzalez, C., & Herreros, B. (1991). Ionic mechanisms for the transduction of acidic stimuli in rabbit carotid body glomus cells. *The Journal of physiology*, **433**, 533-548.

Romanov, R. A., Rogachevskaja, O. A., Bystrova, M. F., Jiang, P., Margolskee, R. F., & Kolesnikov, S. S. (2007). Afferent neurotransmission mediated by hemichannels in mammalian taste cells. *The EMBO journal*, **26**, 657-667.

Romanov, R. A., Rogachevskaja, O. A., Khokhlov, A. A., & Kolesnikov, S. S. (2008). Voltage dependence of ATP secretion in mammalian taste cells. *The Journal of general physiology*, **132**, 731-744.

Rong, W., Gourine, A. V., Cockayne, D. A., Xiang, Z., Ford, A. P., Spyer, K. M., & Burnstock, G. (2003). Pivotal role of nucleotide P2X2 receptor subunit of the ATP-gated ion channel mediating ventilatory responses to hypoxia. *The Journal of neuroscience*, **23**, 11315-11321.

Runold, M., Cherniack, N. S., & Prabhakar, N. R. (1990). Effect of adenosine on isolated and superfused cat carotid body activity. *Neuroscience letters*, **113**, 111-114.

Sapru, H., & Krieger, A. (1977). Effect of 5-hydroxytryptamine on the peripheral chemoreceptors in the rat. *Research communications in chemical pathology and pharmacology*, **16**, 245-250.

Scemes, E., Suadicani, S. O., Dahl, G., & Spray, D. C. (2007). Connexin and pannexin mediated cell–cell communication. *Neuron glia biology*, **3**, 199-208.

Schultz, H. D. (2011). Angiotensin and carotid body chemoreception in heart failure. *Current opinion in pharmacology*, **11**, 144-149.

Schultz, H. D., & Li, Y. L. (2007). Carotid body function in heart failure. *Respiratory physiology & neurobiology*, **157**, 171-185.

Shahar, E., Whitney, C. W., Redline, S., Lee, E. T., Newman, A. B., Javier Nieto, F., O'CONNOR, G. T., Boland, L. L., Schwartz, J. E., & Samet, J. M. (2001). Sleep-disordered breathing and cardiovascular disease: cross-sectional results of the Sleep Heart Health Study. *American journal of respiratory and critical care medicine*, **163**, 19-25.

Shaw, K., Montague, W., & Pallot, D. J. (1989). Biochemical studies on the release of catecholamines from the rat carotid body in vitro. *Biochimica et Biophysica Acta (BBA)-Molecular Cell Research*, **1013**, 42-46.

Shirahata, M., Balbir, A., Otsubo, T., & Fitzgerald, R. S. (2007). Role of acetylcholine in neurotransmission of the carotid body. *Respiratory physiology & neurobiology*, **157**, 93-105.

Shirahata, M., & Fitzgerald, R. S. (1991). Dependency of hypoxic chemotransduction in cat carotid body on voltage-gated calcium channels. *J. Appl. Physiol*, **71**, 1062-1069.

Sprague, R. S., Ellsworth, M. L., Stephenson, A. H., & Lonigro, A. J. (1996). ATP: the red blood cell link to NO and local control of the pulmonary circulation. *American Journal of Physiology-Heart and Circulatory Physiology*, **271**, H2717-H2722.

Spyer, K. M., & Gourine, A. V. (2009). Chemosensory pathways in the brainstem controlling cardiorespiratory activity. *Philosophical Transactions of the Royal Society B: Biological Sciences,* **364**, 2603-2610.

Sridharan, M., Adderley, S. P., Bowles, E. A., Egan, T. M., Stephenson, A. H., Ellsworth, M. L., & Sprague, R. S. (2010). Pannexin 1 is the conduit for low oxygen tension-induced ATP release from human erythrocytes. *American Journal of Physiology-Heart and Circulatory Physiology,* **299**, H1146-H1152.

Tan, Z.-Y., Lu, Y., Whiteis, C. A., Benson, C. J., Chapleau, M. W., & Abboud, F. M. (2007). Acid-sensing ion channels contribute to transduction of extracellular acidosis in rat carotid body glomus cells. *Circulation research,* **101**, 1009-1019.

Teppema, L. J., & Dahan, A. (2010). The ventilatory response to hypoxia in mammals: mechanisms, measurement, and analysis. *Physiological Reviews,* **90**, 675-754.

Thastrup, O., Cullen, P. J., Drøbak, B., Hanley, M. R., & Dawson, A. P. (1990). Thapsigargin, a tumor promoter, discharges intracellular Ca2+ stores by specific inhibition of the endoplasmic reticulum Ca2 (+)-ATPase. *Proceedings of the National Academy of Sciences,* **87**, 2466-2470.

Thomas, D. R. (2006). 5-ht 5A receptors as a therapeutic target. *Pharmacology & therapeutics,* **111**, 707-714.

Thomas, D. R., Soffin, E. M., Roberts, C., Kew, J. N., Raul, M., Dawson, L. A., Fry, V. A., Coggon, S. A., Faedo, S., & Hayes, P. D. (2006). SB-699551-A (3-cyclopentyl-N-[2-(dimethylamino) ethyl]-N-[(4′-{[(2-phenylethyl) amino] methyl}-4-biphenylyl) methyl] propanamide dihydrochloride), a novel 5-ht 5A receptor-selective antagonist, enhances 5-HT neuronal function: evidence for an autoreceptor role for the 5-ht 5A receptor in guinea pig brain. *Neuropharmacology,* **51**, 566-577.

Thompson, R. J., & MacVicar, B. A. (2008). Connexin and pannexin hemichannels of neurons and astrocytes. *Channels (Austin),* **2**, 81-86.

Thompson, R. J., Zhou, N., & MacVicar, B. A. (2006). Ischemia opens neuronal gap junction hemichannels. *Science,* **312**, 924-927.

Tse, A., Yan, L., Lee, A. K., & Tse, F. W. (2012). Autocrine and paracrine actions of ATP in rat carotid body. *Canadian journal of physiology and pharmacology,* **90**, 705-711.

Vandier, C., Conway, A., Landauer, R., & Kumar, P. (1999). Presynaptic action of adenosine on a 4-aminopyridine-sensitive current in the rat carotid body. *The Journal of physiology,* **515**, 419-429.

Varas, R., Alcayaga, J., & Iturriaga, R. (2003). ACh and ATP mediate excitatory transmission in cat carotid identified chemoreceptor units in vitro. *Brain research*, **988**, 154-163.

Venance, L., Stella, N., Glowinski, J., & Giaume, C. (1997). Mechanism involved in initiation and propagation of receptor-induced intercellular calcium signaling in cultured rat astrocytes. *The Journal of neuroscience*, **17**, 1981-1992.

Verkhratsky, A., & Kettenmann, H. (1996). Calcium signalling in glial cells. *Trends in neurosciences*, **19**, 346-352.

Verma, A., Hirsch, D. J., Hanley, M. R., Thastrup, O., Christensen, S. B., & Snyder, S. H. (1990). Inositol trisphosphate and thapsigargin discriminate endoplasmic reticulum stores of calcium in rat brain. *Biochemical and biophysical research communications*, **172**, 811-816.

von Kügelgen, I. (2006). Pharmacological profiles of cloned mammalian P2Y-receptor subtypes. *Pharmacology & therapeutics*, **110**, 415-432.

Wang, Z.-Y., Keith, I. M., Beckman, M. J., Brownfield, M. S., Vidruk, E. H., & Bisgard, G. E. (2000). 5-HT 5a receptors in the carotid body chemoreception pathway of rat. *Neuroscience letters*, **278**, 9-12.

Watt, A., Reid, P., Stephens, M., & Routledge, P. (1987). Adenosine-induced respiratory stimulation in man depends on site of infusion. Evidence for an action on the carotid body? *British journal of clinical pharmacology*, **23**, 486-490.

Watt, A., & Routledge, P. (1985). Adenosine stimulates respiration in man. *British journal of clinical pharmacology*, **20**, 503-506.

Weilinger, N. L., Tang, P. L., & Thompson, R. J. (2012). Anoxia-induced NMDA receptor activation opens pannexin channels via Src family kinases. *The Journal of Neuroscience*, **32**, 12579-12588.

Winter, B. (1991). Carotid body resection in chronic obstructive pulmonary disease. *CHEST Journal*, **100**, 883a-883.

Wyatt, C. N., Mustard, K. J., Pearson, S. A., Dallas, M. L., Atkinson, L., Kumar, P., . . . Evans, A. M. (2007). AMP-activated protein kinase mediates carotid body excitation by hypoxia. *Journal of Biological Chemistry*, **282**, 8092-8098.

Xu, F., Xu, J., Frederick, W. T., & Tse, A. (2006). Adenosine stimulates depolarization and rise in cytoplasmic [Ca2+] in type I cells of rat carotid bodies. *American Journal of Physiology-Cell Physiology*, **290**, C1592-C1598.

Xu, J., Frederick, W. T., & Tse, A. (2003). ATP triggers intracellular Ca2+ release in type II

cells of the rat carotid body. *The Journal of physiology*, **549**(3), 739-747.

Xu, J., Xu, F., Tse, F. W., & Tse, A. (2005). ATP inhibits the hypoxia response in type I cells of rat carotid bodies. *Journal of neurochemistry*, **92**, 1419-1430.

Yokoyama, T., Misuzu, Y.-Y., & Yamamoto, Y. (2013). Immunohistochemical localization of tryptophan hydroxylase and serotonin transporter in the carotid body of the rat. *Histochemistry and cell biology*, **140**, 147-155.

Yoshihara, M., & Littleton, J. T. (2002). Synaptotagmin I functions as a calcium sensor to synchronize neurotransmitter release. *Neuron*, **36**, 897-908.

Zakheim, R., Molteni, A., Mattioli, L., & Park, M. (1976). Plasma angiotensin II levels in hypoxic and hypovolemic stress in unanesthetized rabbits. *Journal of applied physiology*, **41**, 462-465.

Zhang, M., Fearon, I. M., Zhong, H., & Nurse, C. A. (2003). Presynaptic modulation of rat arterial chemoreceptor function by 5-HT: role of K+ channel inhibition via protein kinase C. *The Journal of physiology*, **551**, 825-842.

Zhang, M., & Nurse, C. A. (2000). Does endogenous 5-HT mediate spontaneous rhythmic activity in chemoreceptor clusters of rat carotid body? *Brain research*, **872**, 199-203.

Zhang, M., & Nurse, C. A. (2004). CO2/pH chemosensory signaling in co-cultures of rat carotid body receptors and petrosal neurons: role of ATP and ACh. *Journal of neurophysiology*, **92**, 3433-3445.

Zhang, M., Piskuric, N. A., Vollmer, C., & Nurse, C. A. (2012). P2Y2 receptor activation opens pannexin-1 channels in rat carotid body type II cells: potential role in amplifying the neurotransmitter ATP. *The Journal of physiology*, **590**, 4335-4350.

Zhang, M., Turnbaugh, D., Cofie, D., Dogan, S., Koshida, H., Fugate, R., & Kem, D. C. (1996). Protein kinase C modulation of cardiomyocyte angiotensin II and vasopressin receptor desensitization. *Hypertension*, **27**, 269-275.

Zhang, M., Zhong, H., Vollmer, C., & Nurse, C. A. (2000). Co-release of ATP and ACh mediates hypoxic signalling at rat carotid body chemoreceptors. *The Journal of Physiology*, **525**, 143-158.

Zhong, H., Zhang, M., & Nurse, C. A. (1997). Synapse formation and hypoxic signalling in co-cultures of rat petrosal neurones and carotid body type 1 cells. *The Journal of Physiology*, **503**, 599-612.

Zhong, H., Zhang, M., & Nurse, C. A. (1999). Electrophysiological characterization of 5-HT receptors on rat petrosal neurons in dissociated cell culture. *Brain research*, **816**, 544-

553.

Zimmermann, H. (1992). 5'-Nucleotidase: molecular structure and functional aspects. *Biochemical Journal*, **285**, 345.